Department of Energy
Richland Operations Office
P.O. Box 550
Richland, Washington 99352

10-AMCP-0078

JAN 26 2010

Ms. J. A. Hedges, Program Manager
Nuclear Waste Program
State of Washington
Department of Ecology
3100 Port of Benton
Richland, Washington 99354

Mr. D. A. Faulk, Program Manager
Office of Environmental Cleanup
Hanford Project Office
U.S. Environmental Protection Agency
309 Bradley Boulevard, Suite 115
Richland, Washington 99352

Addressees:

REMEDIATION OF URANIUM IN THE HANFORD VADOSE ZONE USING GAS-TRANSPORTED REACTANTS: LABORATORY-SCALE EXPERIMENTS, PNNL-18879

This letter transmits the Remediation of Uranium in the Hanford Vadose Zone Using Gas-Transported Reactants: Laboratory-Scale Experiments, PNNL-18879, for your information. Three copies of the report were provided to the U.S. Environmental Protection Agency and the State of Washington Department of Ecology during the 200 Area Project Managers Meeting on January 21, 2010.

This completes Hanford Federal Facility Agreement and Consent Order Milestone M-015-54, Submit report on reactive gas testing for sequestration of uranium that will support remedial action decision making, by January 31, 2010. If you have any question, please contact me, or your staff may contact Briant Charboneau, of my staff, on (509) 373-6137.

Sincerely,

Matthew S. McCormick, Assistant Manager
for the Central Plateau

AMCP:JGM

Attachment

cc: See Page 2

cc w/attach:
G. Bohnee, NPT
L. Buck, Wanapum
S. Harris, CTUIR
R. Jim, YN
S. L. Leckband, HAB
K. Niles, ODOE
Administrative Record
Environmental Portal

cc w/o attach:
D. G. Black, CHPRC
R. H. Engelmann, CHPRC
D. L. Foss, CHPRC
R. E. Piippo, MSA
J. G. Vance, FFS

U.S. DEPARTMENT OF
ENERGY

PNNL-18879

Prepared for the U.S. Department of Energy
under Contract DE-AC05-76RL01830

Remediation of Uranium in the Hanford Vadose Zone Using Gas-Transported Reactants: Laboratory-Scale Experiments

in Support of the

Deep Vadose Zone Treatability Test Plan for the Hanford Central Plateau

JE Szecsody
MJ Truex
L Zhong
MD Williams
CT Resch
JP McKinley

January 2010

Pacific Northwest
NATIONAL LABORATORY

Proudly Operated by Battelle *Since 1965*

DISCLAIMER

This report was prepared as an account of work sponsored by an agency of the United States Government. Neither the United States Government nor any agency thereof, nor Battelle Memorial Institute, nor any of their employees, makes **any warranty, express or implied, or assumes any legal liability or responsibility for the accuracy, completeness, or usefulness of any information, apparatus, product, or process disclosed, or represents that its use would not infringe privately owned rights**. Reference herein to any specific commercial product, process, or service by trade name, trademark, manufacturer, or otherwise does not necessarily constitute or imply its endorsement, recommendation, or favoring by the United States Government or any agency thereof, or Battelle Memorial Institute. The views and opinions of authors expressed herein do not necessarily state or reflect those of the United States Government or any agency thereof.

PACIFIC NORTHWEST NATIONAL LABORATORY
operated by
BATTELLE
for the
UNITED STATES DEPARTMENT OF ENERGY
under Contract DE-AC05-76RL01830

Printed in the United States of America

Available to DOE and DOE contractors from the
Office of Scientific and Technical Information,
P.O. Box 62, Oak Ridge, TN 37831-0062;
ph: (865) 576-8401
fax: (865) 576-5728
email: reports@adonis.osti.gov

Available to the public from the National Technical Information Service,
U.S. Department of Commerce, 5285 Port Royal Rd., Springfield, VA 22161
ph: (800) 553-6847
fax: (703) 605-6900
email: orders@ntis.fedworld.gov
online ordering: http://www.ntis.gov/ordering.htm

This document was printed on recycled paper.
(9/2003)

PNNL-18879

Remediation of Uranium in the Hanford Vadose Zone Using Gas-Transported Reactants: Laboratory-Scale Experiments

in Support of the

Deep Vadose Zone Treatability Test Plan for the Hanford Central Plateau

JE Szecsody
MJ Truex
L Zhong
MD Williams
CT Resch
JP McKinley

January 2010

Prepared for
CH2M HILL Plateau Remediation Company
under Contract DE-AC05-76RL01830

Pacific Northwest National Laboratory
Richland, Washington 99352

Abstract

This laboratory-scale investigation focused on decreasing uranium mobility in subsurface contaminated sediments in the vadose zone by in situ geochemical manipulation at low water content. This geochemical manipulation of the sediment surface phases included reduction, pH change (acidic and alkaline), and additions of chemicals (phosphate and ferric iron) to form specific precipitates. Reactants were advected into one-dimensional columns packed with uranium-contaminated sediment from the 200 Area of the Hanford Site as a reactive gas (for CO_2, NH_3, H_2S, SO_2), with a 0.1% water content mist [for NaOH, Fe(III), HCl, PO_4] and with a 1% water content foam (for PO_4).

Uranium is present in the sediment in multiple phases that include (in decreasing mobility) the following: aqueous U(VI) complexes, adsorbed uranium, reduced U(IV) precipitates, rind-carbonates, total carbonates, oxides, silicates, and phosphates. Geochemical changes were evaluated in the ability to change the mixture of surface uranium phases to less mobile forms, as defined by a series of liquid extractions that dissolve progressively less soluble phases. Although liquid extractions provide some useful information as to the generalized uranium surface phases (and are considered operational definitions of extracted phases), positive identification of surface phase changes by electron microprobe analysis is in progress. Some of the changes in uranium mobility directly involve uranium phases, whereas other changes result in precipitate coatings on uranium surface phases. The long-term implication of the uranium surface phase changes to alter uranium mass mobility in the vadose zone was then investigated using simulations of one-dimensional infiltration and downward migration of six uranium phases to the water table.

In terms of the short-term decrease in uranium mobility (in decreasing order), NH_3, NaOH mist, CO_2, HCl mist, and Fe(III) mist showed 20% to 35% change in uranium surface phases. Difference in treatment effectiveness between sediments likely reflects mineralogy. Phosphate addition (mist or foam advected) showed inconsistent change in aqueous and adsorbed uranium, but significant coating (likely phosphates) on uranium carbonates. The two reductive gas treatments (H_2S and SO_2) showed little change. For long-term decrease in uranium reduction, mineral phases created that had low solubility (phosphates and silicates) were desired, so NH_3, phosphates (mist and foam delivered), and NaOH mist showed the greatest formation of these minerals. In addition, simulations of uranium movement in the vadose zone showed that these treatments greatly decreased uranium transport to groundwater. Advection of reactive gasses was the easiest to implement into low water content sediments at the laboratory-scale (and presumably field-scale) experiments. Both mist and foam advection show potential and need further development, but current implementation techniques move reactants shorter distances relative to reactive gasses. Overall, the ammonia and carbon dioxide gas had the greatest overall geochemical performance and ability to implement at field scale. Corresponding mist delivered technologies (NaOH mist for ammonia and HCl mist for carbon dioxide) performed as well or better geochemically, but are not as easily upscaled. Phosphate delivery by mist was rated slightly higher than by foam delivery because of the complexity of foam injection and unknown effect of uranium mobility by the presence of the surfactant.

Acronyms and Abbreviations

adsorbed uranium	mass of uranium extracted from the sediment with a 1M $Mg(NO_3)_2$ solution; second sequential extraction after aqueous uranium
aqueous uranium	mass of uranium extracted from the sediment with Hanford Site 100-N Area groundwater (Ca, Mg-CO_3 saturated) at a sediment/water ratio of 1:1; first of six sequential extractions
autunite	uranium-phosphate precipitate, $Ca(UO_2)_2(PO_4)_2 \cdot XH_2O$
CO_3-U	extracted uranium from sediment with 0.44M acetic acid, 0.1M Ca-NO_3, pH 2.3 for 1 week; fourth sequential extraction
CO_2	carbon dioxide gas
CPS	calcium polysulfide
DMMP	dimethylmethylphosphonate
DOE-RL	U.S. Department of Energy, Richland Operations Office
foam	0.5% solution of sodium laureth sulfate (surfactant) at a water/gas ratio of 1/100 pumped through a porous plate to form bubbles
H_2S	hydrogen sulfide gas
ICP-MS	inductively coupled plasma/mass spectrometry
ISGR	in situ gaseous reduction
K_d	distribution coefficient for uranium defined as fraction uranium adsorbed divided by the fraction uranium in aqueous phase
mist	0.1% to 0.3% water pumped through a venturi with 99.9% gas (air or N_2) to form small droplets of the aqueous solution
Na-boltwoodite	uranium-silicate, (Na, K) $(UO_2)SiO_4$ H_2O
NH_3	ammonia gas
oxide-U	extracted uranium from sediment with 0.1M ammonium oxalate, 0.1M oxalic acid; fifth sequential extraction.
ppb	parts per billion
PRB	Permeable Reactive Barrier
rind-CO_3-U	extracted uranium from sediment with 1M Na-acetate at pH 5 for 1 h; third sequential extraction.
silicate, phosphate-U	extracted uranium from sediment with 8M HNO_3 at 95°C for 2 h; sixth sequential extraction
SMI	sulfur modified iron, Fe^o, S^o, zero valent iron with some zero valent sulfur
SO_2	sulfur dioxide gas
STOMP	Subsurface Transport Over Multiple Phases
TBP	tributyl phosphate

TEP	triethyl phosphate
XRD	x-ray diffraction
vanadate	U-VO_4 mineral phases, tyuyamunite, ($Ca(UO_2)_2(VO_4)_2 \cdot 5\text{-}8H_2O$) and carnotite ($K_2(UO_2)_2(VO_4)_2 \cdot 3H_2O$)
ZVI	zero valent iron

Contents

Abstract iii

Acronyms and Abbreviations v

1.0 Introduction 1.1

1.1 Purpose 1.1

1.2 Scope 1.1

2.0 Background: Natural and Modified Uranium Subsurface Mobility 2.1

2.1 Uranium Mobility in the Hanford Site Vadose Zone 2.1

2.2 Description and Assessment of Candidate Technologies 2.3

2.2.1 Redox Manipulation by H_2S, SO_2 Gas, or ZVI Injection 2.3

2.2.2 Manipulation of pH by CO_2 or NH_3 Gas Injection 2.5

2.2.3 Sequential Redox/pH Manipulation by H_2S or SO_2/NH_3 Gas Injection 2.7

2.2.4 Injection of Organo-PO_4 Reactive Gas to Form Autunite 2.7

2.2.5 Air and Nitrogen Injection for Emplacement of Reactive Solids and Liquids 2.8

2.2.6 Redox/pH Manipulation by Sodium Dithionite Injection 2.9

2.2.7 U(VI)/Fe(III) Coprecipitation by Fe(III) Nitrate Air Injection 2.9

2.2.8 Autunite Precipitation by Phosphate Injection 2.9

2.2.9 Precipitation of Uranium-Vanadate Minerals 2.10

2.3 Selection of Technologies for Laboratory Testing 2.10

3.0 Experimental and Modeling Approach 3.1

3.1 Uranium Sequestration by Treated Sediments 3.1

3.2 Characterization of Reactive Media for Gas Injections in Columns 3.5

3.3 Technology Selection for Larger Scale Studies 3.5

3.4 Electron Microprobe Analysis of Treated Sediments 3.6

3.5 Simulation of Uranium Transport under Field-Scale Conditions 3.8

4.0 Results 4.1

4.1 Uranium Phases in Untreated Sediments 4.1

4.2 H_2S Reactive Gas Treatment of Sediment 4.3

4.3 SO_2 Reactive Gas Treatment of Sediment 4.6

4.4 CO_2 Reactive Gas Treatment of Sediment 4.8

4.5 HCl Liquid Mist Treatment of Sediment 4.10

4.6 NH_3 Gas Treatment of Sediment 4.13

4.7 NaOH Liquid Mist Treatment of Sediment 4.16

4.8 Ferric Nitrate Liquid Mist Treatment of Sediment 4.17

4.9 Phosphate Treatment of Sediment by Mist Injection 4.20

4.10 Phosphate Treatment of Sediment by Foam Injection 4.23

5.0 Discussion 5.1
5.1 Short-Term Geochemical Performance: Change in Uranium Mobility 5.1
5.2 Short-Term Performance: Evaluation of Injection Technology 5.5
5.3 Long-Term Predicted Performance – Simulation of Uranium Transport 5.7
6.0 Summary and Conclusions 6.1
6.1 Technology Influence on Sediment and Uranium Geochemistry 6.1
6.2 Comparison of Technologies and Potential for Field-Scale Use 6.4
7.0 References 7.1
Appendix – Uranium Sequential Extraction Data A.1

Figures

Figure 2.1 Aqueous U(VI) speciation in the presence of Ca, Mg, CO_3, and PO_4 ..... 2.1

Figure 2.2 U(VI) species adsorption to minerals and sediments, and b) change in adsorption with increasing carbonate concentration 2.2

Figure 2.3 U(VI) species reduction and precipitation in batch systems, and oxidation of the reduced sediment/water system after specified reduction time 2.4

Figure 2.4 Remobilization of TcO_2 by oxidation from dithionite-reduced sediment, and NaOH-treated sediment 2.7

Figure 2.5 Abiotic degradation of TEP; abiotic degradation of DMMP; and biodegradation of TEP in Hanford Site groundwater microbial colony 2.8

Figure 3.1 One-dimensional water-saturated column breakthrough of uranium after 1 week, 1 month, or 1 year of ^{233}U-sediment aging: total uranium breakthrough, and ^{233}U breakthrough 3.4

Figure 3.2 Uranium in boltwoodite 3.6

Figure 3.3 Scanning electron microprobe image of a sediment thin section containing 0.033 mg apatite/g sediment 3.7

Figure 3.4 Mineral phase identification of a location with high phosphorous concentration; electron backscatter of the location is indicative of a surface precipitate, with identification of this mineral as apatite by comparison to an spatite standard 3.8

Figure 3.5 Strontium substitution with depth in apatite precipitate with conglomerate morphology, and high magnification image of apatite 3.8

Figure 3.6 ^{238}U concentration profile for initial conditions in STOMP and the corresponding reported inventory 3.9

Figure 4.1 Fraction uranium in different surface phases for the three sediments 4.2

Figure 4.2 Changes in uranium surface phases for H_2S treatment of sediments 2 and 3 ..... 4.4

Figure 4.3 H_2S or SO_2 gas treatment and change in sediment redox potential, and pH 4.5

Figure 4.4 Oxidation of H_2S-treated sediment column with air-saturated water 4.5

Figure 4.5 Changes in uranium surface phases for SO_2 treatment of sediments 2 and 3 ..... 4.7

Figure 4.6 Oxidation of SO_2-treated sediment column with air-saturated water 4.7

Figure 4.7 CO_2 treatment of sediment and resulting pH relative to water content, and natural pH neutralization over time 4.8

Figure 4.8 Changes in uranium surface phases for CO_2 treatment of sediment 2, sediment 3, and sediment 3 at 15% water content 4.10

Figure 4.9 Mist injection into 160-cm-long column, and 620-cm-long column, showing the final water content 4.11

Figure 4.10 Spatial variability in pH over column length for HCl mist injection, and HCl mist followed by NaOH mist injection 4.12

Figure 4.11 Changes in uranium surface phases for HCl mist treatment of sediment 3 ..... 4.13

Figure 4.12 Ammonia gas treatment of sediment showing pH variability with different initial water content, and over time with 7% initial water content 4.14

Figure 4.13 Ammonia gas treatment of sediment showing uranium surface phase changes over time for sediment 2, sediment 3 at 5% water content, and sediment 3 at 15% water content 4.15
Figure 4.14 Sequential mist injection of 0.5M NaOH followed by mist injection of 0.5M HCl after 1 month 4.17
Figure 4.15 Sequential mist injection of ferric nitrate at pH 1.3 followed by mist injection of 0.5M NaOH after 1 week 4.17
Figure 4.16 Ferric and ferrous iron from a 0.5M HCl extraction of the ferric nitrate mist-treated sediment 4.18
Figure 4.17 Ferric iron mist treatment of sediment 2 and sediment 3 ..... 4.19
Figure 4.18 Phosphate injection as a 0.1% mist into a 160-cm-long column showing the resulting water content distribution and phosphate distribution 4.20
Figure 4.19 Phosphate injection as a 0.1% liquid mist and uranium surface phase changes for sediment 1, sediment 2, and sediment 3 ..... 4.22
Figure 4.20 Development of the residual water content halo over time for foam injection in a two-dimensional system 4.23
Figure 4.21 Foam injection with PO_4 into unsaturated one-dimensional columns with 50 mM PO_4 ..... 4.24
Figure 4.22 Foam with 250 mM PO_4 injection into a 150-cm-long sediment column: foam advance and pressure increase over time, O_2 breakthrough, moisture profile, electrical conductivity profile of pore water, phosphate profile of pore water, and surfactant profile of pore water 4.25
Figure 4.23 Pressure profile in 160-cm column 4.26
Figure 4.24 Phosphate treatment of sediments by foam/surfactant delivery with changes in uranium surface phases shown for sediment 1, sediment 2, and sediment 3 ..... 4.27
Figure 5.1 Sediment 3 treatment by NH_3 gas at 5% water content, NH_3 gas at 15% water content, NaOH mist, CO_2 gas at 5% water content, CO_2 gas at 15% water content, HCl mist, ferric iron mist, H_2S gas, SO_2 gas, PO_4 mist, and PO_4 foam 5.3
Figure 5.2. Sediment 2 treatment by NH_3 gas, CO_2 gas, H_2S gas, PO_4 mist, PO_4 foam, SO_2 gas, and ferric iron mist 5.4
Figure 5.3 Simulation of downward uranium migration in the vadose zone for the untreated sediment 5.8
Figure 5.4 Simulation of uranium downward migration for the untreated sediment case directly beneath initial uranium inventory 5.9
Figure 5.5 Simulation of uranium downward migration for the untreated sediment case at 10 ft above the water table 5.11
Figure 5.6 Conceptual diagram of uranium aqueous concentration at the water table 5.12
Figure 5.7 Simulation of uranium downward migration for all treatments at 10 ft above the water table from only the fraction of uranium that was adsorbed 5.12
Figure 5.8 Simulation of uranium downward migration for all treatments at 10 ft above the water table 5.13

Tables

Table 2.1 Summary of Advection, Reaction, and Scale-Up Issues for Proposed Technologies 2.12
Table 3.1 Uranium-Contaminated Sediments used in this Study 3.1
Table 3.2 Sediment Grain Size and Mineralogy Characterization 3.2
Table 3.3 Post-Treatment and Analysis of Uranium Mobility Change 3.3
Table 3.4 Samples for Uranium-Mineral Phase Identification by Electron Microbe Analysis 3.6
Table 3.5 Geochemical Parameters Used in One-Dimensional Infiltration Simulations 3.10
Table 4.1 Results of Sequential Liquid Extractions of Uranium Phases for Untreated Sediment 4.2
Table 4.2 Results of Sequential Liquid Extractions of Uranium Phases for H_2S-Treated Sediment 4.4
Table 4.3 Results of Sequential Liquid Extractions of Uranium Phases for SO_2-Treated Sediment 4.6
Table 4.4 Results of Sequential Liquid Extractions of Uranium Phases for CO_2-Treated Sediment 4.9
Table 4.5 Results of Sequential Liquid Extractions of Uranium Phases for HCl-Mist-Treated Sediment 4.12
Table 4.6 Results of Sequential Liquid Extractions of Uranium Phases for NH_3-Treated Sediment 4.14
Table 4.7 Results of Sequential Liquid Extractions of Uranium Phases for NaOH-Treated Sediment 4.16
Table 4.8 Results of Sequential Liquid Extractions of Uranium Phases for Fe^{III} Mist-Treated Sediment 4.19
Table 4.9 Results of Sequential Liquid Extractions of Uranium Phases for PO_4 Mist-Treated Sediment 4.21
Table 4.10 Results of Sequential Liquid Extractions of Uranium Phases for PO_4 Foam-Treated Sediment 4.27
Table 5.1 Sediment Treatment and Change in Uranium Surface Phases by 3 Months 5.2
Table 6.1 Comparison of Technologies for Decreasing Uranium Mobility 6.5

1.0 Introduction

The *Deep Vadose Zone Treatability Test Plan for the Hanford Central Plateau* (DOE/RL 2008) provides a strategy and framework for evaluating specific vadose zone remediation technologies. To effectively conduct the evaluation, the report includes a comprehensive set of laboratory, modeling, and field tests. Testing of reactive gas technology is one component of the overall treatability test plan, with an initial emphasis on uranium contamination. As discussed in the treatability test plan (DOE/RL 2008), there are several potential technologies for vadose zone treatment of uranium. In previous studies associated with evaluating technologies for application to the 200 Area vadose zone at the Hanford Site, technologies requiring the addition of significant amounts of water to the vadose zone were less preferred because of the potential for inducing uncontrolled migration of contaminants, and difficulties in controlling how added water moves through the vadose zone. Thus, treatability testing efforts for uranium are focused on gas-transported reactants.

This experimental plan provides an initial geochemical evaluation of candidate technologies for uranium contamination in the Central Plateau located at the Hanford Site, and a description of the proof-of-principle experiments to be conducted as the initial step in selecting promising uranium treatment technologies for continued treatability testing. These efforts are the first two steps described in the treatability test plan (DOE/RL 2008) for the portion of the treatability test focused on uranium.

1.1 Purpose

The purpose of this investigation is to evaluate the potential for candidate gas-transported reactant technologies to decrease uranium mobility in vadose zone sediments on the Central Plateau. The investigation is focused on assessing the reaction processes for uranium immobilization through geochemical evaluation and proof-of-principle experiments.

1.2 Scope

A range of candidate technologies are identified in the treatability test plan (DOE/RL 2008) and through additional review of current technology information. Some technologies have already been tested at a field scale for other contaminants (e.g., H_2S, air injection of zero valent iron [ZVI]), whereas other technologies are currently in the developmental stage in laboratory experiments. The technologies evaluated include reactive gases, gas advection to deliver reactive solids (a technology currently used to deliver ZVI at field scale), and advection of air with small amounts of water, and/or water and a surfactant to deliver reactive solids or liquids to the vadose zone. For each of the technologies, the changes in uranium mobility in the sediment were evaluated based on current knowledge of the reaction mechanism and through proof-of-principle experiments as appropriate.

Specific technologies being evaluated include the following:

- **Reactive gas injection**
  - Inject hydrogen sulfide (H_2S or in situ gaseous reduction [ISGR]) gas into the vadose zone to reduce ferric oxides, which will reduce U(VI) carbonate species to $U(IV)O_2$.

- Inject triethyl phosphate (TEP) and dimethylmethylphosphonate (DMMP) gas phase of phosphate into vadose zone sediments to form the uranium-phosphate mineral autunite.
- Inject carbon dioxide gas to lower the pH to dissolve carbonates, then raise the pH to reprecipitate calcite that could coat adsorbed U(VI) species.
- Inject ammonia gas to increase pH to dissolve silica, then decrease the pH to ambient conditions to precipitate aluminosilicate minerals that could coat U(VI) carbonates.
- Inject sequential H_2S/NH_3 gas to reduce U(VI) species (H_2S), then effect some aluminosilicate dissolution/precipitation (alkaline, NH_3) to coat the $U(IV)O_2$.

- **Gas injection to deliver reactants**
  - Inject N_2 (nitrogen) gas of micron-size ZVI or sulfur modified iron (SMI, Fe^o, S^o) into vadose zone sediments, which will reduce U(VI) species to $U(IV)O_2$.
  - Inject N_2 gas (1% water) of sodium dithionite/sodium carbonate (pH 12) to reduce U(VI) phases, and cause aluminosilicate dissolution. Upon return to near-neutral pH, aluminosilicate precipitation will coat the UO_2, resulting in a more permanent immobilization.
  - Inject N_2 gas (1% water) of ferric nitrate to precipitate ferric oxides that co-precipitate U(VI) in the iron oxide structure.
  - Inject air (1% water) of a sodium phosphate mixture into vadose zone sediments to form the uranium-phosphate mineral autunite.
- **Air, surfactant, and water (foam) injection to deliver reactive liquids or solids**
  - Foam (99% gas, 1% water) injection of a liquid containing sodium phosphate and sodium tripolyphosphate to form uranium-phosphate mineral autunite.

2.0 Background: Natural and Modified Uranium Subsurface Mobility

The following sections provide a review of uranium geochemistry relevant to the Hanford Site Central Plateau vadose zone and a description and geochemical assessment of each candidate technology.

2.1 Uranium Mobility in the Hanford Site Vadose Zone

Uranium occurs naturally in the Hanford Site vadose zone sediments and is also present from uranium enrichment processes (surface and subsurface discharges). Natural minerals that contain uranium include betafite C [$Ca_{0.92}U_{1.08}(Ti_2O_7)$], most likely from granitic clasts commonly found in Hanford Site sediments (15% to 35% [Zachara et al. 2007]). Uranium(IV) generally forms insoluble mineral phases, such as uraninite [$UO_{2(s)}$]. Uranium(VI) often exists in species with higher solubility such as Na-boltwoodite [$(Na, K)(UO_2)(SiO_3OH)(H_2O)_{1.5}$], uranophane [$Ca(UO_2)_2(SiO_3OH)_2(H_2O)_5$], soddyite [$(UO_2)_2SiO_4(H_2O)_2$], schoepite [$(UO_2)_8O_2(OH)_{12}(H_2O)_{12}$], and rutherfordine [$UO_2CO_3$] (Finch and Murakami 1999; Liu et al. 2004). Uranium and plutonium enrichment processes at the Hanford Site have resulted in the release of 202,703 kg of uranium to the ground surface (Simpson et al. 2006) in a variety of aqueous solutions (acidic, basic, with organic complexants [citrate, ethylenediaminetetraacetic acid]) and inorganic ligands (CO_3, PO_4), which would influence the uranium migration behavior. Uranium contamination in shallow 200 Area sediments at the Hanford Site has been found as a uranium-silicate (Na-boltwoodite; Liu et al. 2004) and as uranium-calcite coprecipitates (Um et al. 2009). Deeper 200 Area sediments show predominantly natural uranium sorbed to silt- and clay-size fractions and calcite.

Uranium sorption to sediment is highly dependent on pH and carbonate concentration. At the Hanford Site, subsurface pH is 7.5–8.0 in carbonate-saturated groundwater, U^{+6} species present are primarily $Ca_2UO_2(CO_3)_3$ (aq), $CaUO_2(CO_3)_3^{2-}$ (and to a lesser extent Mg equivalent phases), with smaller concentrations of $(UO_2)_2CO_3(OH)_3^-$ and $UO_2(CO_3)_2^{2-}$ (Figure 2.1). U(VI)-carbonate anionic species (and not Ca-U-CO_3 species) would dominate the mid-pH region in low Ca/Mg systems. The Ca-U-CO_3 species are the predominant species in the Hanford Site natural subsurface, caused by the water being saturated and over-saturated in Ca/Mg-CO_3. Uranium migration in the 300 Area sediments is generally from the 21% to 76% fraction of uranium (average percent [Zachara et al. 2007]) that is sorbed (neutral to negatively charged complexes; see Figure 2.1) to sediments and not incorporated into mineral phases. Note also that although adsorption of uranium is

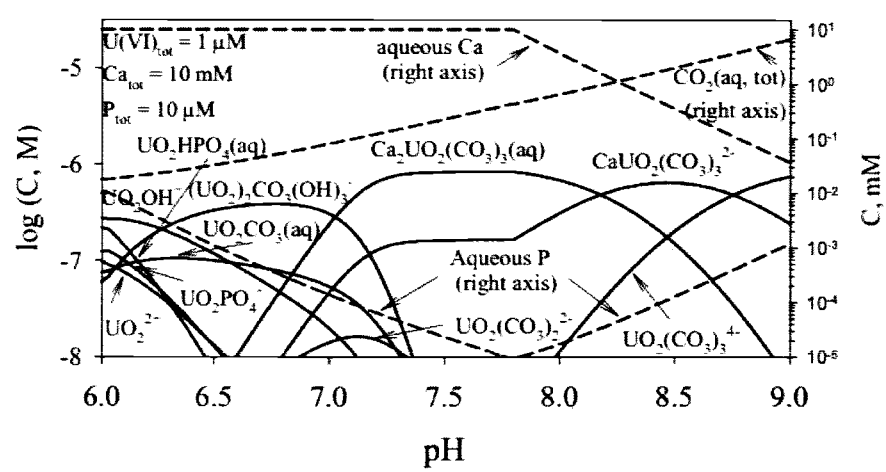

Figure 2.1. Aqueous U(VI) speciation in the presence of Ca (10 mM), Mg (10 mM), CO_3, and PO_4 (Zachara et al. 2007).

assumed to be reversible, additional uranium-mineral phase interactions occur over time that more strongly retain U(VI) species. The mechanisms include stronger adsorption, precipitation, and diffusion of uranium phases into sediment microfractures. Therefore, specific leaching experiments are used in this study to determine the change in uranium mobility that occurs from the presence of the reactive phases emplaced by gas phase advection. These solutions include a 1M $Mg(NO_3)_2$ solution to ion exchange of adsorbed U(VI) species, a high carbonate concentration solution (pH 9.3) to further remove adsorbed and some carbonate-bound precipitates, and an acetic acid solution (pH 2.3) to dissolve some uranium precipitates.

The operationally defined U(VI) sorption K_d in 300 Area sediments averages 0.8 mL/g (range 0.2 to 4.0 [Zachara et al. 2007]), with K_d <0.2 for Ringold Formation gravels and K_d 1.8 to 4.2 mL/g for the Ringold lower mud. The desorption K_d values are higher due to sorption not being completely reversible. For 300 Area sediments, the uranium desorption K_d averages 8.04 ± 8.26 (n = 17 [Zachara et al. 2007]) for <2-mm size fraction, in groundwater. Uranium contamination in 200 Area sediments beneath the BX Tank Farm appears to be mainly in the form of Na-boltwoodite and/or uranophane (Liu et al. 2004) with little adsorbed U(VI) carbonates. The uranium precipitates are somewhat soluble, so introduction of water slowly leaches uranium from these precipitates located in intragranular pore space.

With no change in the groundwater chemistry, U(VI) sorption is fairly linear over a range of uranium concentration up to 1 mg/L. The U(VI) species sorption is generally observed to be anionic (increasing sorption with lower pH) in the weakly alkaline Hanford Site sediments (pH 7–9; see Figure 2.2a), which is also representative of U(VI) species adsorption to major mineral phases (ferrihydrite, kaolinite, and quartz; see Figure 2.2a). Under acidic conditions (pH 3 to 6), U(VI) speciation changes considerably (Figure 2.1) and exhibits cationic behavior (increasing sorption with higher pH, Figure 2.2a). Although relevant in subsurface sediments from an acidic waste stream, the carbonate-laden sediment buffers the pH so long-term U(VI) species migration is generally at neutral to slightly alkaline pH.

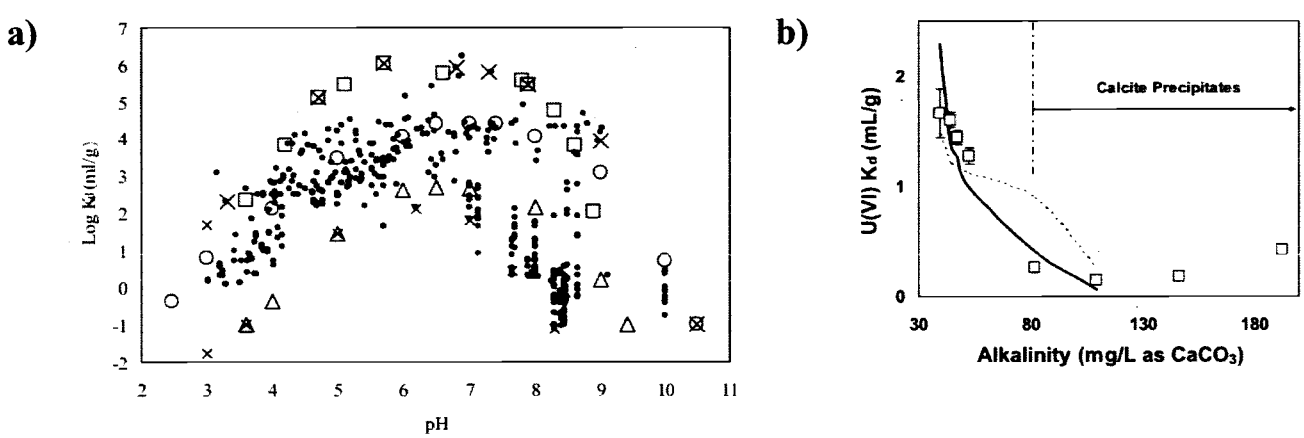

Figure 2.2. a) U(VI) species adsorption to minerals and sediments, and b) change in adsorption with increasing carbonate concentration (Zachara et al. 2007). In (a), data are for sediments (dots), ferrihydrite (open squares), kaolinite (open circles), quartz (open triangles [Waite et al. 1994]), and minimum and maximums (X) given over the pH range.

An increase in ionic strength greater than groundwater would lead to some U(VI) species desorption due to competition for adsorption sites. Because most U(VI) aqueous species are carbonate complexes (Figure 2.1), the subsurface aqueous carbonate concentration has a significant influence on U(VI) sorption (Figure 2.2b), with lower carbonate concentration (i.e., Columbia River water) resulting in much greater U(VI) sorption.

2.2 Description and Assessment of Candidate Technologies

Candidate technologies are evaluated in the following sections and grouped based on the type of reaction or geochemical manipulation.

2.2.1 Redox Manipulation by H_2S, SO_2 Gas, or ZVI Injection

Creation of a subsurface reducing environment results in the reduction of U(VI) phases to U(IV), which typically precipitates rapidly as $U(IV)O_2$ (Figure 2.3a). In the study depicted in Figure 2.3, the initial 10 ppb (4.2E-8 mol/L, squares) uranium in solution decreases due to reduction/precipitation within 1 h. For the treatability test, hydrogen sulfide gas injection, air injection of ZVI, and air injection of sulfur-modified iron depend on this reductive immobilization to occur. While this process is somewhat useful in water-saturated sediments as reducing conditions can be maintained for some period of time, when the reduced zone oxidizes, nearly all of the $U(IV)O_2$ oxidizes and is remobilized (Figure 2.3b). The introduction of sulfur may also lead to some uranium-sulfate precipitates. There is some resistance to oxidation/mobilization due to UO_2-sediment aging (i.e., slightly slower remobilization rate for aged system).

This temporary immobilization of uranium only during reducing conditions likely indicates this process is of limited value in unsaturated sediments if reduction is the only process involved. Reductive immobilization and subsequent remobilization after system oxidation is illustrated in a one-dimensional saturated column containing Hanford sediment that was initially chemically reduced with sodium dithionite (Szecsody et al. 1998). Injection of groundwater levels of U(VI) (10 ppb) and chromate (2.5 mg/L) in oxygen-saturated water results in reduction and precipitation of $U(IV)O_2$ and $Cr(OH)_3$ as long as the system remained reduced (0 to 1000 h, 0 to 500 pore volumes) at a sufficiently rapid rate that no chromium or uranium is initially in the effluent. As the sediment reduced iron phases are oxidized by dissolved oxygen (and the higher concentration of chromate) at 1000–2000 h (500 to 900 pore volumes), there is no longer uranium or chromate reduction. For uranium, 97.8% of the injected mass is remobilized, whereas none of the reduced chromium is remobilized. No further redox reactivity is observed after the system is completely oxidized (2000 to 4000 h). In the vadose zone, the predicted barrier lifetime in the vadose zone for H_2S reduced sediment was estimated to range from a few years to more than 100 years (Thornton et al. 2007).

ISGR treatment of vadose zone reduces sediments with diluted hydrogen sulfide (H_2S) (Thornton and Amonette 1999; Thornton 2000) provides a possible means for immobilization of uranium(VI) in a vadose zone environment. This technology uses low concentration (~200 ppm v/v) H_2S gas as a reductant for immobilization of contaminants that show substantially lower mobility in their reduced oxidation states. It is conceivable that the ISGR approach can be used in two ways: 1) to immobilize or stabilize pre-existing contaminants in the vadose zone by direct H_2S treatment; or 2) to create a permeable reactive barrier in which a gaseous mixture of H_2S diluted in nitrogen or air is passed through an interval in the

vadose zone to produce a volume of reduced sediment. The reduced phases (which contained ferrous oxyhydroxides and ferrous sulfide) would form a permeable reactive barrier that could immobilize possible future releases of contaminants from surface facilities or waste sites, such as during the process of waste tank decommissioning at the Hanford Site.

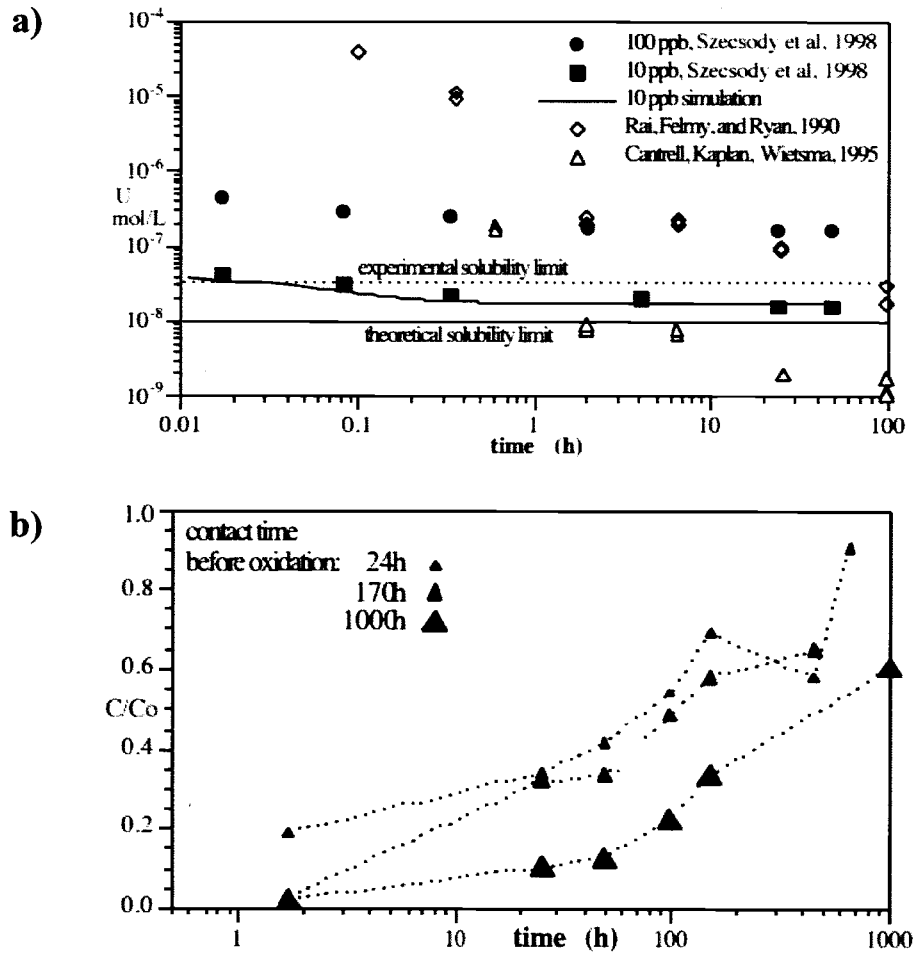

Figure 2.3. a) U(VI) species reduction and precipitation in batch systems, and b) oxidation of the reduced sediment/water system after specified reduction time (Szecsody et al. 1998).

The general reaction for H_2S with ferric hydroxide and ferric oxides, in the absence of oxygen, can be expressed as shown in Equation (2.1) (Cantrell et al. 2003; Davydov et al. 1998):

$$2Fe(OH)_3(s) + 3H_2S(g) \rightarrow 2FeS(s) + 1/8S_8(s) + 6H_2O \qquad (2.1)$$

For uranium immobilization, the ferrous iron generated in the treatment zone can act as the reductive reagent to reduce U(VI) to U(IV) when uranium contaminated water infiltrates through the zone. Reductive immobilization of U(VI) by ferrous iron has been observed by several groups of researchers (e.g., Charlet et al. 1998; Liger et al. 1999; Livens et al. 2004; Sani et al. 2004; Behrends and van Cappellen 2005). The efficiency and life time of the Permeable Reactive Barrier (PRB) depend on the reductive capacity of the barrier, which is determined by the amount and the phase(s) of iron (hydr)oxides and the H_2S treatment duration. In the vadose zone, although chemical reduction of sediment by H_2S gas

was found to produce about a quarter of the reductive capacity as an aqueous reductant in water-saturated sediments (sodium dithionite [Szecsody et al. 2004]), the predicted barrier lifetime in the vadose zone for H_2S reduced sediment was a few years to more than 100 years (Thornton et al. 2007).

Laboratory-scale experiments were conducted to study the reaction between U(VI) and hydrogen sulfide, and to evaluate the feasibility of using gaseous H_2S to immobilize U(VI) in sediments under vadose zone conditions. No intermediate-scale laboratory tests or field-scale demonstration on the treatment of U(VI) contamination by H_2S gas have been conducted.

In batch studies, the rate of U(VI) reduction by hydrogen sulfide in aqueous systems strongly depended on solution pH and carbonate concentrations (Hua et al. 2006). The reaction stoichiometry could be best represented by $UO_2^{2+} + HS^- = UO_2 + S^o + H^+$. Mobility of U(VI) in H_2S-treated sediments was investigated using laboratory batch and column experiments to assess the potential of applying ISGR for U(VI) immobilization in the vadose zone (Zhong et al. 2007). The study revealed that the gas-treated sediments have the potential for U(VI) immobilization. Addition of moisture to the H_2S-N_2 gas mixture enhanced the uranium immobilization. The primary mechanisms for uranium immobilization included U(VI) sorption to the sediments, reduction of U(VI) to insoluble U(IV), and enhanced adsorption of U(VI) to newly formed iron oxides.

Sulfur dioxide, SO_2, can also be used to reduce and immobilize redox sensitive contaminants in the subsurface and/or wastewater. For example, a common treatment of chromium(VI) [Cr(VI)] in wastewater is the reduction by SO_2 at low pH (Lancy 1954). The reaction rate is pH sensitive. At pH values below pH 4, the reaction is very rapid with half-reaction time less than 1 min; at pH 7, the half-reaction time is about 45 min (Lancy 1954). The effect of pH on the reaction rates has been attributed to the S(IV) species distribution when SO_2 dissolves in water. When SO_2 dissolves in water, it produces sulfurous acid (H_2SO_3), which dissociates to form HSO_3^- and SO_3^{2-}.

A study was conducted to characterize and evaluate the application of SO_2 for vadose zone Cr(VI) remediation (Ahn 2003). Batch tests were used to characterize the stoichiometry and kinetics of Cr(VI) reduction by SO_2 in water and in soil. When tests were conducted in water, the half-reaction time was about 45 min and 16 h for pH 6 and pH 7, respectively. When the reduction was conducted in soil, the reaction was much faster, with half-reaction time less than 2 min. The faster reaction in soil was caused by the lower pH in the soil than in water. The stoichiometry of S(IV) removed to Cr(VI) was almost 2. This ratio was higher than that for reaction in water. It was concluded that this higher value might be caused by S(IV) oxidation by Fe(III) in sediment minerals. No literature is available on the treatment of uranium contamination by sulfur dioxide gas.

2.2.2 Manipulation of pH by CO_2 or NH_3 Gas Injection

Although changing the pH may be useful to dissolve and reprecipitate a mineral phase to coat adsorbed U(VI) species, a change in pH from natural Hanford Site groundwater conditions (pH equals 8) to either acidic or more alkaline conditions would greatly increase U(VI) species mobility (Figure 2.2a). This effect would be a problem in a groundwater system with relatively high advection (centimeters to tens of centimeters per day), but would not likely be significant as a short-term transient effect on uranium mobilization in the vadose zone because of extremely low advection rates of water. The use of reactive gases, such as CO_2 and NH_3, to manipulate the geochemical conditions by altering the pore-water chemistry through altering of the pH can have a profound effect on a number of different processes that

influence contaminant migration. These include chemical speciation, solubility, adsorption, desorption, precipitation, and dissolution. Furthermore, the aforementioned processes are also influenced by the rate and extent of key reactions and the length-scale (e.g., micro- versus macro-environment) at which these reactions occur. For example, changes in pore-water pH can have a profound effect on many of the dominant soil minerals present in the Hanford Site vadose zone such as calcite, feldspar, iron-oxides, and quartz. Dissolution experiments conducted by Chou and Wollast (1984) illustrate the rate of feldspar dissolution has been shown to increase by two to three orders of magnitude with an increase in pH from 8 to 12 at 23°C. A review of the open literature has not provided any additional details on the viability of using pH manipulation by CO_2 or NH_3 gas injection; therefore, this review focuses more generally on the impact of pH changes.

A decrease in Hanford Site sediment pH to acidic conditions would result in a number of geochemical changes that include increased carbonate dissolution, mobilization of cations, and less adsorption of U(VI) species (Figure 2.2a). The injection of CO_2 gas (proposed by E. Dresel, PNNL) may lead to mildly acidic conditions (pH 4 to 6), depending on the CO_2 concentration, which could cause some dissolution of carbonate minerals, although this aqueous dissolution reaction would likely be significantly more limited at low water content. A subsequent increase in pH (by air or N_2 injection) could lead to carbonate mineral precipitation that could coat $U(IV)O_2$ precipitates and possibly adsorbed U(VI) species. In water-saturated systems, advection of aqueous complexes in the porous media redistributes reactant mass, so carbonates dissolved in one location can coat surface phases in another location. At low-water saturation, the very slow advection of water near surfaces will result in significantly less redistribution of reactants (i.e., more difficulty in carbonate precipitates coating other phases without a mechanism for redistribution). Carbonate coatings on mineral phases have been previously observed to influence U(VI) adsorption (Dong et al. 2005). The slow timescale for carbonate dissolution/precipitation of weeks or longer (although pH dependent [McKinley et al. 2007]) may be of concern.

Alternatively, increasing the pH to affect dissolution of mineral phases by the injection of ammonia gas (proposed by N. Qafoku, PNNL) could lead to mineral phase dissolution of silica and aluminum (and other metals). Advection in the limited aqueous solution at low-water content would be much more limited than in water-saturated systems. The subsequent decrease in pH to natural conditions (~pH 8) would lead to precipitation of aluminosilicates, which could potentially coat adsorbed U(VI) species. The increase in pH and aluminosilicate precipitation has been previously observed in aqueous Hanford Site sediment under highly alkaline conditions (pH 14, 4M NaOH) and is somewhat effective for technetium immobilization. In that study, injection of a high-NaOH solution through sediments caused the dissolution of several mineral phases as evidenced by aqueous silica, aluminum, and iron effluent concentrations. There was significant mobilized silica (up to 10 g/L). The released ferrous iron was sufficient to reduce the pertechnetate ($Tc(VII)O_4^-$) to $Tc(IV)O_2$, which precipitated in the system. As the pH was subsequently reduced to natural groundwater (pH 8, Figure 2.3b), only 23% of the TcO_2 precipitate was remobilized upon reoxidation. Thus, 77% of the technetium remained immobilized in the oxic environment, presumably by aluminosilicate mineral phase coatings. In contrast, chemical reduction of the same sediment (using sodium dithionite) also immobilized all the injected pertechnetate, but subsequent oxidation (Figure 2.4a) remobilized 98.7% of the pertechnetate (Szecsody et al. 2001). In these tests, the chemical reduction of sediment and pertechnetate (Figure 2.4a) initially showed no mobilization of technetium as long as the sediment remained reduced, but by 300 pore volumes of oxygen-saturated water (230 h), essentially all of the technetium was oxidized to pertechnetate and

remobilized. In contrast, the reduction and aluminosilicate precipitation at high pH (Figure 2.4b) had very little reductive capacity, so the injection of oxygen-saturated water quickly mobilized any reduced

TcO_2 on the surface was not coated in other precipitates (0–20 pore volumes, 0–180 h), but the remaining 77% of mass was not mobilized by further oxidation. The experiment was terminated at 300 h (33 pore volumes) and technetium in the effluent was still below detection limits.

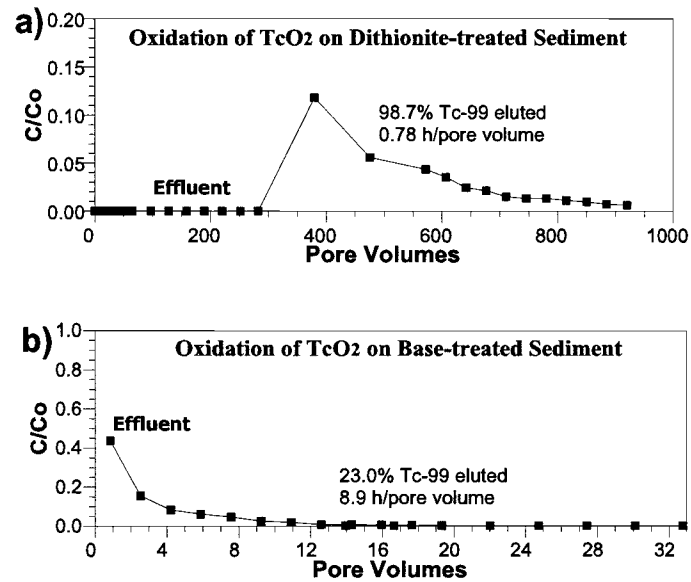

Figure 2.4. a) Remobilization of TcO_2 by oxidation from dithionite-reduced sediment, and b) NaOH-treated sediment.

While this aqueous example involved highly alkaline (pH 14, 4M NaOH) treatment of the sediment, the injection of ammonia gas would produce mildly alkaline conditions. It is unknown whether these mildly alkaline conditions at low-water saturation would affect sufficient pH change to cause some aluminosilicate dissolution. Additionally, in oxic conditions an increase in the system pH would mobilize U(VI) species (Figure 2.2a), but with the very low advection rate of water in vadose zone sediments, this effect would likely not cause any real migration during this process.

2.2.3 Sequential Redox/pH Manipulation by H_2S or SO_2/NH_3 Gas Injection

To enhance the impact of uranium immobilization by a mineral coating, combined use of a reductant and a gas that creates conditions for a mineral coating may be effective. In this process, a gaseous reductant (e.g., H_2S or SO_2) may convert some portion of the uranium to a precipitate that—when followed by NH_3—would then potentially dissolve and then reprecipitate aluminosilicate coatings on the uranium precipitates. There are significant issues to investigate with this approach that include the following: 1) the acidic conditions created by H_2S creates uranium and other metal mobilization in water-saturated systems, which may not be an issue at low-water content with very low-water advection; 2) ammonia gas needs to create sufficiently alkaline conditions to cause some mineral phase dissolution; and 3) stability of the mixed aluminosilicate-U(IV)O2-U(VI) phase. The temporarily immobilized UO_2 should remain as a precipitate if the ammonia gas is introduced without oxygen. At a large scale, this sequential process involves the use of two toxic gasses.

2.2.4 Injection of Organo-PO_4 Reactive Gas to Form Autunite

The formation of a Ca-U-PO_4 mineral phase autunite $[Ca(UO_2)_2(PO_4)_2 \cdot XH_2O]$ by injection of sodium phosphate or polyphosphate mixture into sediment is well established in water-saturated sediment as well

as in unsaturated sediment (Wellman et al. 2006a, 2006b; 2007; 2008a). The injection of low volatility TEP or DMMP as a gas phase into sediments has been previously investigated (Denham and Looney 2007; Rockhold et al. 2008) as a means of introducing inorganic phosphate into subsurface sediments at low water content. In addition, tributyl phosphate (TBP) in water-saturated systems has previously been shown to biodegrade with naturally occurring microbial isolates in sediment, and removing uranium from aqueous solution (Thomas and Macaskie 1996). Researchers leading a small project (funded by the Laboratory Directed Research and Development Program at Pacific Northwest National Laboratory) investigated abiotic and biotic TEP/DMMP degradation to produce PO_4, as well as air advection of the TEP/DMMP vapor. Both TEP and DMMP could be abiotically degraded, but under extreme conditions and only very slowly (half-life of years). TEP and DMMP degradation produced measurable PO_4 in aqueous sediment/water systems at pH > 13, or under reducing conditions (Figure 2.5a, b), or both. TEP and DMMP could also be biotically degraded (Figure 2.5c). However, in all cases, the degradation rate of these compounds was on the order of years (half-life). In addition, attempts to inject TEP and DMMP vapor from elevated temperature liquid sources produced very limited transport (Rockhold et al. 2008). In addition, there may be increased uranium mobility change as a result of the formation of uranium-organic aqueous complexes before complete TEP or DMMP degradation occurs, and the presence of the organic intermediates may interfere with the formation of autunite. These compounds could be injected in liquid form by air with 1% water, as described earlier (but inorganic PO_4 could be injected by the same means). The very slow abiotic and biotic degradation rates of TEP and DMMP make formation of available PO_4 (then autunite) very slow (years), which would not be suitable for the Hanford Site vadose zone. Therefore, these compounds were not investigated further.

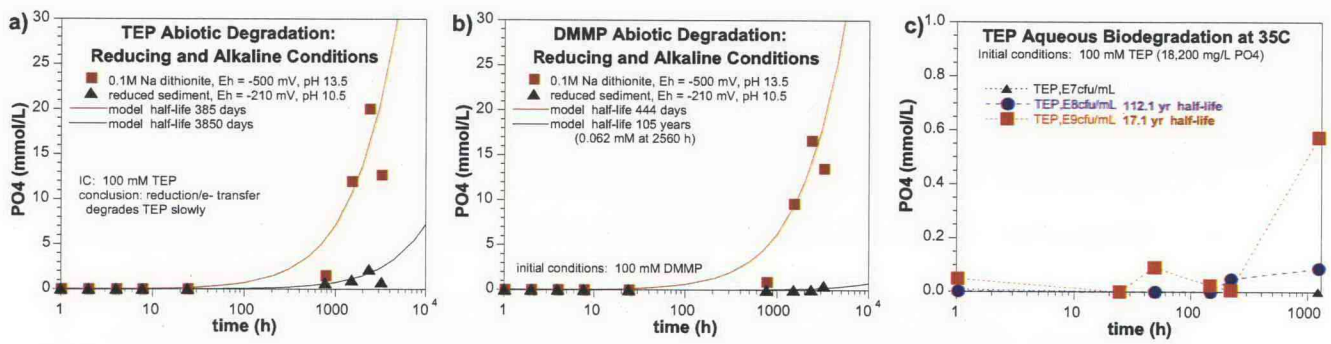

Figure 2.5. a) Abiotic degradation of TEP; b) abiotic degradation of DMMP; and c) biodegradation of TEP in Hanford Site groundwater microbial colony (Rockhold et al. 2008).

2.2.5 Air and Nitrogen Injection for Emplacement of Reactive Solids and Liquids

Air injection has been used for over a decade for emplacement of ZVI (15–70 micron particle size) in the subsurface by ARS Technologies, Inc. and other companies. Typical well injection scheme is 500 to 1500 cubic feet per minute (cfm) air injection with 20–70 gallons per minute (gpm) (2.67–9.35 cfm) ZVI/water slurry, which corresponds to 0.18% to 1.9% water content. This water content is on the same order of magnitude (or lower) than foam injection (about 1% water content). Gas transport of solid media into porous media results in two general patterns; with lower injection pressure and/or a tight formation, a dendritic pattern of fractures forms with fine veins observed up to 40 ft away from the injection well. In contrast, with higher injection pressure and/or a looser formation, the formation is fluidized, and the

injected particles mix with the formation somewhat more homogeneously, which is observed up to 20 ft from the injection well. A typical loading is 2% or less ZVI per gram of sediment. These field experiments have not quantified the distribution of particles with distance from the injection well.

2.2.6 Redox/pH Manipulation by Sodium Dithionite Injection (1% Water)

Sodium dithionite is an effective uranium and iron phase reductant that can be injected under highly alkaline (aqueous) conditions, as demonstrated in laboratory and field scale (Szecsody et al. 2004; Vermeul et al. 2004). Dithionite can be used to reduce and precipitate UO_2, then dissociates to sulfate over a period of days. The carbonate solution can maintain pH at 12, so the solution may affect some silica dissolution over time, as described in Section 2.2.2. These solutions are proposed to be injected in 1% water relative to 99% air. Air with a small mass of water injection has been successfully used at field scale for placement of solid phase ZVI particles.

2.2.7 U(VI)/Fe(III) Coprecipitation by Fe(III) Nitrate Air Injection (1% Water)

Laboratory experiments in water-saturated sediments have demonstrated that a ferric nitrate solution will result in ferric oxide precipitation, which will coprecipitate U(VI) in the iron oxide structure. The injection of ferric nitrate into unsaturated sediments at low water content could be accomplished using 1% water content with primarily air injection. A technology similar to this proposed technology has been somewhat unsuccessfully tested at Fry Canyon, Utah (Naftz et al. 2002). In that study, solid phase Fe(III) oxides were emplaced in a trench, forming a PRB that would presumably adsorb U(VI) phases, with subsequent dissolution of some of the iron oxides to reprecipitate as mixed Fe-U(VI) oxides.

2.2.8 Autunite Precipitation by Phosphate Injection (Mist and Foam-Delivered)

As described earlier, the formation of autunite [$Ca(UO_2)_2(PO_4)_2 \cdot XH_2O$] by injection of sodium phosphate or polyphosphate mixture into sediment is well established in water-saturated sediment as well as in unsaturated sediment (Wellman et al. 2006a, 2006b; 2007, 2008a). To date, a polyphosphate mixture (i.e., mixture of ortho-, pyro-, and tripolyphosphate) has been injected at field scale in the Hanford Site 300 Area aquifer to sequester U(VI) species. At the laboratory scale, a modified mixture of polyphosphate has been infiltrated into unsaturated sediments at high water content and low water content to sequester U(VI) species. Low water content transport experiments were conducted in a centrifuge using an unsaturated flow apparatus. For the Hanford Site Central Plateau, phosphate could be delivered either through air injection or foam (Zhong et al. 2009a, 2009b) injection. The presence of the surfactant in the foam may cause increased U(VI) mobility. In addition, with this phosphate and organic carbon source injection, the possibility of increased microbial activity must be considered. The mixture of 85% Na_2HPO_4 and 15% NaH_2PO_4 will maintain the pH at 7.5 ± 0.1. Note also that a 3-year field study at Fry Canyon, Utah (Naftz et al. 2002), was conducted comparing the uranium remediation performance of ZVI to bone char pellets (phosphate) to amorphous ferric oxyhydroxide. Both the phosphate and amorphous iron oxide barriers showed weak performance, but the ZVI barrier showed relatively efficient uranium removal. This placement of apatite was intended to adsorb U(VI) species, and is not the same process as proposed here, with precipitation of autunite by injection of aqueous phosphate, which has been shown to be effective in laboratory- and field-scale studies.

Delivery of phosphate or polyphosphate to the deep vadose zone uranium source is a challenge. The use of foam for delivery may provide better control of the volume of fluids injected and the ability to contain the migration of contaminant-laden liquids (Chowdiah et al. 1998). Foam is a shear-thinning non-Newtonian fluid that enables more uniform sweeping over a heterogeneous system when forced through the system. Jeong et al. (2000) and Kovscek and Bertin (2003) reported the injection of a surfactant-foam mixture enhances the flooding efficiency of surfactant flushing in heterogeneous porous medium systems, resulting in better sweeping efficiency over the contamination zone and higher contaminant removal.

Foam application in environmental remediation has been evaluated for nonaqueous phase liquids removal (Kovscek and Bertin 2003; Rothmel et al. 1998; Wang and Mulligan 2004b; Mulligan and Eftekhari 2003; Peters et al. 1994; Enzien et al. 1995; Jeong et al. 2000; Huang and Chang 2000) and heavy metal cleanup (Mulligan and Wang 2006; Wang and Mulligan 2004a) from vadose zones. In these studies, however, the surfactant-foam itself was used as the reactant but not as a delivery means for other remedial amendments.

A study on foam delivery of the amendment calcium polysulfide (CPS) to sediment under vadose zone conditions for Cr(VI) immobilization has been recently completed (Zhong et al. 2009a, 2009b). It was reported that foam flow can effectively deliver CPS to sediments for Cr(VI) immobilization under vadose zone conditions. Sediment reduction by foam-delivered CPS was observed. Minimized Cr(VI) mobilization from the sediment by foam-delivered solution was reported. Immobilization of more than 90% of total Cr(VI) in the sediment was achieved in this study.

2.2.9 Precipitation of Uranium-Vanadate Minerals

The formation of vanadate minerals tyuyamunite ($Ca(UO_2)_2(VO_4)_2 \cdot 5\text{-}8H_2O$) and carnotite ($K_2(UO_2)_2(VO_4)_2 \cdot 3H_2O$) as a remediation technology is reasonable because these minerals are stable in most oxic natural environments. These minerals occur naturally as uranium-mineral deposits. These mineral phases have been investigated in the water-saturated zone (Tokunaga et al. 2009) and may be advantageous due to low solubility (lower than phosphates) and high stability in many natural geochemical environments. The precipitation of these minerals would involve injection of potassium and vanadate (VO_4) under the proper pH conditions. The lowest solubility of these minerals is under somewhat acid conditions (pH 5.0 to 6.5), with significantly higher uranium solubility at pH 8 (Hanford Site groundwater). Therefore, under the slightly alkaline conditions at the Hanford Site, these minerals may not be as stable as phosphates.

2.3 Selection of Technologies for Laboratory Testing

Some of the above-listed technologies have been tested at field scale (ISGR for chromate at White Sands, New Mexico; air injection of ZVI particles at dozens of sites by ARS Technologies, Inc.). Other technologies have been investigated in small to large laboratory-scale experiments (TEP/DMMP gas, foam, or polysulfide). Finally, some technologies are concepts that have not been tested even in the laboratory. Table 2.1 summarizes the evaluation of the candidate technologies to determine whether proof-of-principle laboratory experiments are needed as part of treatability test efforts at the Hanford Site. This evaluation is based on the analysis presented in Sections 2.1 and 2.2, and an assessment of the ability to advect the reactant(s) into vadose zone, reactions with either the sediment or uranium, and applying the technology at the field scale. While Table 2.1 indicates that laboratory experiments will not be conducted

for some technologies as part of the efforts described in this plan, these technologies may still be considered in subsequent evaluations. For instance, ZVI particles were not selected for experimentation because the reaction processes are well known, the particles have been injected in the field at other sites, and remaining issues related to the Hanford Site are best addressed at the field scale. Thus, while ZVI is still a candidate technology, laboratory experiments were not conducted.

As shown in Table 2.1, reactive gas technologies that were investigated included H_2S, SO_2, CO_2, and NH_3, with CO_2 having the best rating of the reactive gases. Injection of CO_2 gas to decrease pH, cause carbonate dissolution, and subsequently raise the pH to cause carbonate precipitation (to result in carbonate coatings on uranium surface phases) is based on a naturally occurring process that may be possible to enhance. A potential problem with CO_2 gas injection processes is lack of reactivity that could result at the very low water content in vadose zone sediments.

In contrast, gas advection of aqueous reactants (as 1% liquid in an injected air or nitrogen stream) would result in a significantly greater reactive mass in the vadose zone, but in a smaller zone around the injection well (relative to reactive gas injection). Injection of sodium phosphate is potentially the best reactant (Table 2.1), as the formation of autunite will likely immobilize uranium from further advection. The use of sodium phosphate (with and without tripolyphosphate [Wellman et al. 2008a]) has been tested at low water content. Unknowns associated with this technology include the distribution of phosphate mass that would result from 99% gas/1% water injection. Advection of sodium phosphate with a surfactant received a lower rating for this treatability test (Table 2.1), because the surfactant (sodium laurel sulfate) may influence the formation of autunite and/or increase uranium mobility. In addition, issues related to aqueous reactant mass advection using a surfactant (pressure buildup, distribution in heterogeneous sediments) need to be resolved.

Gas advection of solid reactants (ZVI, sulfur modified iron, or other nanoparticles) is likely to result in a very high mass of reactant (dendritic pattern or homogeneous) in an even smaller zone around the injection well compared to an air/water or gas injection. However, because reactions are known and the primary issues for reactive solids are related to emplacement, solid reactants were not included in the initial laboratory experiments.

Table 2.1. Summary of Advection, Reaction, and Scale-Up Issues for Proposed Technologies

Technology	Maturity	Advection Issues*	Reaction Issues*	Scale-up Issues*	Rating**	Test in lab?
Reactive gas						
H_2S	tested in field	low concentration, reduction over large area	H_2S-sediment: reduces U(VI) and Fe(III) phases; $U(IV)O_2$ remains immobile only if reduced	safety issues H_2S gas, low reductant mass injected, field tested	9	yes
SO_2	concept	untested, less reactive than H_2S	untested. Likely to have less pH decrease compared to H_2S	safety issues H_2S gas, low reductant mass injected	8	yes
CO_2	concept	none, no retardation, but only advecting a small reactive mass into sediment, need humidity added to CO_2	small reactant mass, ability to change pH in vadose zone at low water content, CO_3 diss./ppt. time scale (weeks), ppt coating of U phases	may need some water addition, gas is inexpensive	12	yes
NH_3	concept	unknown, likely retardation	ability to increase pH sufficiently at low water content, time scale of silicate dissolution (months/years)	safety issues NH_3 gas	8	yes
H_2S, then NH_3	concept	unknown	more complex than individual gas (NH_3 concept untested)	safety issues	5	no
triethyl phosphate (TEP) dimethyl methyl phosphonate (DMMP)	small lab. scale	significant issues due to low vapor pressure	very slow (years) to abiotically or biotically degrade, might form autunite	long time scale for degradation, very small advection radius	3	no
Gas advection (+0.1 to 1% H_2O)						
dithionite/CO_3	aqueous tested in field	smaller transport radius than gas, more than solid injection	stronger reductant than H_2S, immobile only if reduced (weeks-years)	high reactant mass injected, % water added, radius of reactivity	8	no
Fe(III)NO_3	small lab. scale	smaller transport radius than gas, more than solid injection, may clog pore space	depends on forming $(U/Fe)O_3$ coprecipitate, moderate longevity	high reactant mass injected, % water added, radius of reactivity, pore clogging	10	yes
Na_2HPO_4	aq. tested in field, low water content tested in lab	smaller transport radius than gas, more than solid injection	tested, relatively simple geochemistry, forms autunite	% water added, radius of reactivity low	13	yes
zero valent iron (zvi) or sulfur modified iron (smi)	tested in field	<3% (high mass) into a small (10 ft) radius	retains some reduction reactivity even when sediment system is oxic, reduced U(IV)-S phases may be more difficult to oxidize than $U(IV)O_2$	% water added, small radius of reactivity	6	no
specialized nanoparticles (e.g., SAMMS)	ex-situ field tested	<3% (high mass) into a small (10 ft) radius	can be tailored for uranium sequestration	% water added, small radius of reactivity	7	no
foam advection (+1% H_2O)						
Na_2HPO_4	2-D large lab. scale tested	moves low mass of PO_4 very slowly into sediment (adsorption), elevated pressure, mainly in high-K	might form autunite (does w/o surfactant), but influence of surfactant unknown (U mobilization)	% water + surfactant added, radius of reactivity, surfactant residue	9	yes

*Scale of 1• (low) to 5• (high, positive) rating of technology in category. Advection rated based on radius of influence and mass delivered per volume. Reaction rated based on reaction with uranium, complexity of reaction, probability of occurring, longevity of uranium immobilization, and dependence on sediment conditions. Scale-up rated based on difficulty at large scale, radius of likely effectiveness, safety, and secondary effects such as water addition or residues.
**Sum of category ratings (maximum = 15).

3.0 Experimental and Modeling Approach

3.1 Uranium Sequestration by Treated Sediments

Each gas delivery technology was used to dose three to six different uranium-contaminated sediment columns to quantify the efficiency of uranium immobilization, retardation, and longevity. Because of the potential application to the deep vadose zone in the 200 Area of the Hanford Site, four sediment sources were used that exhibit a range of expected behavior in the 200 Area (Table 3.1 sediments provided by Wooyong Um and Jeff Serne, PNNL).

Table 3.1. Uranium-Contaminated Sediments used in this Study

#	Uranium surface phase	Location	Depth (ft)	Sample ID	Formation	U (ug/g)	$CaCO_3$(%)
1	U-silicate: Na-boltwoodite*3	BX-102	131	SO1014-61A*	Hanford	415	–
2	adsorbed U(VI) species	BX-102	152	SO1014-72*	Hanford	~49*2	–
3a	U-calcite coprecipitate*4, 5	TX-104	69.3	C3832-69B	Hanford	18.4	~1.78%*1
3b	ads. U(VI) + U-calcite coppt*4, 5	TX-104	110.3	C3832-110B	Cold Creek	55	ND

*1 1.78% calcite for sample 69A.
*2 40 µg/g for sample 72A.
*3 Liu et al. (2004).
*4 Um et al. (2009).
*5 Wellman et al. (2008b).
*6 Borehole 299-E33-45, Serne et al. (2002, 2008a, 2008b).

Uranium-contaminated shallow sediments from the 200 Area beneath the BX Tank Farm (primarily containing uranium in Na-boltwoodite as shown in Table 3.1) will exhibit slow uranium mobility as this phase slowly dissolves into aqueous solution from intragranular precipitates. Aqueous, adsorbed, and carbonate-associated uranium in Hanford Site sediment are considered mobile or labile phases. Carbonate-associated uranium is the predominant uranium surface phase in deep 200 Area sediments (Table 3.1). In addition, uranium coprecipitated with calcite is found in some shallow sediments (Um et al. 2009). Uranium-contaminated sediments from the Hanford Site 300 Area were not used [mixture of uranium solid phases and adsorbed U(VI) carbonate species] because the precipitate phases are significantly different from those expected in the 200 Area.

The mineralogy in sediments from the BX and TX Tank Farm boreholes were characterized in other studies (Serne et al. 2008a, 2008b). This characterization was conducted in the same BX-102 borehole as sediments 1 and 2 in this study (and similar depth, as shown in Tables 3.1 and 3.2). Characterization was also conducted near where sediments 3a and 3b were collected (near tank TX-104). Mineralogy shown in Table 3.2 from borehole C4105 is between tanks TX-106 and TX-109, so near tank TX-104. The three sediment samples in the Hanford H2 formation were sandy gravels (Table 3.2) and did not vary significantly in major mineralogy or clay mineralogy. The average moisture content for the Hanford H2 formation was 6.3% (2.8% to 13% range), with 1.5% calcite and total uranium (by 8M HNO_3) of 0.5 to 2.5 µg/g (uncontaminated sediment). In contrast, the fine-grained Cold Creek formation sample contained significant calcite (55%), but the clay mineralogy was similar to the Hanford formation samples. The Cold Creek formation had an average moisture content of 14.2% (range 13% to 23%) and total uranium of 3.3 µg/g. The calcite content in the Cold Creek formation varies considerably with depth. In this study, the calcite content of the mixture of sediments 3a and 3b should average ~1% (Table 3.2), so other than this calcite content, the higher clay content of the Cold Creek and Hanford

formation sediments at the TX Tank Farm (8% to 10%, compared to 2.5% to 5.5%) could result in higher reactivity for sediment 3 compared to sediments 1 and 2.

Table 3.2. Sediment Grain Size and Mineralogy Characterization

			Grain Size			Mineralogy (< 2 mm)							Clays (< 60 um)			
Sample Locatio	Depth (ft)	Formation	gravel, sand (%)	silt (%)	clay (%)	quartz	plagioclase	mica	K-feldspar	amphibole	chlorite	calcite	illite	smectite	chlorite	kaolinite
E33-45, BX-102	120	Hanford	87	7.5	5.5	34	27	17	13	6	4		55	24	14	7
E33-45, BX-102	151.5	Hanford	95.5	2	2.5	28	33	19	14	2	5		47	28	20	5
C4105, TX-106	61	Hanford	63.5	29	8	34	39		15	2		1	47	26	20	7
C4105, TX-106	92	Cold Creek	11	79	10	11	18			7		55	50	35	10	5

Data from Serne et al. (2008a, 2008b).

The objective of this task is to demonstrate a change in the total uranium mobility as a result of the treatment. Although the intended effect of each technology is to reduce uranium mobility, in some cases there may be increased uranium at short timescales before steps of the treatment have been completed; e.g., precipitation of mineral phases that may coat adsorbed U(VI) phases. For these studies, it is not the intention to optimize delivery of reactive phases to the sediment column, but to evaluate under ideal conditions whether the technology can result in a decrease in uranium mobility. As such, each gas phase injection technology (H_2S, CO_2, NH_3) was dosed into the sediment column for 1 month. Gas advection technologies ($Fe(III)NO_3$, $Na\text{-}PO_4$) deliver a greater mass of reactant, so were dosed into the sediment column for 1 day. In each case, an attempt was made to characterize the amount of reactive media added to the columns. Because of the long timescale of some of the mineral phase precipitation processes for some technologies, the sediment columns were aged after treatment: 1) 30 days at 22°C, and 2) 60 days at 82°C (Table 3.3).

The elevated temperature was used to accelerate the aging process. It is recognized the elevated temperature crystallize some amorphous iron oxides (and associated uranium phases may be further sequestered [Payne et al. 1994]). A series of control columns were used (no treatment) that were subjected to the same treatment so that any change in uranium mobility was measured. Technologies that rely upon reduction were also evaluated for changes in uranium mobility after system oxidation.

Because these treatment technologies are intended for use on the vadose zone, the technologies were conducted at low water content. Reactive gas technologies (H_2S, CO_2, NH_3) were conducted with an initial water content of 5 wt% (approximate field conditions) and 15 wt% (about half saturation) in separate sets of columns. Higher water content experiments were conducted because some reactions occur in aqueous solution; therefore, the influence of water content on the technology performance was investigated by these two water contents. Gas advection (and surfactant) technologies [$Fe(III)NO_3$, $Na\text{-}PO_4$] use 1% water (in either the air injection or air/surfactant injection); thus, water was introduced and as such the technologies were conducted with an initial water content of 5 wt%.

Table 3.3. Post-Treatment and Analysis of Uranium Mobility Change

Technology	%H_2O	Sed. #	Aging Times: 1 mo 22C	1 mo 22C, oxic 1 mo	2 mo 82C	2 mo 82C, oxic 1 mo	U Sequential Extractions: #1 aq. U*1	#2 ads. U*2	#3 acetate pH 5 *3	#4 acetate pH2.3*4	#5 oxalate *5	#6 8M HNO_3*6	Minerals: Electron Micro-probe
no treatment	5%, 15%	1,2,3	+	+	+	+	+	+	+	+	+	+	+
reactive gas													
H_2S	5%	2, 3	+	+	+	+	+	+	+	+	+	+	+
SO_2	5%	2, 3	+	+	+	+	+	+	+	+	+	+	
CO_2	5%, 15%	2, 3	+		+		+	+	+	+	+	+	+
NH_3	5%, 15%	2, 3	+		+		+	+	+	+	+	+	+
gas advection (0.1% aq.)													
Fe(III)NO_3	5%	2, 3	+		+		+	+	+	+	+	+	+
HCl	5%	3			+		+	+	+	+	+	+	
NaOH	5%	3			+		+	+	+	+	+	+	
Na_2PO_4	5%	1,2,3	+		+		+	+	+	+	+	+	+
foam advection (1% aq.)													
Na_2PO_4	5%	1,2,3	+		+		+	+	+	+	+	+	+

(1) Hanford groundwater, aqueous extraction for 1 h
(2) 1M Mg(NO3)2 pH8, ion exchangable extraction for 1 h
(3) 1M Na-acetate, pH 5 with acetic acid, 1 h
(4) 0.44 mol/L acetic acid, 0.1 mol/L $Ca(NO_3)_2$, pH 2.3, 1 week
(5) 0.1M NH_4-oxalate, 0.1M oxalic acid, 4 h
(6) 8M HNO_3, 95°C, 2 h

The following sequential extraction tests were used to evaluate the change in uranium mobility of the control and treated columns for each aging treatment:

1. Aqueous uranium by addition of Hanford Site groundwater
2. Readily desorbed uranium by 1M Mg-nitrate batch extraction
3. Dissolution of the thin rind of uranium-carbonate precipitate (acetate at pH 5, 1 h)
4. Dissolution of most carbonates (acetic acid, pH 2.3, 1 week)
5. Dissolution of amorphous oxides (0.1M oxalic acid, 0.1 M ammonium oxalate, 4 h)
6. Dissolution of hard-to-extract uranium in oxides, silicates, and phosphates (8M HNO_3, 95°C, 2 h).

Electron microprobe analysis of thin sections of treated sediments that are likely to contain different uranium surface phases or coatings on uranium were also conducted for positive identification of the uranium surface phase changes. With any of the proposed treatments, thin reacted rinds on the solid phase uranium surface phases may occur, leaving the underlying U(VI) phase unaltered, so the change in uranium mobility may be fractional. Note that other studies of Hanford Site 200 Area and 300 Area sediments show that while there is a labile fraction of uranium that is relatively quickly released from the sediment, additional uranium is slowly released from sediment over long timescales (years [Zachara et al. 2007]). After decades of uranium contamination contact with the sediment, some uranium has diffused into sediment microfractures, so the slow release of uranium from sediment is partially controlled by mineral phase solubility (i.e., chemical kinetic control) and partially by slow diffusion out of microfractures (i.e., physical kinetic control; see Figure 3.2).

Total uranium concentration was measured by kinetic phosphorescence analysis and inductively coupled plasma/mass spectrometry (ICP-MS). As illustrated in Figure 2.3b, adsorbed uranium in contact with sediments exhibit stronger attachment with greater contact time due to stronger adsorption binding

and/or some uranium precipitates forming. This process is illustrated with the addition of ^{233}U to sediment at low water content and aging for 1 week, 1 month, or 1 year. There is additional uranium-sediment binding with greater aging, as less ^{233}U mass is eluded with greater aging (Figure 3.1b). Note that the total uranium breakthrough does not show the same effect of aging (Figure 3.1a) because the amount of ^{233}U added is small (3%) relative to the total uranium in the sediment. Several of these technologies depend on mineral phases combining with U(VI) or mineral phases precipitating on top of $U(IV)O_2$ precipitate. Future experiments could use the addition of ^{233}U (and ICP-MS analysis) to clearly understand the retention mechanisms. This technique was not used for this screening study because of the additional cost (i.e., experiments are radioactive).

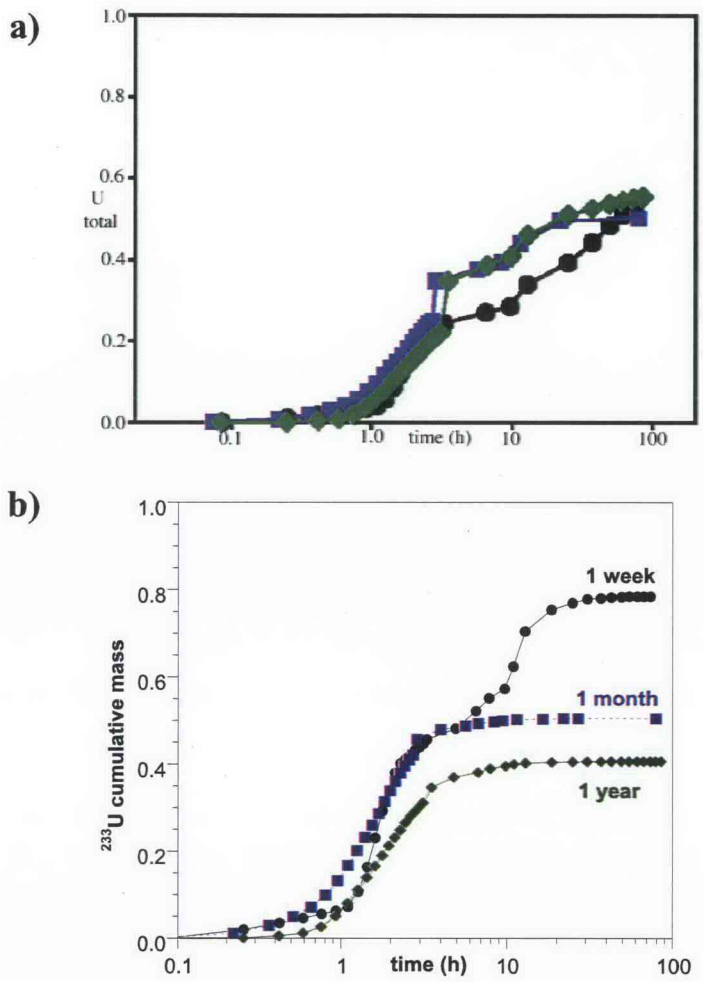

Figure 3.1. One-dimensional water-saturated column breakthrough of uranium after 1 week, 1 month, or 1 year of ^{233}U-sediment aging: a) total uranium breakthrough, and b) ^{233}U breakthrough (Smith and Szecsody 2009).

3.2 Characterization of Reactive Media for Gas Injections in Columns

Given the most ideal conditions for delivery of each gas, liquid, or solid reactive media by predominantly gas phase advection, experiments in this task quantified the amount of reactive media delivered at different distances from the injection location. Stainless steel or PEEK columns 0.2 to 1.0 m in length by 1.9 cm (3/4 in.) diameter were used in the experiments. The porous media conditions evaluated included the following: 1) coarse sand and fine sediment (sand, silt, and clay); and 2) low and moderate water content (2% to 15%). Reductive technology reactive phase delivery was characterized by reductive capacity measurements and redox potential measurements. Reductive capacity measurements consisted of slow oxidation of reduced porous media in a small sediment column using air-saturated water for 2–3 weeks and automated monitoring of oxygen consumption until oxygen was no longer consumed by reduced phases. The reactive phase delivery for phosphate technologies was characterized by acid extraction and analysis of total phosphate of sediment samples. For the foam technology, the change in water content along the column length was also characterized.

3.3 Technology Selection for Larger Scale Studies

The experiments in this report focus on verifying and quantifying reaction processes for candidate technologies at a small scale. The tests do not directly measure the impact of the reaction on the transport rate. Instead, these test data primarily interpreted the impact of the reaction processes on transport rates based on how the reaction process changes the geochemical state of the uranium in the sediment. Tests used uranium-contaminated sediments such that comparison to untreated sediments can be used to evaluate the impact on uranium mobility for the type of uranium compounds found within the contaminated vadose zone in the Central Plateau of the Hanford Site.

After sediment columns were treated with the specific reagent for each candidate technology, a sequential extraction procedure was used to evaluate changes to the uranium geochemistry (Table 3.5). The portion of the total uranium within each bin defined by these extractions was quantified and compared to the distribution for untreated sediment. The first three extracted phases (aqueous uranium, adsorbed uranium, and rind-carbonate uranium) are considered mobile. The balance of uranium mass (carbonate-associated uranium, oxide-associated uranium, and silicates/phosphates) are considered progressively more immobile. A treatment is considered successful if it moves uranium into less mobile bins.

For treatments that were successful based on the sequential extraction assessment, additional tests were conducted to further quantify the geochemical changes through 1) measuring the uranium that can be eluted from a saturated treated sediment column in comparison to untreated sediment column, and 2) using electron microscopy to examine the type of uranium-mineral phases present after treatment (for treatments expected to produce minerals that can be detected with this method). This information provided additional confirmation that the candidate technology has altered the uranium in a way that decreases its mobility in comparison to untreated sediments.

The experimental plan also included testing of reagent dosing for those candidate technologies that are successful in decreasing uranium mobility. Reagent dosing used uncontaminated sediments and focused on quantifying the amount of reagent retained in the sediment or amount of sediment geochemical change that can be induced per unit of reagent added to a soil column and for a specified

contact time. These data do not directly indicate the ability to immobilize uranium. Rather, these data were used to interpret reagent loading as part of computing the transport and stoichiometry associated with how the candidate technologies may be applied in the field. As such, these data quantified the ability to implement the uranium immobilization technologies. Numerical modeling was used to assist in this comparison process. The specific comparisons depended on the results of initial testing.

3.4 Electron Microprobe Analysis of Treated Sediments

The use of x-ray diffraction (XRD) to identify the small concentrations of uranium-mineral phases in sediment has not been used because of the very low uranium concentrations. XRD is typically limited to 0.5% or above for proper identification. The electron microprobe has successfully been used in other studies to identify small uranium-mineral phases, as shown in Figure 3.2. The process involves taking a small sediment sample (0.5 g), encasing it in epoxy, then creating a thin section of the sediment sample, which shows both surface precipitates and crystal structure of the sediment minerals. The process involves scanning the thin sections to make two-dimensional maps of specific elements (described below) that indicate possible uranium-mineral phases, then placing the thin section back into the microprobe to focus on the specific spots of interest to identify the uranium-mineral phase. The elemental association process can be conducted manually (i.e., manually look for elemental associations), or automatically by making additional two-dimensional maps of just associations. This mineral phase is identified by comparing the relative amounts of elements present at that spot to known minerals.

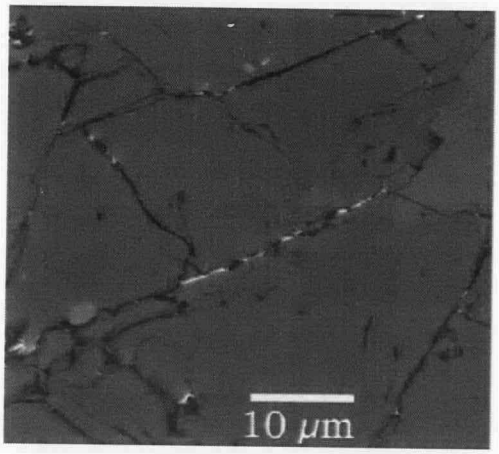

Figure 3.2. Uranium in boltwoodite (bright spots) (Liu et al. 2004).

Table 3.4. Samples for Uranium-Mineral Phase Identification by Electron Microbe Analysis

Name	Sediment No.	Treatment
Z-10	1	None, background
Z-11	2	None, background
Z-13	3	None, background
Z-39	3	SO_2 gas
Z-48	3	CO_2 gas
Z-57	3	NH_3 gas
Z-63	3	Fe(III)
Z-72	3	PO_4 mist
Z-81	3	PO_4 foam

A total of eight thin sections were made in this study (Table 3.4). The elemental detectors (or Energy dispersive spectroscopy detector) on the electron microbe can identify elements at an extremely small point (~10 micron beam width, adjustable), so to identify small uranium-mineral phases as precipitates around sediment grains, an automated scanning routine was used. Using a beam width of 10 microns and scan time of 500 milliseconds per point, a 200 × 200 grid was scanned on each sample (i.e., 4000 points, 2 mm × 2 mm), which took ~20 h per sample. The microprobe used had multiple high-sensitivity elemental detectors, set for uranium, iron, silica, phosphorus, calcium, aluminum, and sulfur. Analysis is in progress and preliminary results are reported. The elemental maps show associations, which can indicate possible uranium-mineral phases, that will be evaluated by additional microprobe analysis at specific spots.

An example of microprobe analysis that identifies very small concentrations of apatite precipitate in sediment (Figures 3.3 and 3.4) is shown to illustrate the type of analysis that is in progress for the uranium-laden samples in this study. In this example, the first image is electron backscatter showing the minerals (brighter) set in epoxy (Figure 3.3a). The calcium image (in Figure 3.3b, the warmer color indicates higher concentration) shows many minerals that contain calcium, whereas the phosphorus image (Figure 3.3c) shows very few mineral phases containing phosphorus. Note that some mineral phases contain phosphorus, so the combination of phosphorus plus calcium (Figure 3.3d, in yellow) identify locations requiring further analysis.

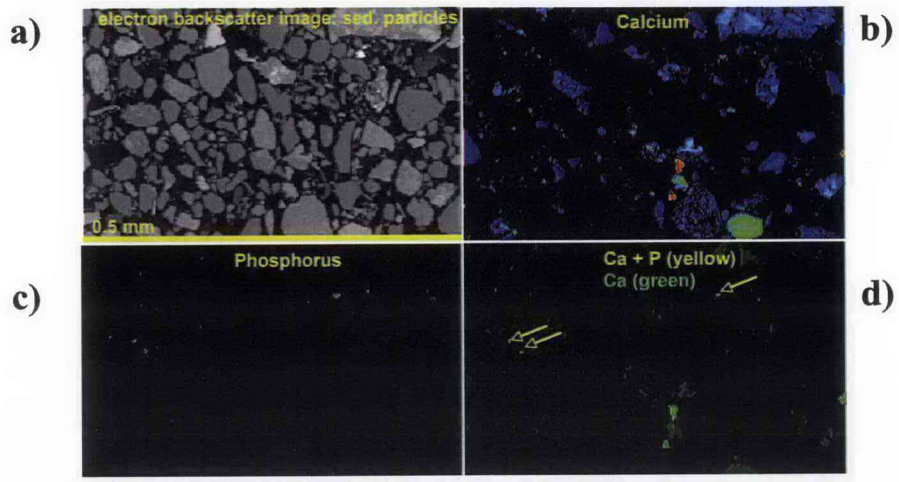

Figure 3.3. Scanning electron microprobe image of a sediment thin section containing 0.033 mg apatite/g sediment (Szecsody et al. 2009). Microprobe analysis by JP McKinley (PNNL). Images are as follows: a) electron backscatter illustrating sediment grains (grey) in the black epoxy background; b) calcium density; c) phosphorus density; and d) addition of Ca + P.

The identification of the mineral phase involves focusing the electron beam on the potential mineral (a few microns across) at high magnification (Figure 3.4a, b). This electron backscatter image shows that this crystal is likely precipitated apatite, as sediment grains are generally far larger and this small crystal is located on the surface of a mineral grain. An EDS detector scan of this grain (Figure 3.4c) with peaks clearly shows the crystal structure is apatite.

Additional analysis can also be conducted to determine, for example, whether uranium is associated with just the near surface carbonate or is relatively evenly distributed with depth in the carbonate precipitate. In a previous study conducted (Szecsody et al. 2009), strontium in solution was slowly substituted for calcium in the precipitated apatite structure. Samples taken after 1.3 years of strontium solution (in groundwater) in contact with apatite were analyzed with the electron microprobe at high beam intensity to slowly remove the mineral surface to characterize the amount of strontium with depth in the apatite crystal (Figure 3.5a). These results showed very little change in strontium substitution with depth (averaging 16.1% mole/mole substitution for calcium). The reason why strontium was evenly distributed is due to the morphology of the apatite precipitate, which is similar to the porous microcrystalline structure (Figure 3.5b).

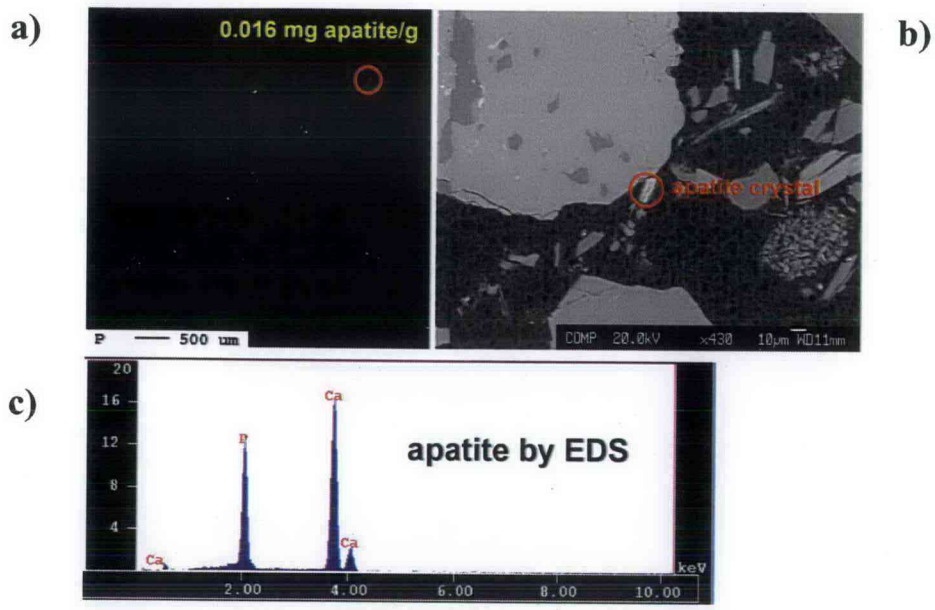

Figure 3.4. a) Mineral phase identification of a location with high phosphorous concentration; b) electron backscatter of the location is indicative of a surface precipitate, with c) identification of this mineral as apatite by comparison to an spatite standard.

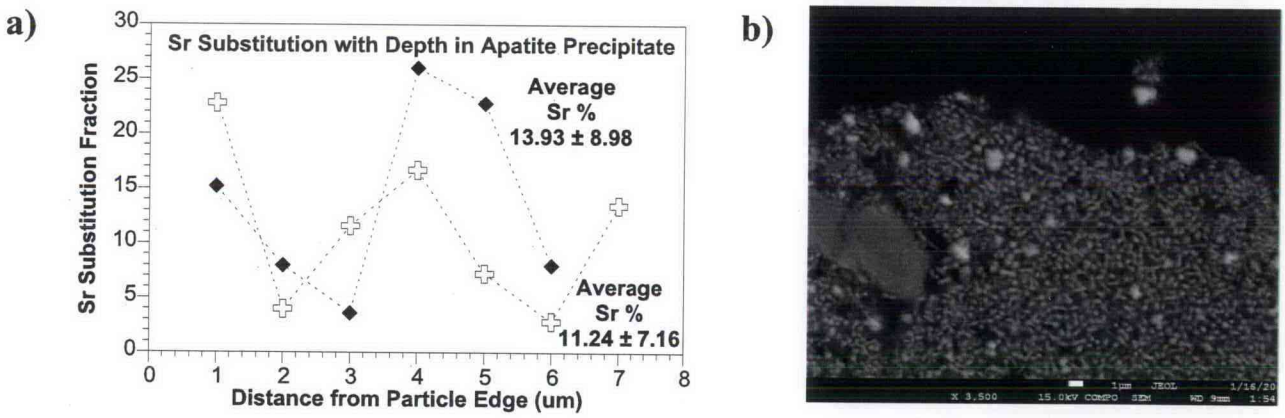

Figure 3.5. a) Strontium substitution with depth in apatite precipitate with conglomerate morphology, and b) high magnification image of apatite.

3.5 Simulation of Uranium Transport under Field-Scale Conditions

Gas delivery technologies were simulated to quantify long-term effectiveness at a large scale, based on uranium surface phase changes characterized in laboratory experiments. Simulation cases were selected from existing Subsurface Transport Over Multiple Phases (STOMP) simulations from the numerous tank farm field investigation reports and tank farm closure studies in the Hanford Site 200 Area (e.g., S-SX, B-BX-BY, T-TX-TY, and C Tank Farms). These earlier modeling studies developed STOMP finite difference grids, hydrostratigraphy, material properties, and boundary conditions along with uranium concentration profiles and source term cases for the vadose zone under these sites. More specifically, the hydrostratigraphy for this one-dimensional infiltration model was chosen from borehole

299-E33-45 in the B-BX-BY Tank Farm (Serne et al. 2002; Freedman et al. 2002), with surface backfill (269- to 260-ft elevation), H2 gravelly sand (235 to 260 ft), H2 sand (100 to 235 ft), H3 gravelly sand (51 to 100 ft), a silty sand (51 to 31 ft), and the aquifer at a 10-ft elevation. Unsaturated physical properties are based on laboratory measurements and values used in prior simulations (Freedman et al. 2002; White et al. 2002; Serne et al. 2002). The uranium profile in the B-BX-BY Tank Farm used in previous simulations (Figure 3.6, based on Freedman et al. 2002 based on borehole data from Serne et al. 2002) was located at 99- to 170-ft elevation, with additional mass at 185- to 200-ft elevation. For this study, a uniform mass of uranium at 99- to 170-ft elevation was used to evaluate breakthrough curves due to the change in mass between different surface phases, rather than the distribution vertically in the sediment profile. Water infiltration at 60 mm/year (high due to the surface gravel) results in a tracer in the 99- to 170 ft uranium-laden zone reaching the water table in 90 years. Simulation results in this study are breakthrough curves for the different uranium species directly beneath the initial inventory (i.e., at 97-ft elevation) and 10 ft above the water table (i.e., at a 27-ft elevation).

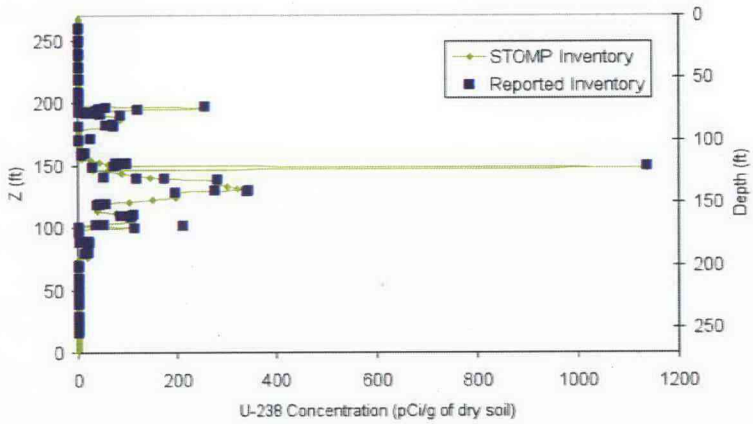

Figure 3.6. ^{238}U concentration profile for initial conditions in STOMP and the corresponding reported inventory.

The geochemical reactions used for these preliminary simulations are relatively simple, and are representative of some aspects of uranium phases and transport. These simulations do not include aqueous speciation (Figure 2.1), nor the behavior that would be observed for multiple species sorption or transformation, nor slow diffusion release of uranium from sediment. Although these simulations are more informative than uranium transport using a K_d model (model that includes only equilibrium sorption of a single uranium species), but without the full geochemistry, cannot represent changes in uranium mobilization associated with pH, Eh, carbonate concentration, or other geochemical changes.

One equilibrium and four kinetic reactions were used in this modeling approach:

1. Equilibrium sorption: U(VI) species (mobile) ⇔ >U(VI) adsorbed
2. Dissolution of rind-CO_3-U: U-rind CO_3 (immobile)➔ U(VI) species (mobile)
3. Dissolution of CO_3-U: U-CO_3 bound (immobile)➔ U(VI) species (mobile)
4. Dissolution of oxide, silicate, phosphate bound U: U(ox,si,PO_4) ➔U(VI) species (mobile)
5. Time-delayed desorption: U(VI) species (mobile) ⇔ >U(VI) adsorbed.

Reactions 2 through 5 are kinetic, with time-dependent parameters. Dissolution reactions 2 through 4 are assigned dissolution rates equal to 1800 years half-life (rxn 2), 10,500 years (rxn 3), and 18,000 years (rxn 4). Reaction 4 is intended to represent uranium mass that was reduced (for H_2S and SO_2 treatments), where in a reduced state the surface UO_2 is immobile, but after the subsurface system is oxidized, the uranium mass is again mobile. The most optimistic set of parameters was used for this reaction, where uranium mass remains immobile for 100 years (Thornton et al. 2007), and only half of the mass is remobilized (i.e., assuming aging has sequestered half of the mass into a less mobile phase). In addition to the dissolution half-lives, surface phases for reactions 2 through 4 are assumed to be in equilibrium with the natural geochemical environment, and therefore dissolve and reprecipitate at a slow rate down gradient. Retardation factors were set for these different surface phases as: a) Rf = 10 for rind-CO_3 (water table breakthrough at 900 years), b) Rf = 60 for carbonate uranium (water table breakthrough at 5400 years), and c) Rf = 100 for oxide, silicate, and PO_4-associated uranium (water table breakthrough in 18,000 years).

A base case (no treatment) simulation was conducted using uranium mass extracted from different surface phases for sediment 3 (Table 3.5). Nine additional simulations were conducted for the different treatments, with differences in uranium mass determined in experiments.

Table 3.5. Geochemical Parameters Used in One-Dimensional Infiltration Simulations

	U (aq+ads)		**U (rind-CO_3)**		**U (CO_3)**		**U (PO_4, silicate)**		**Reduced U**	
	Kd = 0.1		Rf=10, t/2=1800yr		Rf=60, t/2=10800yr		Rf=100, t/2=18000yr		oxidation by 100 yr	
Simulation	initial %	ug U/ cm^3 sed	initial %	ug U/ cm^3 sed	initial %	ug U/ cm^3 sed	initial %	ug U/ cm^3 sed	initial %	ug U/ cm^3 sed
No Treatment	19.4	63.5	33	108.1	40	131.0	7.6	24.9		
CO_2 Gas	19.4	63.5	17	55.7	35	114.6	28.6	93.7		
Fe(III)NO_3 Mist	3.4	11.1	22	72.1	53	173.6	21.6	70.7		
NH_3 Gas	10.4	34.1	16	52.4	37	121.2	36.6	119.9		
NaOH Mist	9.1	29.8	22	72.1	42.3	138.5	26.6	87.1		
HCl Mist	5.1	16.7	14	45.9	64	209.6	16.9	55.4		
PO_4 Mist	21	68.8	34	111.4	8	26.2	37	121.2		
PO_4 Foam	23	75.3	35	114.6	11	36.0	31	101.5		
H_2S Gas	17	55.7	25.2	82.5	41	134.3	8.6	28.2	8.2	26.9
SO_2 Gas	13	42.6	24.4	79.9	43	140.8	10.3	33.7	9.3	30.5

4.0 Results

Laboratory experiments conducted in 2009 primarily focused on the change in uranium mobility as a result of the reactive gas or gas-advected treatment. All experiments used actual field sediments, which contained a variety of uranium surface phases (Table 3.1). This change in uranium mobility was characterized by a series of six liquid extractions on the sediments (Table 3.3), with positive identification of uranium surface phase change by electron microprobe. Additional uranium mobility experiments conducted included water-saturated one-dimensional column experiments. To interpret the changes in uranium surface phases, an additional focus of some experiments was to identify changes in the sediment geochemistry from the reactive gas or gas-advected treatment. Simulations of one-dimensional downward migration of a hypothetical uranium plume were then conducted for each treatment case to determine the influence of the uranium surface phase changes.

The six sequential liquid extractions used in this study were used to account for uranium on the surface in different phases (adsorbed and in mineral phases). The first liquid extraction is Hanford Site groundwater ($CaCO_3$ saturated), added in a sediment/water ratio of 7.5 g to 10 mL of water. The uranium aqueous fraction under field conditions (much higher sediment/water ratio) is approximately 10 times less (shown in Appendix tables). The second extraction (ion exchangeable) used a 1.0 mol/L $Mg(NO_3)_2$ solution. The distribution coefficient (K_d) was then calculated from the ratio of sorbed uranium (by ion exchange, extraction 2) to aqueous uranium (extraction 1). Note also that changes in the K_d for treatments was not useful, as in a case where both ion exchangeable and aqueous uranium fractions decrease (with a larger decrease in the ion exchangeable fraction) results in a smaller K_d (apparent more uranium mobility), but in reality, there is less uranium mobility because both of these fractions decreased. The third extraction (1M Na-acetate, pH 5) is designed to remove a portion of the carbonate (or "rind" on carbonates), thus targeting any contaminant uranium that formed carbonate. The fourth extraction (acetic acid, pH 2.3, 1 week) is designed to remove nearly all of the carbonate on the sediment. This extraction solution is in contact with the sediment for a week. The fifth extraction (0.1 mol/L ammonium oxalate) is designed to remove oxides. The final extraction (8M HNO_3, 95°C for 2 h) is designed to remove hard-to-extract uranium phases, including crystalline phosphates and silicates. Although this sequential extraction technique provides a general description of the uranium surface phases and their leachability (i.e., mobility), the complex mineral phases in sediments are not perfectly separated using this technique. A more resistant phase (e.g., phosphate) can coat a more mobile phase (e.g., carbonate), showing less carbonate. Electron microbe analysis (in progress) of the uranium surface phases and changes that result from the geochemical treatments was used for more positive mineral phase identification. Additional experiments are likely needed to test specific hypotheses and surface phase changes that are difficult to identify.

4.1 Uranium Phases in Untreated Sediments

Four sediment samples taken from the 200 Area of the Hanford Site were used for this study (Table 3.1). Sediments 3a and 3b were combined, as both contained uranium associated with carbonate. The sequential uranium extractions were conducted on the untreated sediments, with three to six duplicate samples to estimate the mean and standard deviation of the uranium extraction values. Table 4.1 shows the fractions of total uranium mass extracted for each category of uranium represented by the extraction

solution. The actual extracted masses (ng U/g of sediment) are listed in the Appendix. The standard deviation of the extractions ranged from 3.6 to 16%, averaging 12%.

Table 4.1. Results of Sequential Liquid Extractions of Uranium Phases for Untreated Sediment

						Sequential Extractions, fraction of total U mass						
Sed.	Treat-ment	Time (months)	T (°C)	H2O (%)	Total U (ug/g)	#1 aq.	#2, ion exch.	#3, pH 5 acetate	#4, pH2.3 acetate	#5 oxalate	#6 8M H+	K_d (cm^3/g)
1	none	0 (3 samples)	22	5	376.6±6.2	0.0152	0.01	0.028	0.800	0.0818	0.065	1.45
2	none	0 (5 samples)	22	5	74.3±2.3	0.0129	0.011	0.039	0.744	0.137	0.051	0.87
3	none	0 (6 samples)	22	5	28.1±1.8	0.0606	0.107	0.291	0.336	0.061	0.149	1.84
3	none	0 (3 samples)	22	15	27.7±1.8	0.0864	0.110	0.270	0.331	0.099	0.104	1.90
						±12%	±12%	±8.8%	±3.6%	±11%	±16%	

Sediment 1 (BX-102, 61') contained significant uranium mass (376.6 μg U/g sediment), which was mainly bound as carbonate (83% of the uranium was associated with carbonate, shown in yellow in Figure 4.1). A small fraction was bound as oxides (8.2%) and as difficult to extract surface uranium phases (silicates, phosphates, 6.5%). This sediment contains the uranium phase sodium boltwoodite (Table 3.1), which is extracted in the 8M HNO_3 (extraction 6), although it is present as only a small fraction of the total uranium in the sediment. About 1.5% of the uranium in this sediment was present in the aqueous phase (at the laboratory experiment sediment/water ratio). The distribution coefficient (K_d) calculated from the ion exchangeable uranium and aqueous uranium was 1.45 cm^3/g. Under field-scale conditions of high bulk density and low porosity (20%) and 4% water content, the fraction of uranium in the aqueous phase is 0.16%.

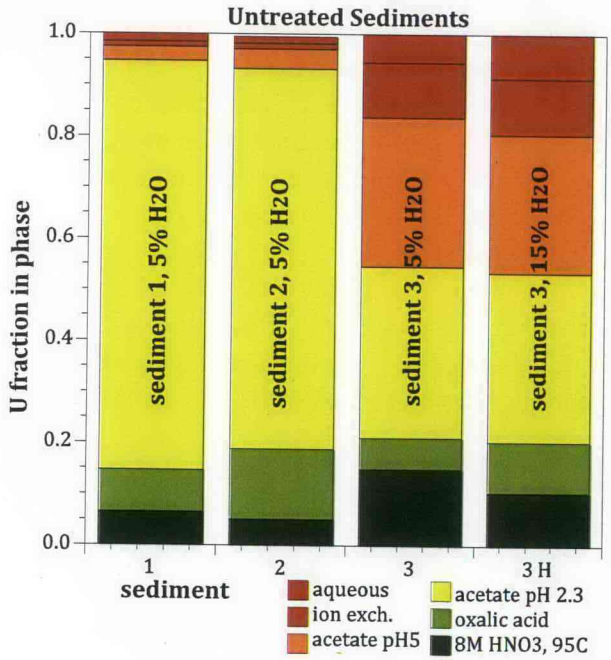

Figure 4.1. Fraction uranium in different surface phases for the three sediments.

Sediment 2 (BX-102, 102 ft) contained less uranium mass (74.3 μg U/g sediment) relative to sediment 1, and the sequential extractions showed generally the same distribution between phases. Most of the uranium was bound as carbonate (78% of the uranium was associated with carbonate, shown as a yellow center bar graph in Figure 4.1). Of this fraction, the weak carbonate extraction (or carbonate "rind") was 3.8% compared to 2.8% for sediment 1. A small fraction was bound as oxides (13.7%) and it was hard to extract surface uranium phases (silicates, phosphates, 5.1%). About 1.3% of the uranium in this sediment was present in the aqueous phase (at the laboratory experiment sediment/water ratio), and calculated K_d was 0.87 cm^3/g. Under field-scale conditions of high bulk density and low porosity (20%) and 4% water content, the fraction of uranium in the aqueous phase is 0.24%. Note that these extractions provide a general guide to the different uranium phases, but do not identify the specific uranium-oxides, silicates, or phosphates. Although sediments 1 and 2 appear

similar in the distribution of uranium between the different phases, significantly different behavior was observed with many of the treatments, implying that uranium is in different surface phases for these two sediments.

Sediment 3 (5% and 15% water content) contained a small uranium mass (28.1 μg U/g sediment), and was a mixture of TX-104 samples from 69 and 110 ft depth. The distribution between different extracted phases was significantly different from the other two sediments. Uranium was present in a significant quantity as a carbonate rind (27%, shown in orange in third and fourth bar graphs in Figure 4.1), and as the balance of the carbonate (33.1%) for a total carbonate uranium quantity of 60.1%). There was significant aqueous uranium (6.1%) and ion exchangeable uranium (10.7%). The oxide fraction (6.1%) and hard to extract uranium phases (14.9%) were similar to the other sediments. Under field-scale conditions of high bulk density and low porosity (20%) and 4% water content, the fraction of uranium in the aqueous phase is 0.9%. The uranium surface phase distribution did not change significantly for the different water contents (i.e., 5% versus 15% as shown in Table 4.1). Sediment 3 was used for all treatments, and sediments 1 and 2 for selected treatments. Preliminary electron microbe analysis (not shown) shows higher uranium abundance associated with calcium (presumed to be carbonates), silica, and iron. Additional microbe analysis on these mineral phases will be conducted and may indicate uranium-silicate and uranium-iron oxide minerals.

4.2 H_2S Reactive Gas Treatment of Sediment

Hydrogen sulfide has been used at laboratory- and field-scale studies to create weak iron reducing conditions in different sediments (Thornton et al. 2007), including Hanford Site sediments. The hydrogen sulfide treatment has been applied and successfully treated chromate at the White Sands, New Mexico, field scale. Uranium requires a greater reduction potential than chromate to reduce mobile U(VI) carbonate phases to U(IV) phases [UO_2 (ppt)]. In addition, when the sediment system becomes oxidized over time, U(IV) phases are reoxidized. Therefore, the reduction in uranium mobility associated with hydrogen sulfide gas treatment mainly depends on the rate at which the sediment is reoxidized at the field scale. Diffusion of gasses into a treated zone has been estimated to take between 1 and 100 years to reoxidize (Thornton et al. 2007), although advection due to atmospheric pumping by barometric pressure changes was not accounted for in those calculations. There are additional processes that occur with greater contact time of uranium surface phases with sediment. Aging of the surface phases, even as short as hundreds of hours to 1 year (Szecsody et al. 1998; Smith and Szecsody 2009; Payne et al. 1994) decreases the mass of uranium that desorbs. At field scale, this significantly larger desorption K_d compared to adsorption K_d (with freshly adsorbed uranium) is attributed to aging of the uranium surface phases (Zachara et al. 2007). Therefore, use of hydrogen sulfide gas for uranium remediation would depend on several processes that would be difficult to quantify: a) field-scale oxidation rate of the reduced sediment zone (years to tens of years), and b) rate of transformation of reduced uranium phases to other surface phases that are less mobile (also years to tens of years).

In this study, hydrogen sulfide treatments were conducted on small sediment columns to keep the sediment reduced for 1 or 2 months, with changes in uranium surface phases characterized by the sequential extractions (Table 4.2). A concentration of 200 ppm (by volume) H_2S was used at a flow rate of six pore volumes per minute for 24 h. Additional columns that were reduced for 1 or 2 months were oxidized for 1 month to observe the amount of uranium that was remobilized.

Table 4.2. Results of Sequential Liquid Extractions of Uranium Phases for H_2S-Treated Sediment

Sed.	Treat-ment	Time (months)	T (°C)	H2O (%)	Total U (ug/g)	Sequential Extractions, Fraction of Total U Mass #1 aq.	#2, ion exch.	#3, pH 5 acetate	#4, pH2.3 acetate	#5 oxalate	#6 8M H+	K_d (cm^3/g)
2	none	0 (5 samples)	22	5	74.3±2.3	0.0129	0.011	0.0385	0.744	0.137	0.0507	0.87
	H2S	1 mo.	22	5	68.0	0.0136	0.009	0.0456	0.783	0.120	0.0282	1.07
	H2S	1mo, 1mo oxic	22	5	74.9	0.0133	0.008	0.0891	0.728	0.090	0.0715	1.13
	H2S	2 mo.	82	5	72.6	0.0068	0.013	0.0907	0.689	0.094	0.1055	3.25
	H2S	2mo, 1mo oxic	82	5	79.5	0.0203	0.013	0.0397	0.759	0.087	0.0811	0.99
3	none	0 (6 samples)	22	5	28.1±1.8	0.0606	0.107	0.291	0.336	0.061	0.149	1.84
	H2S	1 mo.	22	5	34.1	0.108	0.118	0.188	0.380	0.116	0.0905	3.30
	H2S	1mo, 1mo oxic	22	5	31.6	0.0332	0.095	0.250	0.376	0.0955	0.150	8.43
	H2S	2 mo.	82	5	25.9	0.0549	0.096	0.257	0.370	0.0959	0.126	5.23
						Fraction Change to End of Experiment						Mobile*
2	H2S	3 months	82	5		0.0074	0.0020	0.0012	0.0152	-0.050	0.0304	0.011
3	H2S	3 months	82	5		-0.0057	-0.0107	-0.0345	0.034	0.035	-0.023	-0.051

fraction loss (-) or gain (+) *sum of extractions 1, 2, and 3

After 1 month of hydrogen sulfide treatment, and in the subsequent 2 months of either oxidation or under reducing conditions, there were little changes in uranium surface phases for sediments 2 and 3 (Figure 4.2). Sediment 3 also showed a slight decrease in carbonate associated uranium, which may be caused by the acidic conditions created by the hydrogen sulfide treatment (measured and shown in Figure 4.3b). For sediment 2, there was a 5.6% increase in mobile uranium phases (aqueous, ion exchangeable, and carbonate-rind), compared to sediment 3 with a 7.3% decrease in mobile uranium phases. Because these laboratory experiments represent high concentration of hydrogen sulfide treatment, the results show fairly weak performance. This observation of little apparent change is clear when the data are plotted in cumulative bar graphs (Figure 4.2).

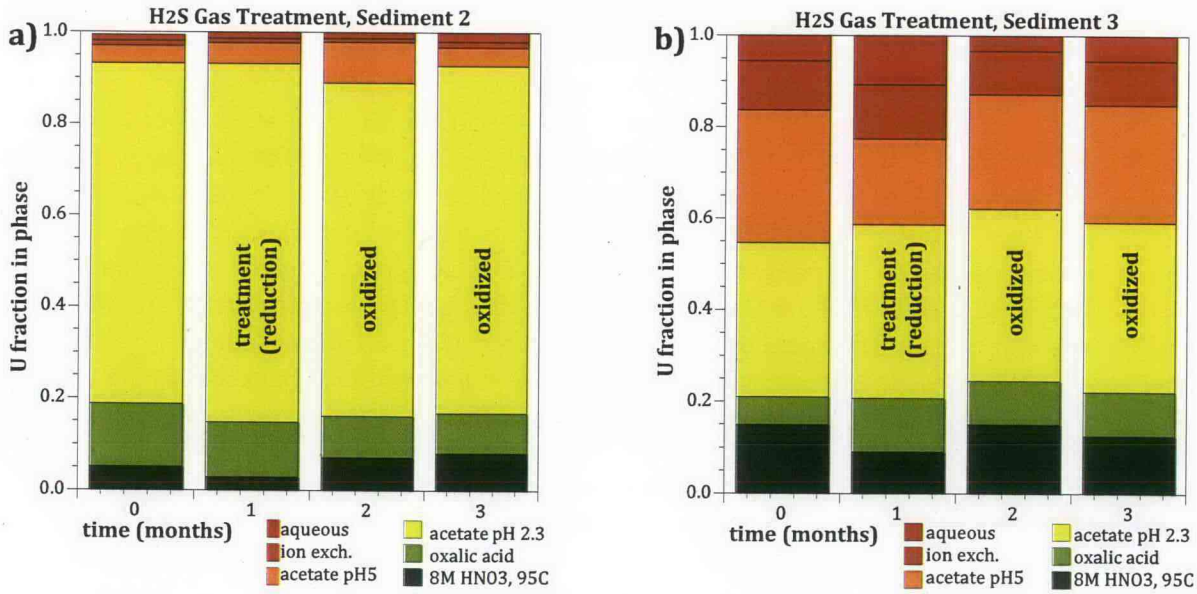

Figure 4.2. Changes in uranium surface phases for H_2S treatment of sediments 2 and 3.

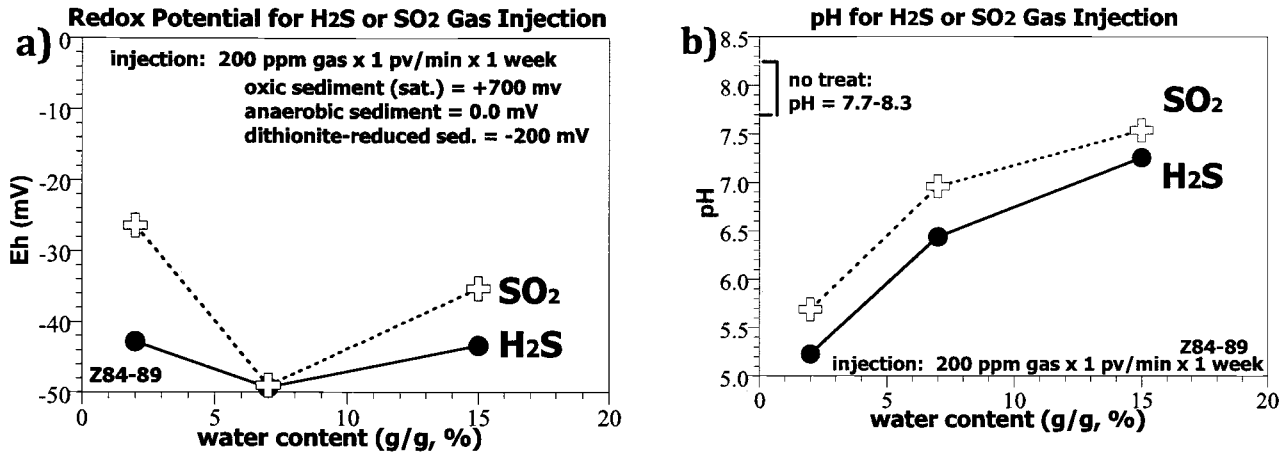

Figure 4.3. H_2S or SO_2 gas treatment and change in a) sediment redox potential, and b) pH.

Hydrogen sulfide gas treatment to sediment does result in mildly reducing conditions (Figure 4.3a), which do not appear to be a function of the water content. Sulfur dioxide treatment appears to produce somewhat weaker reducing conditions. Because there is a pH change of the pore water (pH 5.2 at 2% water content shown in Figure 4.3b), uranium mobilization is greatly increased. Mobilization of some uranium in carbonates or oxides (Table 4.2) may be caused by the slight acidic conditions created by the hydrogen sulfide treatment (pH 7.0 at 2% water content). The pH was not as influenced at higher water contents (Figure 4.3b). Treatment experiments were conducted with an initial water content of 5% (Table 4.2). In comparison, sulfur dioxide treatment did not produce as acidic conditions as the hydrogen sulfide at all the water contents.

To measure the reductive capacity created by the treatment, hydrogen sulfide treatment of sediment 3 was oxidized in a water-saturated system in which air-saturated water (8.2 mg/L dissolved oxygen) was slowly pumped into the column (70 h/pore volume, Figure 4.4), with dissolved oxygen being monitored at the effluent using two separate microelectrodes. The consumption of oxygen by the reduced sediment was used to calculate the reductive capacity of the sediment (1.2 μmol electron equivalence/g of sediment). This value was low relative to sediment from the Hanford Site 100-D Area that was reduced with an aqueous reductant (sodium dithionite at pH 12; reductive capacity of 11.3 μmol/g), although the sediments were not the same. In a water-saturated system, introduction of air-saturated water would oxidize the sediment in ~2.5 pore volumes, as shown in Figure 4.4 (oxidation in 172 h, a pore volume is 70 h).

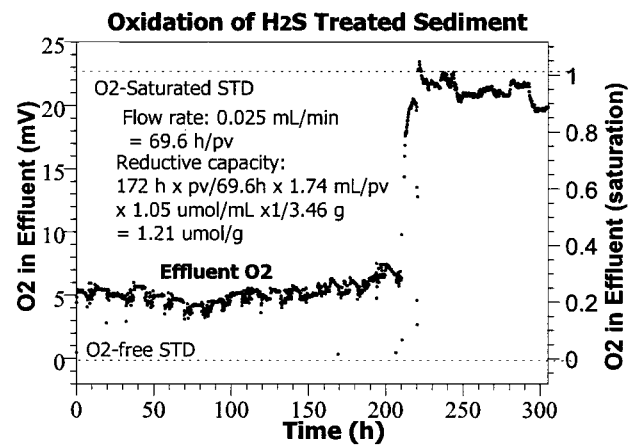

Figure 4.4. Oxidation of H_2S-treated sediment column with air-saturated water.

4.3 SO_2 Reactive Gas Treatment of Sediment

Sulfur dioxide treatment of sediment should also produce slightly reducing conditions in sediments, as some ferric oxide phases are slightly reduced. In contrast to hydrogen sulfide, sulfur dioxide has not been used previously for field reduction experiments. In this study, SO_2 treatments were conducted on small sediment columns to keep the sediment reduced for 1 or 2 months, with changes in uranium surface phases characterized by the sequential extractions. A concentration of 200 ppm (by volume) SO_2 was used at a flow rate of 6 pore volumes per minute for 24 h. Sulfur dioxide did create weak reducing conditions in the sediment (Figure 4.3a), as well as some acidification of the sediment (Figure 4.3b). The effect was not as strong as H_2S, because the SO_2 is a weaker reductant.

Uranium extractions on the SO_2-treated sediment after 1 and 2 months (Table 4.3, Figure 4.5) showed an increase in aqueous, ion exchangeable, and rind-carbonate uranium fractions. The total carbonate-bound uranium remained constant, but the oxide-bound uranium phases increased (which was expected). The total change in uranium surface phases varied from 3% to 7.6% (Table 4.3). This performance was similar to that of the H_2S-treated sediments.

Sulfur dioxide treatment of sediment 3 was oxidized in a water-saturated system in which air-saturated water (8.2 mg/L dissolved oxygen) was slowly pumped into the column (70 h/pore volume as shown in Figure 4.6), with dissolved oxygen being monitored at the effluent using two separate microelectrodes. The consumption of oxygen by the reduced sediment was used to calculate the reductive capacity of the sediment (1.3 μmol electron equivalence/g of sediment). This capacity was slightly larger than the H_2S-treated sediment (1.2 μmol/g), but still had low reductive capacity; thus, it can be readily oxidized.

Table 4.3. Results of Sequential Liquid Extractions of Uranium Phases for SO_2-Treated Sediment

						Sequential Extractions, Fraction of Total U Mass						
Sed.	Treat-ment	Time (months)	T (°C)	H2O (%)	Total U (ug/g)	#1 aq.	#2, ion exch.	#3, pH 5 acetate	#4, pH2.3 acetate	#5 oxalate	#6 8M H+	K_d (cm^3/g)
2	none	0 (5 samples)	22	5	74.3±2.3	0.0129	0.011	0.0385	0.744	0.137	0.0507	0.87
	SO2	1 mo.	22	5	76.5	0.0208	0.018	0.0396	0.7855	·	0.1356	1.38
	SO2	1mo, 1mo oxic	22	5	75.1	0.0168	0.014	0.0763	0.7091	0.0965	0.0876	1.26
	SO2	2 mo.	82	5	77.6	0.0121	0.011	0.0876	0.7051	0.0901	0.0937	1.55
	SO2	2mo, 1mo oxic	82	5	76.1	0.0359	0.014	0.0618	0.7286	0.0821	0.0776	0.66
3	none	0 (6 samples)	22	5	28.1±1.8	0.0606	0.107	0.291	0.336	0.061	0.149	1.84
	SO2	1 mo.	22	5	29.9	0.109	0.135	0.230	0.389		0.136	3.58
	SO2	1mo, 1mo oxic	22	5	30.0	0.0234	0.094	0.263	0.406	0.0947	0.119	12.3
	SO2	2 mo.	82	5	27.6	0.0483	0.084	0.240	0.407	0.0938	0.126	5.12
	SO2	2mo, 1mo oxic	82	5	33.6	0.0414	0.0522	0.110	0.641	0.0656	0.090	4.84
						Fraction Change to End of Experiment						Mobile*
2	SO2	3 months	82	5		0.0230	0.0033	0.0233	-0.015	-0.055	0.269	0.050
3	SO2	3 months	82	5		-0.0192	-0.0548	-0.181	0.305	0.005	-0.059	-0.255

fraction loss (-) or gain (+) *sum of extractions 1, 2, and 3

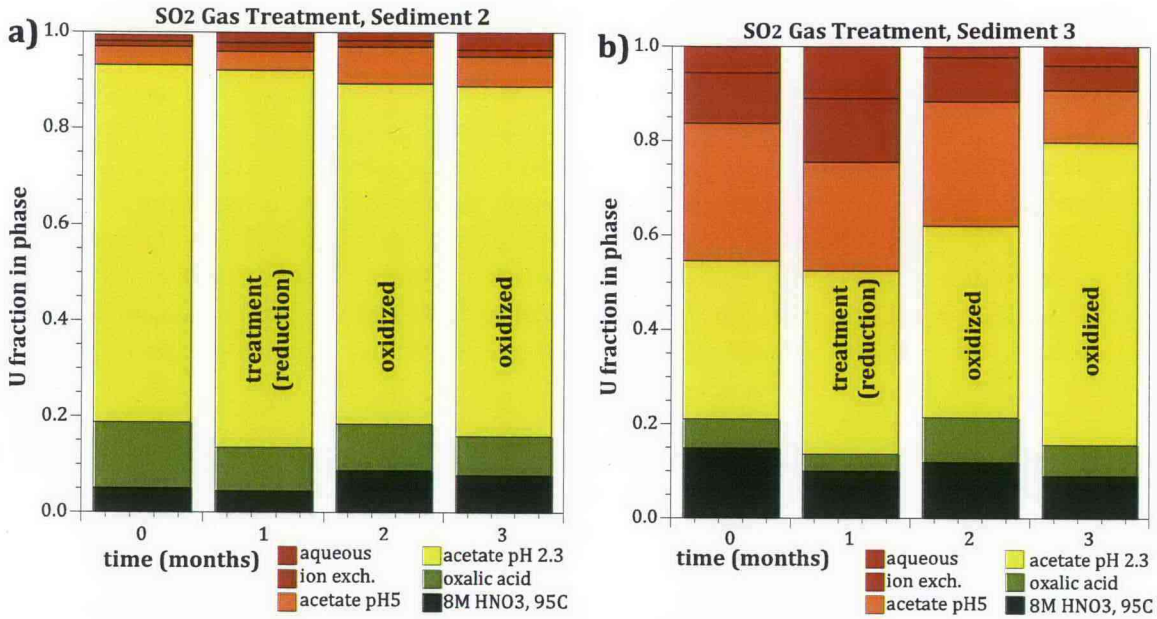

Figure 4.5. Changes in uranium surface phases for SO_2 treatment of sediments 2 and 3.

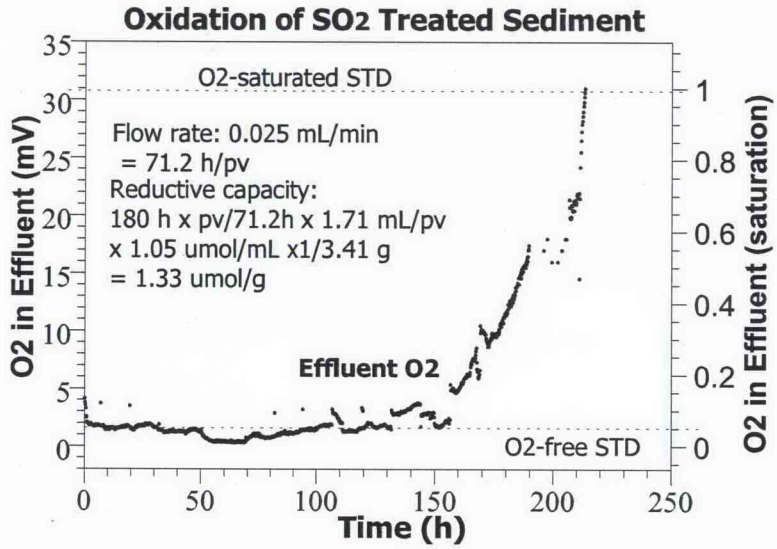

Figure 4.6. Oxidation of SO_2-treated sediment column with air-saturated water.

Overall, the performance of the H_2S- and SO_2-treated sediments was weak, with a small reductive capacity, low reducing potential created, and minimal effect on changing the uranium mobility. In general, a small fraction of the mobile uranium was immobilized by the sediment reduction, but that fraction was remobilized upon sediment oxidation. Although this result appears to not be very useful for a field-scale application, what is not apparent from these short-term (months in duration) tests is the following: a) sediment oxidation may take considerable time (decades), and b) long contact time of the uranium surface phases with the sediment will result in some resistance to remobilization (Payne et al. 1994; Zachara et al. 2007). Those long-term processes were not quantified in these experiments, but need to be addressed for consideration of H_2S or SO_2 treatment.

4.4 CO_2 Reactive Gas Treatment of Sediment

A temporary increase in the carbonate concentration in sediments at low water saturation is likely to result in an increase in uranium mobility because some uranium surface phases can form additional U(VI)-carbonate aqueous complexes. In addition, there may be a slight decrease in the system pH, which will result in less adsorption. The increased carbonate concentration by CO_2 gas can be neutralized by subsequent flushing using an inert gas, which may then lead to a greater fraction of the mobile uranium precipitating as uranium-carbonate phases. Carbonate coatings on mineral phases have been observed to influence U(VI) adsorption (Dong et al. 2005). At low water saturation, the very slow advection rate of water near surfaces will result in low redistribution of reactants, which may negatively impact treatment performance.

Carbon dioxide treatment of sediments does result in a slight decrease in the sediment pH, as tested in small one-dimensional columns filled with the sediment 3 with a porosity of 34% to 38%. At the lowest water content (2%), the pH in the sediment column changed considerably (pH 5.4 as shown in Figure 4.7a). At higher water contents, the acidification of the pore water was less pronounced, as expected. Note the pH values shown (Figure 4.7) are corrected for the dilution effect for pH measurement. For example, 10 g of sediment at 2% water content contains 0.2 mL of pore water. A total of 3 mL of deionized water was added to the sediment for the pH measurement (20x dilution).

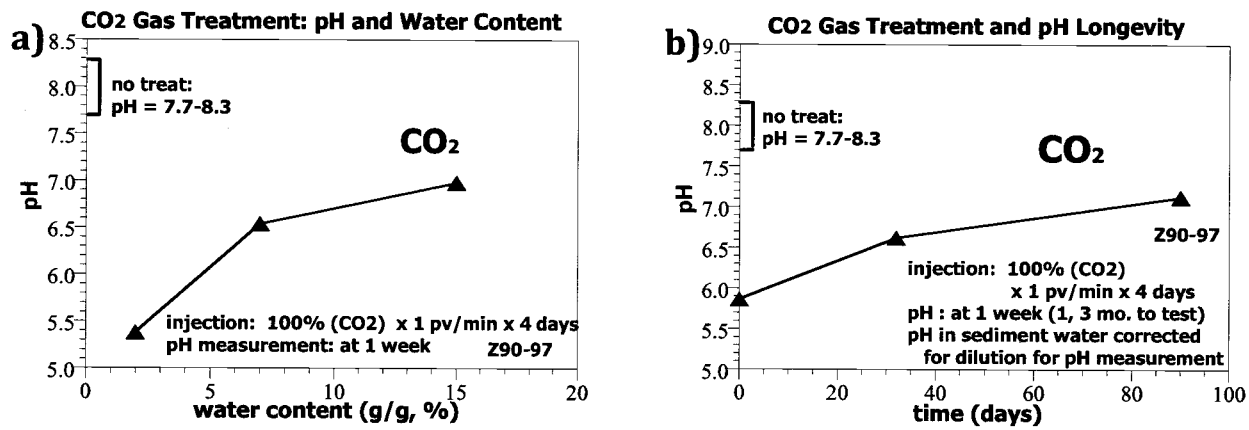

Figure 4.7. CO_2 treatment of sediment and a) resulting pH relative to water content, and b) natural pH neutralization over time.

An additional three columns at 7% water content were gassed with 100% CO_2, and then the pH was measured after 1 and 3 months to quantify whether the sediment had the buffering capacity to neutralize the pH (Figure 4.7b, Table 4.4). After 1 week, the sediment pore-water pH was 5.8; after 1 month, the pH was 6.6; and after 3 months, the pH was 7.1. While the sediment was not neutralized to the natural pH (pH 7.7 to 8.3), it appears that process was occurring. Thus, CO_2 gas treatment at field scale may be possible by gassing the sediment with no neutralization at a later point in time.

Table 4.4. Results of Sequential Liquid Extractions of Uranium Phases for CO_2-Treated Sediment

Sed.	Treat-ment	Time (months)	T (°C)	H2O (%)	Total U (ug/g)	#1 aq.	#2, ion exch.	#3, pH 5 acetate	#4, pH2.3 acetate	#5 oxalate	#6 8M H+	K_d (cm^3/g)
						Sequential Extractions, Fraction of Total U Mass						
2	none	0 (5 samples)	22	5	74.3±2.3	0.0129	0.011	0.0385	0.744	0.137	0.0507	0.87
	CO2	1 month	22	5	83.0	0.322	0.164	0.071	0.361		0.082	0.77
	CO2	2 mo., N2 flush	82	5	91.9	0.0137	0.004	0.028	0.603	0.153	0.197	0.41
	CO2	3 mo., N2 flush	82	5	71.3	0.0144	0.006	0.034	0.690	0.115	0.140	0.64
3	none	0 (6 samples)	22	5	28.1±1.8	0.0606	0.107	0.291	0.336	0.061	0.149	1.84
	CO2	1 month	22	5	28.8	0.110	0.148	0.162	0.353		0.227	1.38
	CO2	2 mo., N2 flush	82	5	22.1	0.039	0.040	0.150	0.347	0.1401	0.284	1.07
	CO2	3 mo., N2 flush	82	5	25.3	0.0339	0.0356	0.167	0.3015	0.1197	0.342	1.08
3	none	0 (3 samples)	22	15	27.7±1.8	0.0864	0.110	0.270	0.331	0.099	0.104	1.90
	CO2	1 month	22	15	29.7	0.170	0.181	0.132	0.306		0.212	1.21
	CO2	2 mo., N2 flush	82	15	24.1	0.0397	0.035	0.178	0.291	0.0223	0.434	1.01
						Fraction Change to End of Experiment						**Mobile***
2	CO2	3 months	82	5		0.0015	-0.0043	-0.0049	-0.054	-0.022	0.089	-0.008
3	CO2	3 months	82	5		-0.027	-0.0710	-0.124	-0.0350	0.059	0.193	-0.222
3	CO2	3 months	82	15		-0.047	-0.0747	-0.0919	-0.0402	-0.077	0.330	-0.213

fraction loss (-) or gain (+) *sum of extractions 1, 2, and 3

For the uranium-extraction experiments, 100% CO_2 gas was advected into batch vials containing 5 to 10 g of sediment for 1 month, with regassing once per week. The headspace in the vials was equivalent to 20 pore volumes in packed porous media (porosity 35%). It was expected to see increased uranium mobilization in that first month. After 1 month, the CO_2 was evacuated to simulate long-term pH neutralization and replaced by air for the remaining 1 to 2 months of the extraction experiments. Because there was considerable change in the sediment pH with water content (Figure 4.7a), two different water contents (5%, 15%) were investigated in the uranium extraction experiments.

After 1 month of 100% CO_2 in the pore space in contact with the sediment, there was a substantial increase in aqueous uranium (Table 4.4 and Figure 4.8) for sediments 2 and 3 (at both water contents), and a substantial decrease in the rind-CO_3 associated uranium for sediment 3. Untreated sediment 3 had 29.1% uranium associated with rind-CO_3 (i.e., a thin layer of carbonate that is dissolved by a weak carbonate extraction). The total carbonate associated uranium for sediment 2 also significantly decreased after 1 month of CO_2 contact. There was little observed difference in the increased uranium mobilization after 1 month for sediment 3 at the two different water contents (5%, 15%). The CO_2 gas was removed from the columns after 1 month, and after 2 additional months, the final result of the CO_2 gas treatment was an increase in hard to extract uranium phases (8M acid extraction) for both sediment 2 (9% increase) and sediment 3 (25% to 33% increase as shown in Table 4.4). Because the fraction of uranium associated with carbonate decreased in all cases, it appears that other aluminosilicates (dissolved in the 8M acid extraction) either containing uranium or coated uranium surface phases were the cause of the effect. This fairly significant positive effect was minor for sediment 2 (which contained minor uranium associated with rind-CO_3 – 3.8%) but substantial for sediment 3 (containing 29% uranium associated with rind-CO_3), even though the carbonate-extracted uranium actually decreased in all cases. Clearly, uranium associated with rind-CO_3 is being dissolved (as demonstrated after 1 month), but it is unclear what uranium surface phases are produced, which are less mobile after the pH is neutralized.

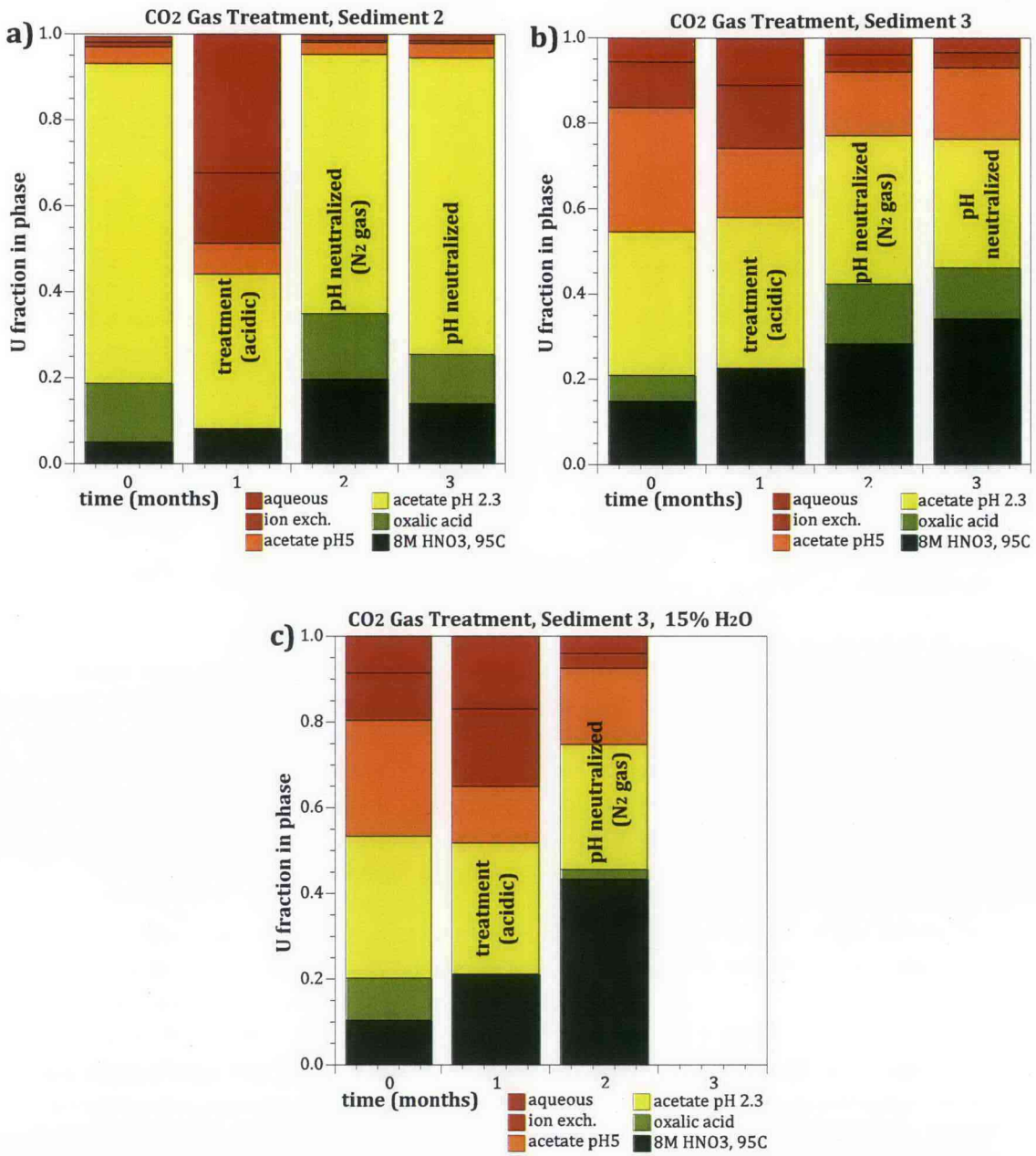

Figure 4.8. Changes in uranium surface phases for a) CO_2 treatment of sediment 2, b) sediment 3, and c) sediment 3 at 15% water content.

4.5 HCl Liquid Mist Treatment of Sediment

The use of a mist containing 0.5M HCl to acidify sediment was originally intended to parallel the CO_2 gas phase treatment of sediment. The HCl mist provides a similar pH decrease to the CO_2 gas, but does not increase the carbonate concentration in the sediment. Mist injection is a high volume of air injected into sediment with a small amount of water. A venturi was used to atomize the water into small droplets in the gas stream. For these experiments, 0.125-in. tubing was used for air (or nitrogen) gas

flow, and a "T" fitting was added so that water injection occurred from a small (0.001-in.) inner diameter tube located in the T fitting. The liquid stream was operating at 60 psi and the air stream at <5 psi, so the substantial pressure drop resulted in a fine liquid particle size. Qualitative measurements of the droplet size (on a glass plate) were ~0.008 to 0.02 in. (0.2 to 0.5 mm) in diameter.

Mist injection into a 160-cm-long column (Figure 4.9a) at 329 mL/min air flow and 1.0 mL/min water flow (0.3% water by volume) showed the mist was exiting the column, and after 10 min, a relatively uniform water content of 2% was observed to 100 cm, beyond which there was a decrease in water content. In a second mist injection experiment into a 610-cm-long (25-ft) column, mist injection was not as uniform, and the resulting water content was 12% at 20 cm, decreasing to below 1% by 90 cm (Figure 4.9b). Results in this second mist injection experiment likely reflect the problems with the liquid injection pump. Mist injection of HCl at 0.1% water content by volume into a 160-cm-long sediment column resulted in a nonuniform spatial distribution of the final pH (Figure 4.10a). Although the water content deposition can be uniform (Figure 4.9a) or decreasing with distance from the injection location (Figure 4.9b), the HCl mist injection appeared to result in greater deposition of the acid near the injection location (Figure 4.10a). The sediment pH at the injection point was 5.06, and gradually increased to ~8.0 by 100 cm (natural sediment pH).

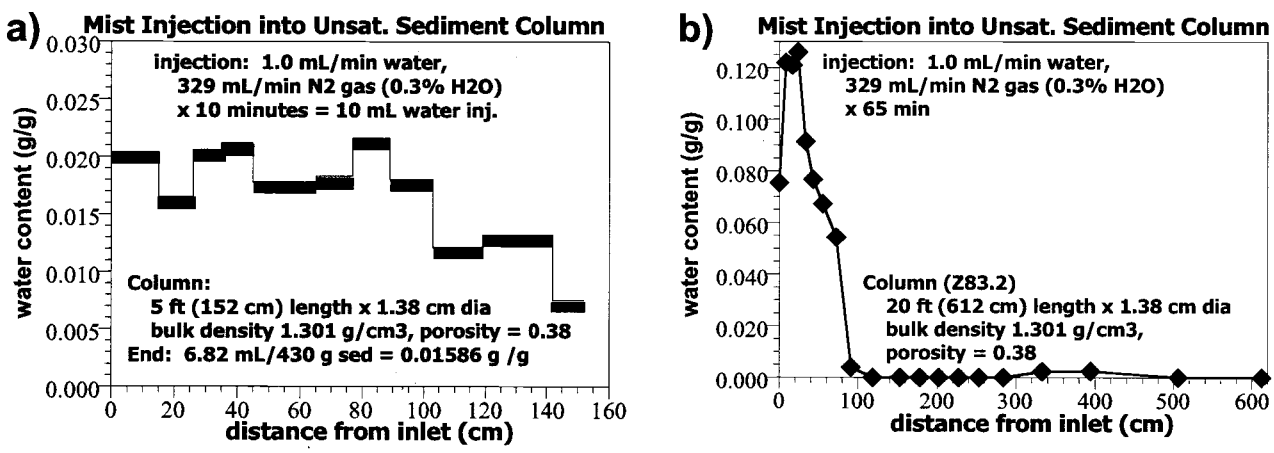

Figure 4.9. Mist injection into a) 160-cm-long column, and b) 620-cm-long column, showing the final water content.

If this technology (or CO_2 gas) were to be injected into sediment at a field scale, the lower pH (and the addition of carbonate for the CO_2 gas) will increase uranium surface phase mobilization. The subsequent pH neutralization is needed to precipitate carbonates and other oxides/silicates to either incorporate uranium or coat uranium surface phases. The pH neutralization may occur naturally by the Hanford Site sediment buffering capacity (primarily carbonate), as shown in Figure 4.7b over several months. Alternatively, mist can be used to inject a base approximately equal in volume to the acid mist to neutralize the pH. In one 160-cm-long column, the mist injection of HCl was followed by a mist injection of NaOH (both at 0.1% liquid content by volume; Figure 4.10b). The resulting pH profile with distance from the injection point illustrates the complexity of a two-stage approach. Although the quantity of liquid injected into the column was the same for HCl and NaOH (which should have resulted in neutral pH pore water if evenly mixed), the second mist injection (NaOH) was deposited even more closely to the injection location (within 40 cm) than the initial mist injection of HCl (about 100 cm). The

resulting pH varied with distance, with alkaline conditions between 0 and 20 cm, slightly lower than natural pH for 20 cm to 100 cm, then natural sediment pH (8.0) for 100 to 160 cm. Although the mist injection process was not fully developed, these few experiments illustrate that while mist could possibly be used for delivery of aqueous reactants to the vadose zone at low water content, there is additional development work needed to achieve uniform and predictable results.

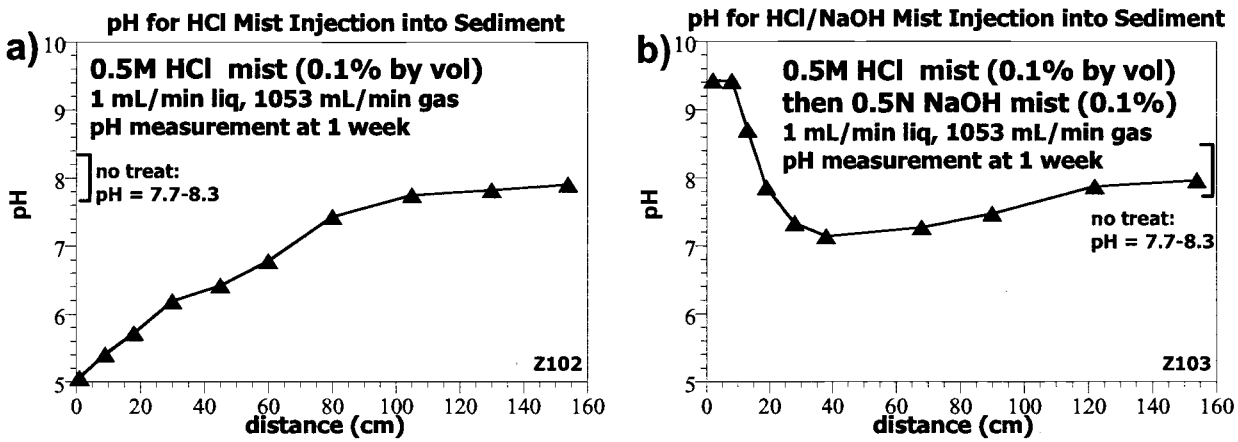

Figure 4.10. Spatial variability in pH over column length for a) HCl mist injection, and b) HCl mist followed by NaOH mist injection.

The changes in uranium surface phases for sediment that was treated with a 0.5M HCl mist for 1 month, after which time 0.5M NaOH was injected into the column as a mist. The uranium extractions were conducted only after 3 months. The results (Table 4.5, Figure 4.11) showed large decreases in aqueous, ion exchangeable, and CO_3 rind-associated uranium (mobile and labile phases), and an increase in uranium associated with carbonate-, oxide-, and hard-to-extract phases. Overall, 33% of the uranium mass was redistributed from the labile to less mobile phases. The primary change was a 19% decrease in carbonate-rind associated uranium, and an 18% increase in carbonate-associated uranium, indicating the acid treatment appeared to reprecipitate the uranium in carbonates that are somewhat more difficult to extract. Uranium associated with oxides increased some (7%), as did hard-to-extract uranium phases (increase of 8%).

Table 4.5. Results of Sequential Liquid Extractions of Uranium Phases for HCl-Mist-Treated Sediment

						Sequential Extractions, Fraction of Total U Mass						
Sed.	Treat-ment	Time (months)	T (°C)	H2O (%)	Total U (ug/g)	#1 aq.	#2, ion exch.	#3, pH 5 acetate	#4, pH2.3 acetate	#5 oxalate	#6 8M H+	K_d (cm^3/g)
3	none	0 (6 samples)	22	5	28.1±1.8	0.0606	0.107	0.291	0.336	0.061	0.149	1.84
	HCl	3 months	82	5	22.4	0.0138	0.0112	0.105	0.514	0.130	0.228	2.13
						Fraction Change to End of Experiment						Mobile*
3	HCl	3 months	82	5		-0.047	-0.096	-0.186	0.178	0.069	0.079	-0.329

fraction loss (-) or gain (+) *sum of extractions 1, 2, and 3

A comparison of the changes in uranium mobility for CO_2 gas treatment (Table 4.6) to HCl mist treatment (Table 4.8) show significant differences. There were several data points over time (8) for two sediments in which the CO_2 gas treatment was used versus a single set of extractions for the HCl treatment at 3 months—thus, the comparison is incomplete. Although both ultimately decreased aqueous and ion exchangeable uranium phases, the CO_2 gas treatment actually decreased the total uranium associated with carbonates (both rind and total carbonate) in contrast to the HCl treatment that resulted in a significant increase in uranium associated with total carbonate. The uranium associated with oxides (extraction 5) decreased for the CO_2 gas treatment (8%), versus a 7% increase for the HCl treatment. Finally, both resulted in a 33% change in uranium phases extracted, and both increased the less mobile phases (total carbonate, oxide, and hard-to-extract phases). For field-scale application, the CO_2 gas treatment would be easier to implement. One potential downside of the CO_2 gas treatment is the initial large increase in aqueous uranium (samples after 1 month) before the CO_2 gas was removed.

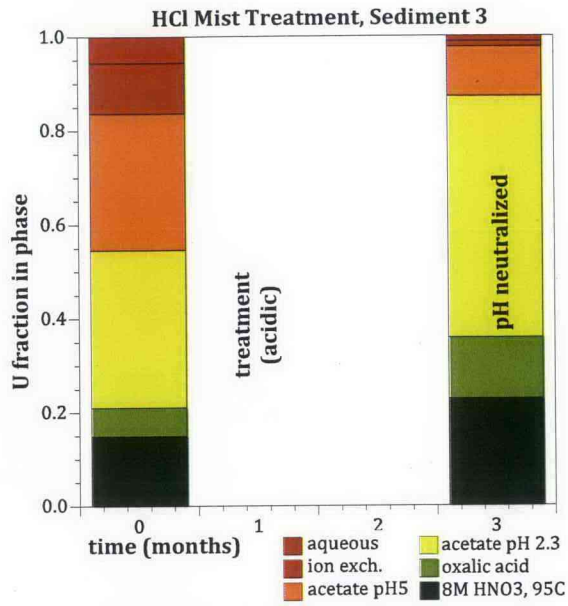

Figure 4.11. Changes in uranium surface phases for HCl mist treatment of sediment 3.

4.6 NH_3 Gas Treatment of Sediment

The use of ammonia gas injection into sediment at low water saturation is hypothesized to increase the pore-water pH, leading to dissolution of aluminosilicates. An analogous process is previously observed in water-saturated sediments, in which highly alkaline solutions (to 4M NaOH, which is present in some single-shell tanks at the Hanford Site) are dissolving significant phases to result in g/L concentrations of silica and alumina (Qafoku et al. 2004). Dissolution of biotite and/or magnetite has produced minor aqueous ferrous concentrations, which is sufficient to reduce chromate (Qafoku et al. 2004) and pertechnetate. When the sediment was oxidized, the reduced technetium ($Tc^{IV}O_2$) was generally remobilized (similar to UO_2); however, in this case only 23% of the technetium remobilized. The immobilized technetium was hypothesized as coated by aluminosilicates. Whether similar processes could occur for ammonia gas treatment of sediment depends on how much pH change can be produced.

In this study, 10% ammonia (balance N_2) was injected into small sediment columns at a flow rate of six pore volumes per hour for 24 h. Three columns at different initial water content (2%, 7%, 15%, Figure 4.12a) showed that a pH of 11.5 to 12 was achieved. As was observed with other reactive gasses, greater reactivity is observed at lower water content.

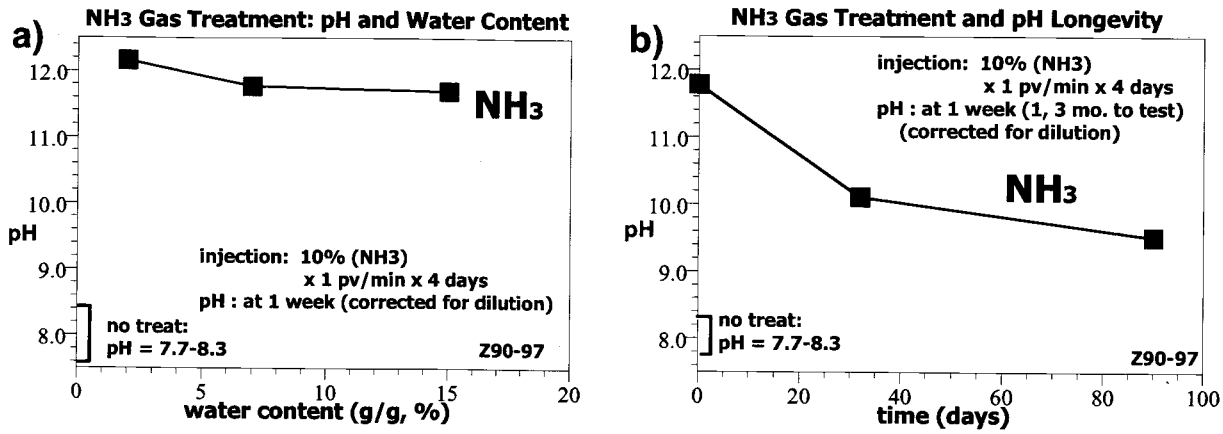

Figure 4.12. Ammonia gas treatment of sediment showing pH variability a) with different initial water content, and b) over time with 7% initial water content.

Three additional sediment columns at 7% initial water content were treated with ammonia gas and analyzed for pH over 3 months (Figure 4.12b). These results showed that the pH was returning to the natural sediment pH (pH = 10 by 1 month, pH = 9.5 by 2 months). Therefore, neutralization of the alkaline conditions may be possible with just the natural sediment buffering capacity.

The changes in uranium surface phases for sediments 2 and 3 (and at 5% and 15% water content for sediment 3) were quantified using the sequential liquid extractions (Table 4.6, and shown in Figure 4.13). For both sediments and at different water contents, the ammonia gas was reacted with the sediment for 1 month, after which the nitrogen gas was flushed into the sediment columns. After 1 month, there was an increase in aqueous uranium and carbonate uranium, but by 3 months (after the pH was neutralized)—in all cases—there were consistent decreases in the aqueous, adsorbed, and carbonate-rind associated uranium, and a significant increase in hard-to-extract uranium phases (8M HNO_3, silicates; Table 4.6).

Table 4.6. Results of Sequential Liquid Extractions of Uranium Phases for NH_3-Treated Sediment

						Sequential Extractions, Fraction of Total U Mass						
Sed.	Treat-ment	Time (months)	T (°C)	H2O (%)	Total U (ug/g)	#1 aq.	#2, ion exch.	#3, pH 5 acetate	#4, pH2.3 acetate	#5 oxalate	#6 8M H+	K_d (cm^3/g)
2	none	0 (5 samples)	22	5	74.3±2.3	0.0129	0.011	0.0385	0.744	0.137	0.0507	0.87
	NH3	1 month	22	5	70.4	0.0145	0.016	0.051	0.771		0.147	1.66
	NH3	2 months	82	5	44.8	0.0038	0.0007	0.041	0.665	0.117	0.172	0.27
	NH3	3 months	82	5	78.2	0.0127	0.008	0.020	0.743	0.093	0.123	0.95
3	none	0 (6 samples)	22	5	28.1±1.8	0.0606	0.107	0.291	0.336	0.061	0.149	1.84
	NH3	1 month	22	5	26.2	0.008	0.012	0.307	0.440	0.000	0.233	1.46
	NH3	2 months	82	5	22.6	0.0074	0.004	0.108	0.380	0.1491	0.352	0.52
	NH3	3 months	82	5	24.6	0.0345	0.0431	0.124	0.301	0.1018	0.396	1.27
3	none	0 (3 samples)	22	15	27.7±1.8	0.0864	0.110	0.270	0.331	0.099	0.104	1.90
	NH3	1 month	22	15	29.7	0.015	0.007	0.332	0.423		0.223	0.49
	NH3	2 months	82	15	24.1	0.0058	0.001	0.108	0.417	0.1421	0.326	0.18
						Fraction Change to End of Experiment						Mobile*
2	NH3	3 months	82	5		-0.0002	-0.0024	-0.0185	-0.001	-0.045	0.0728	-0.021
3	NH3	3 months	82	5		-0.026	-0.0640	-0.167	-0.035	0.041	0.247	-0.257
3	NH3	2 months	82	15		-0.081	-0.109	-0.162	0.086	0.043	0.222	-0.352

fraction loss (-) or gain (+) *sum of extractions 1, 2, and 3

For sediment 2, there was a 7.3% increase in hard-to-extract uranium phases, and for sediment 3 there was a 29% to 35% increase in hard-to-extract uranium phases (Table 4.6).

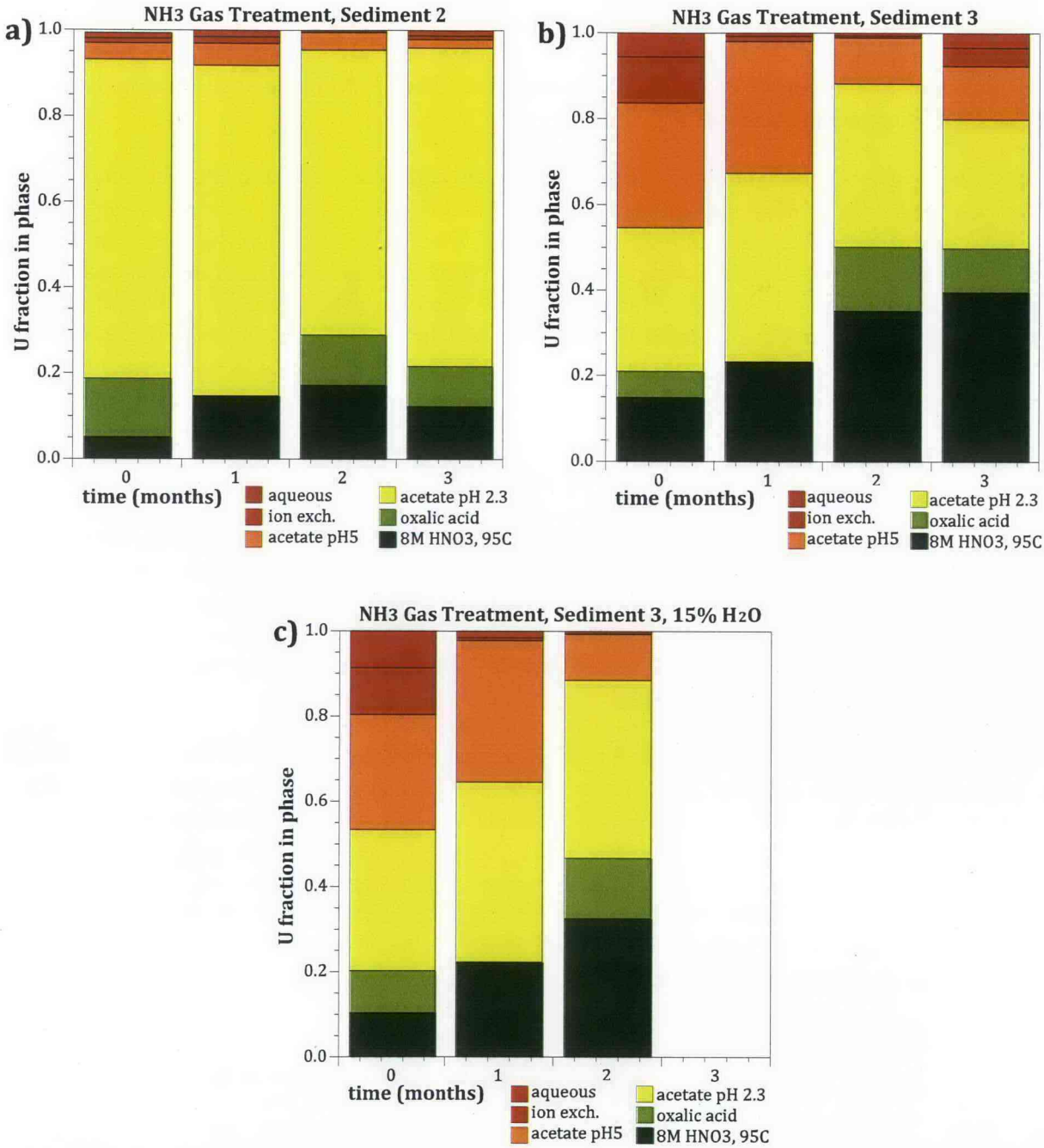

Figure 4.13. Ammonia gas treatment of sediment showing uranium surface phase changes over time for a) sediment 2, b) sediment 3 at 5% water content, and c) sediment 3 at 15% water content.

For the ammonia gas (Table 4.6) and carbon dioxide gas (Table 4.4) treatment, higher water content (15% versus 5%) resulted in a slightly greater uranium phase transformation. This effect does appear counter intuitive, as it was shown that gas phase treatments generally effect more change at lower water

content (i.e., NH_3 gas in Figure 4.11b; CO_2 gas in Figure 4.4a; and H_2S and SO_2 gas in Figure 4.1a). For these reduction or precipitation processes to be effective, there needs to be some redistribution of uranium in the pore water, so higher water contents may lead to somewhat more effective uranium redistribution. The changes in uranium surface phases are in the process of being identified with electron microprobe analysis of the treated sediments. Preliminary electron microbe analysis of NH_3 gas treated sediment shows significant association of uranium abundance associated with silica, which may be more frequent compared with the untreated sediment.

Over the long term, the addition of ammonia gas at field scale may increase subsurface microbial activity, as nitrogen is a limiting nutrient. Nitrogen is not added to the system at the natural sediment pH (8.0), but under strongly alkaline conditions (pH 11 to 12), which is likely to cause significant microbial death. Previous analysis of the natural microbial population subjected to pH 12 with aqueous sodium dithionite (Szecsody et al. 2004) showed 90% death, but the surviving population was still able to biodegrade organic compounds after the pH had returned to natural conditions. In addition, the microbial oxidation of ammonia to nitrate is likely not significant. None of these potential NH_3-microbial interactions were evaluated in fiscal year 2009, but should be evaluated to assess the potential impact.

4.7 NaOH Liquid Mist Treatment of Sediment

The use of a mist containing 0.5M NaOH to create alkaline conditions in the low water saturation sediment was intended to parallel the ammonia gas phase treatment of sediment. The mist technology described in Section 4.5, although somewhat inconsistent, can be used to inject an aqueous reductant into sediment maintaining low water saturation. NaOH mist was injected into a 160-cm-long sediment column (Figure 4.10b) that was previously treated with HCl (by mist injection; see Figure 4.10a) and significant alkaline conditions was achieved.

The changes in uranium surface phases for sediment 3 (at 5% water content) for NaOH mist injection was conducted on a single sediment column in which the NaOH mist treatment remained in the column for 1 month; afterwards, an HCl mist was used to neutralize the pore water pH. Uranium sequential extractions were conducted after 3 months (Table 4.7). In general, the NaOH mist treatment resulted in similar uranium surface phase changes as the ammonia gas, with losses in the aqueous, adsorbed, and CO_3 rind phases, and a gain in the oxide and phosphate/silicate phases (Figure 4.14). The total change in uranium surface phases (as a fraction of the total extractable, Table 4.7) was 25%, as compared to 29% for the ammonia gas for the same sediment (3) at the same initial water content (5%).

Table 4.7. Results of Sequential Liquid Extractions of Uranium Phases for NaOH-Treated Sediment

						Sequential Extractions, Fraction of Total U Mass						
Sed.	Treat-ment	Time (months)	T (°C)	H2O (%)	Total U (ug/g)	#1 aq.	#2, ion exch.	#3, pH 5 acetate	#4, pH2.3 acetate	#5 oxalate	#6 8M H+	K_d (cm^3/g)
3	none	0 (6 samples)	22	5	28.1±1.8	0.0606	0.107	0.291	0.336	0.061	0.149	1.84
	NaOH	3 months	82	5	19.5	0.0008	0.0042	0.202	0.388	0.155	0.250	13.3
						Fraction Change to End of Experiment						Mobile*
3	NaOH	3 months	82	5		-0.06	-0.103	-0.089	0.052	0.094	0.101	-0.252

fraction loss (-) or gain (+) *sum of extractions 1, 2, and 3

Note that the NaOH mist resulted in a very significant decrease in the aqueous and adsorbed uranium (most mobile uranium phases). A comparison of the K_d values (changes) that occur for both the ammonia gas and NaOH mist treatments appear to show vast increases and decreases (somewhat inconsistent values for K_d). Because K_d is a ratio of adsorbed to aqueous uranium, in cases where both quantities are changing, the K_d value can appear worse (i.e., more mobile; for example, sediment 3, 15% water content, 2 months, $K_d = 0.18$ or 10x worse than the base case $K_d = 1.9$). However, the adsorbed uranium decreased 100x (from 11% to 0.1%) and the aqueous uranium decreased 15x (from 8.6% to 0.6%), so this is a very substantial decrease in uranium mobile phases, even though the K_d value shows an apparent worse case.

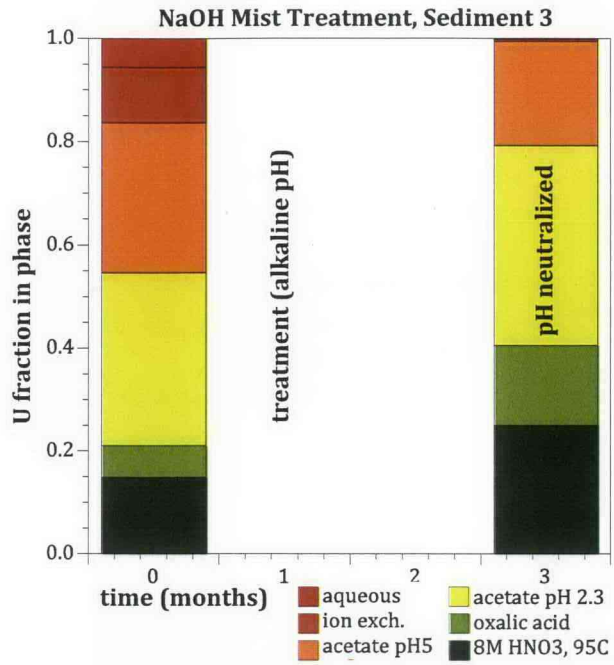

Figure 4.14. Sequential mist injection of 0.5M NaOH followed by mist injection of 0.5M HCl after 1 month. Uranium surface phases shown.

4.8 Ferric Nitrate Liquid Mist Treatment of Sediment

Aqueous ferric iron can only occur under highly acidic conditions (pH < 2.0), as it will precipitate under pH neutral to alkaline conditions of the natural Hanford Site sediment (pH 7.7 to 8.3). Under oxic conditions, addition of ferric iron (in this case as ferric nitrate) at pH 1.5 as a mist is then pH neutralized with the mist injection of a 0.5M NaOH solution (Figure 4.15) to cause precipitation in situ. As shown in Figure 4.10, while this approach appears straightforward, the spatial distribution of the water content after the first mist injection influences the spatial deposition of the NaOH during the second mist injection. The pH needs to be >4.0 to precipitate amorphous $Fe(OH)_3$, but sufficient NaOH was added to achieve pH 7.0. The same spatial distribution of pH was observed for this sequential ferric nitrate (pH 1.3), then NaOH mist injection (Figure 4.14), with a high pH in the first 20 cm of the column, then slightly acidic conditions between 20 and 100 cm, then natural sediment pH 100 to 160 cm. In addition, over time, the natural buffering capacity of the sediment will return the pH to 8.0, as illustrated in Figure 4.4 for CO_2 injection, which resulted in acidic sediment pore water that was slowly returning to natural conditions after 90 days.

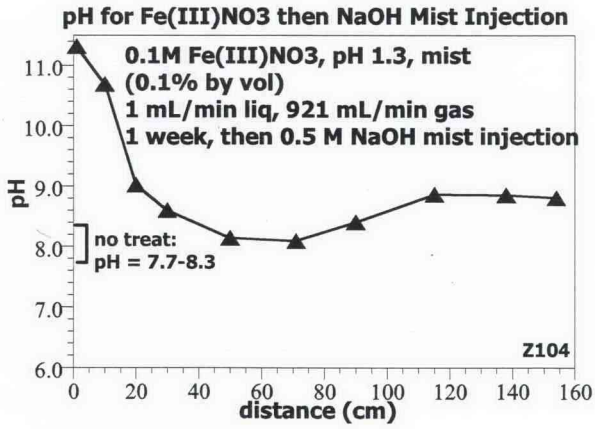

Figure 4.15. Sequential mist injection of ferric nitrate at pH 1.3 followed by mist injection of 0.5M NaOH after 1 week.

The purpose of a mist injection of ferric iron in this study is that U(VI) will substitute for the ferric iron, forming a mixed oxide [$(Fe_{1-x}, U_x)(OH)_3$]. In one 160-cm long column, ferric nitrate (pH 1.3) was injected as a mist (0.1% water content by volume); a week later, the pH was neutralized by the injection of NaOH mist (Figure 4.15). Note that mist was exiting the 160-cm-long column during both injections. Samples were also taken to characterize the ferric and ferrous iron surface phases to quantify the effect of the ferric nitrate injection (Figure 4.16).

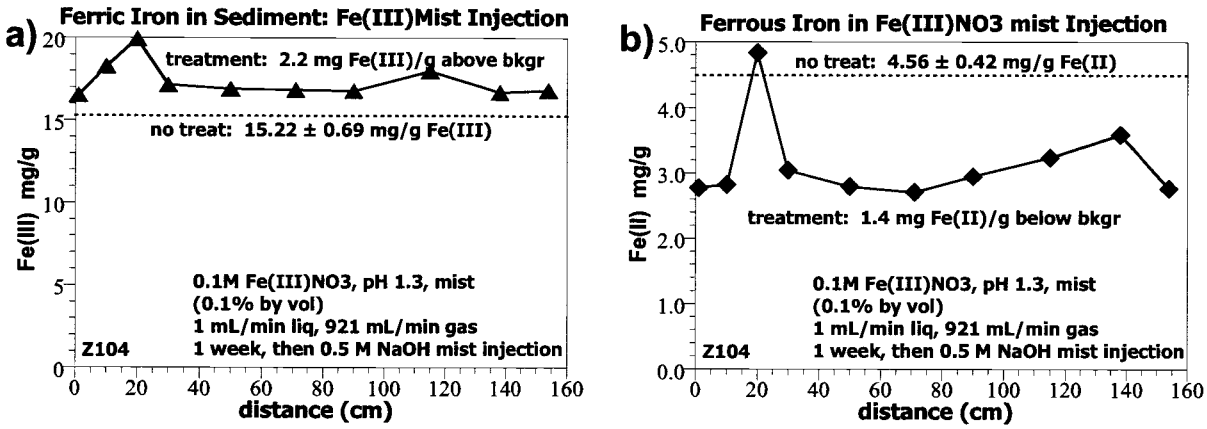

Figure 4.16. Ferric (a) and ferrous (b) iron from a 0.5M HCl extraction of the ferric nitrate mist-treated sediment.

Three untreated sediment samples were used to quantify the natural ferric and ferrous iron surface phases. Untreated sediment averaged 15.2 ± 0.7 mg ferric iron per gram of sediment and for the 10 samples taken in the ferric nitrate-treated column, all were significantly above this average (Figure 4.16a). The average ferric iron in the treated column was 17.4 ± 1.1 mg/g of sediment. The average ferrous iron in the untreated sediment was 4.56 ± 0.42 mg/g, and the treated column averaged 3.14 ± 0.65 mg/g. This decrease in ferrous iron may have been caused by some unidentified dissolution/precipitation during the pH changes.

The changes in uranium surface phases for sediments 2 and 3 were characterized by sequential extractions (Table 4.8). These experiments were conducted in small (10-cm long) columns in which the ferric nitrate at pH 1.3 was injected as a mist; then after 1 day, a second mist injection of 0.5M NaOH was conducted to neutralize the pH. In contrast to other two-step processes (CO_2 gas, NH_3 gas, HCl mist, NaOH mist), there was no need for a long time period between these two steps. The ferric iron addition to sediment resulted in a significant decrease in aqueous and adsorbed uranium for both sediments. The results for the balance of the phases were mixed (Table 4.8). The uranium associated with CO_3 rind, total CO_3, and oxides either increased or decreased for sediments 2 and 3. In both cases, the hard to extract uranium (8M HNO_3 extraction) increased, and accounted for 1/5 to 1/3 of the total uranium phase changes. Overall, there was 23% to 26% change in uranium in surface phases. Preliminary electron microprobe analysis of the ferric iron treated sediment shows locations of associated iron and uranium, which could be iron oxides with uranium substitution (to be confirmed with additional analysis).

Table 4.8. Results of Sequential Liquid Extractions of Uranium Phases for Fe^{III} Mist-Treated Sediment

Sed.	Treat-ment	Time (months)	T (°C)	H2O (%)	Total U (ug/g)	Sequential Extractions, Fraction of Total U Mass: #1 aq.	#2, ion exch.	#3, pH 5 acetate	#4, pH2.3 acetate	#5 oxalate	#6 8M H+	K_d (cm^3/g)
2	none	0 (5 samples)	22	5	74.3±2.3	0.0129	0.011	0.0385	0.744	0.137	0.0507	0.87
	Fe^{III}mist	1 month	22	5	63.6	0.0031	0.0004	0.366	0.513		0.117	0.16
	Fe^{III}mist	2 months	82	5	62.9	0.0059	0.0013	0.105	0.660	0.124	0.103	0.33
	Fe^{III}mist	3 months	82	5	40.9	0.0033	0.010	0.182	0.512	0.126	0.167	4.49
3	none	0 (6 samples)	22	5	28.1±1.8	0.0606	0.107	0.291	0.336	0.061	0.149	1.84
	Fe^{III}mist	1 month	22	5	21.2	0.0025	0.0027	0.508	0.372		0.114	3.04
	Fe^{III}mist	2 months	82	5	19.7	0.004	0.0012	0.484	0.337	0.065	0.108	0.80
	Fe^{III}mist	3 months	82	5	16.5	0.0025	0.0011	0.217	0.464	0.119	0.197	1.15
						Fraction Change to End of Experiment						Mobile*
2	Fe^{III}mist	3 months	82	5		-0.010	-0.0005	0.143	-0.232	-0.011	0.116	0.133
3	Fe^{III}mist	3 months	82	5		-0.058	-0.106	-0.074	0.128	0.058	0.048	-0.238

fraction loss (-) or gain (+) *sum of extractions 1, 2, and 3

Over the 3-month time period, nearly all of the uranium phase changes remained stable (Figure 4.17), indicating that after the initial precipitation event, the surface phases were relatively stable. As noted with other treatments, the K_d value does not accurately reflect the uranium mobility in the system, as minor changes in both aqueous and adsorbed uranium phases can change the K_d to a smaller value (apparent indication of more mobility of uranium), even though both the aqueous and adsorbed uranium after treatment are significantly smaller than before treatment (i.e., actual data show decreased uranium mobility).

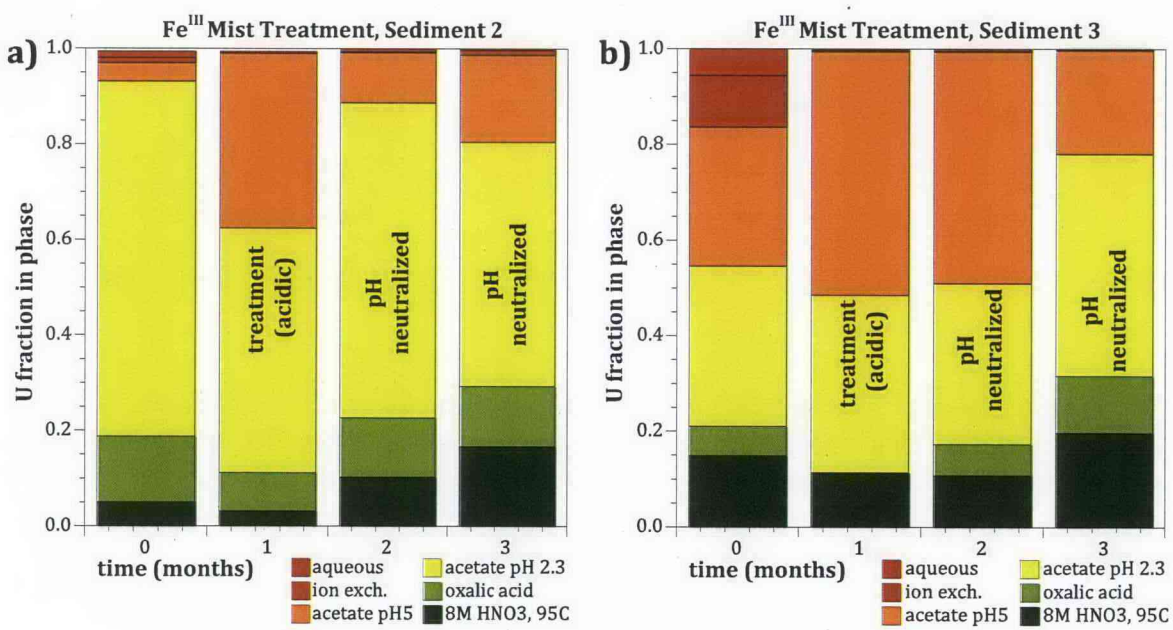

Figure 4.17. Ferric iron mist treatment of a) sediment 2 and b) sediment 3.

4.9 Phosphate Treatment of Sediment by Mist Injection

The addition of phosphate to sediment either by a liquid mist (this section) or by foam injection (following section) will result in the formation of autunite [$Ca(UO_2)_2(PO_4)_2 \cdot XH_2O$] and excess phosphate will form mono- or di-calcium phosphate and apatite [$Ca_{10}(PO_4)_6 \cdot 2H_2O$] in this mid-pH range. The formation of autunite by injection of sodium phosphate or polyphosphate mixture into sediment is well established in water-saturated sediment, as well as in unsaturated sediment (Wellman et al. 2006a, 2006b; 2007; 2008a). In this study, the phosphate mixture used for both the mist and foam injection consisted of the following: 39.9 mM Na_2HPO_4, 7.5 mM NaH_2PO_4, and 1.75 mM sodium tripolyphosphate, which creates a solution with a pH of 7.5 to 7.6 (measured).

Phosphate injection as a mist (0.1% liquid by volume) into a 160-cm column resulted in a roughly uniform moisture distribution (Figure 4.18a) averaging 6% water content (initial water content was <1%), but with greater moisture at 20 to 60 cm. Phosphate adsorbs to sediment quickly and slowly precipitates (hours to hundreds of hours), so is well known to lag relative to a conservative tracer. For this mist injection of phosphate, there was a decreasing amount of phosphate from 0 to 90 cm, with the highest concentration of 0.85 mg PO_4/g of sediment at 0 to 10 cm (Figure 4.18b).

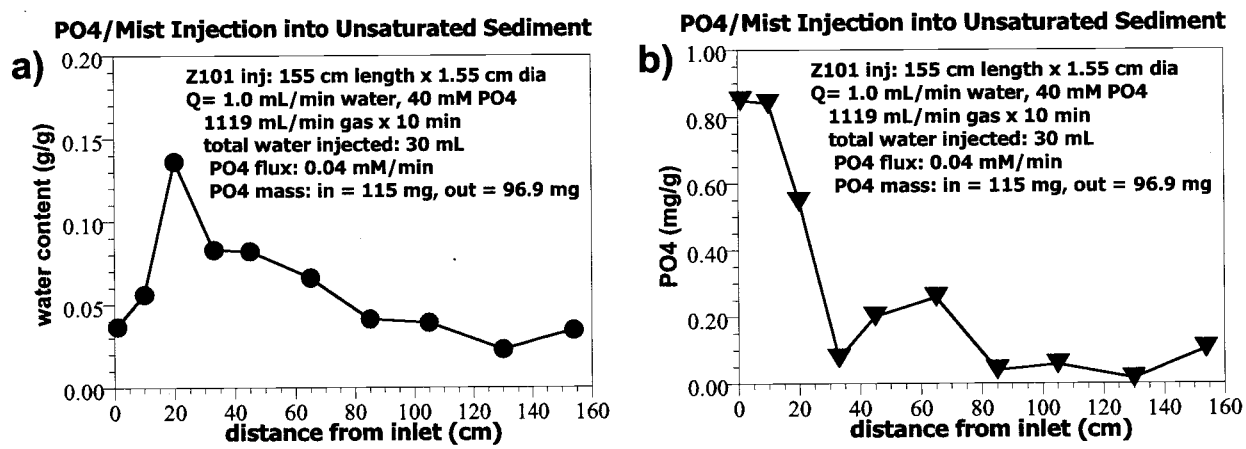

Figure 4.18. Phosphate injection as a 0.1% mist into a 160-cm-long column showing the a) resulting water content distribution and b) phosphate distribution.

The calculated phosphate mass injected into the column was within 20% of the phosphate mass injected into the column (Figure 4.18b). In conclusion, this column experiment demonstrated that some phosphate can be injected into a sediment column at low water saturation, and significant phosphate mass can be injected, allowing the water content to increase to half saturation. Note there was no attempt to optimize this process. A much higher concentration of phosphate (to 400 mM) is soluble in water, so mist injections could achieve higher phosphate concentrations in the sediment while still maintaining low water content.

Changes in uranium surface phases for sediments 1, 2, and 3 were characterized by sequential extractions. These experiments were conducted on small (10-cm long) sediment columns in which the phosphate was injected as a mist. Because these are very short columns, there should be a high concentration of phosphate deposited. For samples taken at 1 month, there was a substantial decrease in

aqueous uranium (all three sediments); however, by 3 months, aqueous uranium was actually greater than in the untreated sediment. The major changes to uranium surface phases included a substantial decrease in uranium associated with carbonate (either as a rind or the total carbonate-bound uranium), and an increase in oxide and silicates/phosphates (Table 4.9). Preliminary electron microbe analysis does show some locations with phosphorous and uranium associations. Additional analysis will be used to identify the mineral phase.

Table 4.9. Results of Sequential Liquid Extractions of Uranium Phases for PO_4 Mist-Treated Sediment

						Sequential Extractions, Fraction of Total U Mass						
Sed.	Treat-ment	Time (months)	T (°C)	H2O (%)	Total U (ug/g)	#1 aq.	#2, ion exch.	#3, pH 5 acetate	#4, pH2.3 acetate	#5 oxalate	#6 8M H+	K_d (cm^3/g)
1	none	0 (3 samples)	22	5	376.6±6.2	0.0152	0.01	0.0277	0.800	0.0818	0.0649	1.45
	PO4 mist	1 month	22	5	292.9	0.0041	0.0072	0.017	0.751		0.220	2.79
	PO4 mist	2 months	82	5	302.3	0.0605	0.0093	0.004	0.082	0.219	0.625	0.24
	PO4 mist	3 months	82	5	244.5	0.0838	0.0145	0.018	0.062	0.168	0.653	0.28
2	none	0 (5 samples)	22	5	74.3±2.3	0.0129	0.011	0.0385	0.744	0.137	0.0507	0.87
	PO4 mist	1 month	22	5	70.4	0.0008	0.0118	0.045	0.341		0.601	21.2
	PO4 mist	2 months	82	5	72.6	0.019	0.0084	0.053	0.149	0.345	0.425	0.70
	PO4 mist	3 months	82	5	53.1	0.028	0.0107	0.054	0.145	0.349	0.414	0.54
3	none	0 (6 samples)	22	5	28.1±1.8	0.0606	0.107	0.291	0.336	0.061	0.149	1.84
	PO4 mist	1 month	22	5	26.9	0.0091	0.0333	0.345	0.253		0.359	9.43
	PO4 mist	2 months	82	5	23.2	0.0373	0.0182	0.273	0.198	0.157	0.316	1.30
						Fraction Change to End of Experiment						Mobile*
1	PO4 mist	3 months	82	5		0.0686	0.0042	-0.0095	-0.738	0.086	0.588	0.063
2	PO4 mist	3 months	82	5		0.015	0.0000	0.015	-0.599	0.212	0.363	0.030
3	PO4 mist	3 months	82	5		-0.023	-0.089	-0.0184	-0.138	0.096	0.167	-0.131

fraction loss (-) or gain (+) *sum of extractions 1, 2, and 3

The loss of carbonate-bound uranium was substantial; for sediment 1, there was a 74% decrease, for sediment 2, there was a 60% decrease, and for sediment 3, there was an 11% decrease in carbonate uranium, and an additional 19% decrease in rind-CO_3 (Table 4.9, Figure 4.19). Previous work with polyphosphate addition to sediment (Wellman et al. 2007, 2008b) indicates that phosphates coat other mineral phases (including the extensive carbonate). Therefore, the apparent decrease in carbonate reported here from sequential extractions is likely incorrect, but rather carbonates are coated with phosphates resistant to the acetic acid used to extract carbonates. Uranium phase changes are not likely as extensive as reported. The oxide extraction (which may dissolve some of the autunite) resulted in a 6% to 22% increase, and the phosphate/silicate extraction resulted in a 17% to 59% increase. Overall, the performance of adding phosphate to sediment resulted in a large apparent immobilization of carbonate associated uranium, but very little change in the aqueous and adsorbed uranium. Because the addition of phosphate was at pH 7.5, it is not possible to actually dissolve the carbonates, so it is likely the sequential extraction data is reflecting phosphate precipitate coating on top of the carbonates, which limits how much carbonate can be extracted with extractions 3 (acetate at pH 5) and 4 (acetic acid at pH 2.3). Although these most mobile aqueous and adsorbed phases were initially decreased (at 1 month), the same or greater aqueous and/or adsorbed uranium gives the appearance of little treatment, especially in a field site where only the aqueous uranium is monitored (for example, through wells). This may result from incomplete time to fully form autunite during the 3-month experiments. The results suggest the phosphate should be combined with another technology for complete treatment. Certainly, the phosphate addition results in the formation of a very low solubility mineral (autunite) of lower solubility than iron

oxides. Ammonia gas treatment results in a consistent loss in all mobile phases and a gain in the phosphates/silicates (extraction 6), but the amount of fractional change was smaller than the phosphate treatment (7.3 to 24.7% compared to 26 to 75% for PO_4 addition). Therefore, one possible treatment would be to combine phosphate (mist) and ammonia gas treatments.

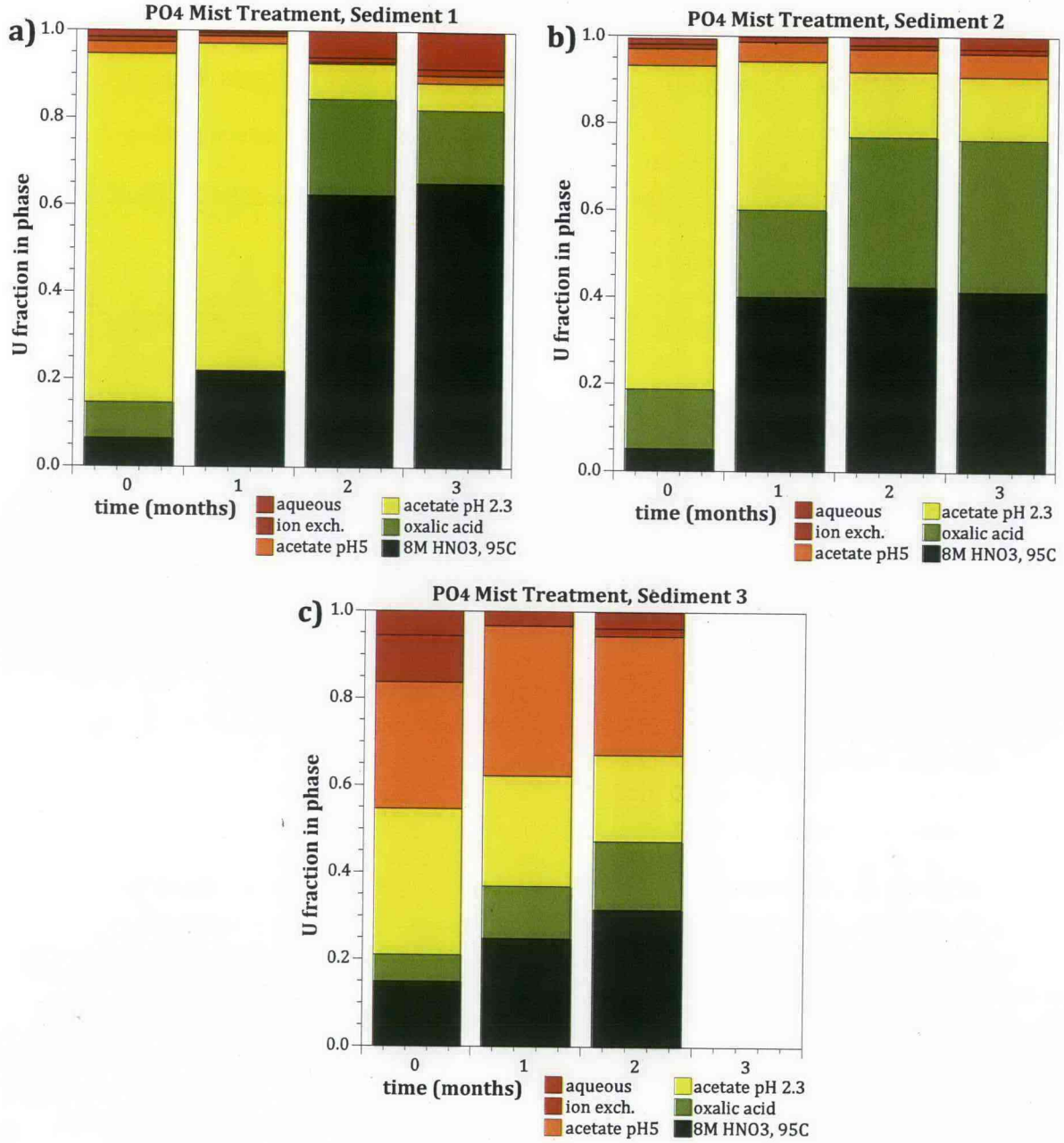

Figure 4.19. Phosphate injection as a 0.1% liquid mist and uranium surface phase changes for a) sediment 1, b) sediment 2, and c) sediment 3.

4.10 Phosphate Treatment of Sediment by Foam Injection

The addition of phosphate to sediment at slightly acidic pH (6.2) forms the low solubility mineral autunite [$Ca(UO_2)_2(PO_4)_2 \cdot XH_2O$], as described in detail in the previous section. For experiments described in this section, a surfactant (sodium laureth sulfate, as STEOL-CS-330) was used to create a foam (bubble size 0.5 to 1.0 mm) and 1% liquid (by volume) containing the phosphate solution (39.9 mM Na_2HPO_4, 7.5 mM NaH_2PO_4, and 1.75 mM sodium tripolyphosphate, pH of 7.5) was included to treat sediments. The difference between this surfactant advection of phosphate and the mist injection of phosphate (previous section) is the presence of the surfactant. Therefore, a performance decrease of the phosphate injected with foam may be attributed to additional interactions between uranium surface/ solution phases and the surfactant. Experiments conducted for this foam injection were used to a) quantify the general aspects of the foam injection process, and b) evaluate the phosphate treatment by foam injection on uranium surface phases. There was no attempt to optimize the performance of the foam injection process, nor fully evaluate uranium-surfactant complexes.

The foam injection technology uses 0.5% sodium laureth sulfate solution (30% purity) containing the phosphate mixture to inject a 0.5% to 1% water content foam into sediment. The foam has a high viscosity so it requires pressure to be advected through the sediment. Over time, pore water initially in the sediment is pushed ahead (or aside in a two-dimensional flow system) of the foam front, as the foam travels in air-filled pores. The pressure required to advect the foam into the sediment increases over time (30 to 100 psi for a 1.5-cm-diameter by 150-cm-long column), depending on the injection rate and foam quality. This is a result of a one-dimensional system because water is pushed ahead of the wetting front. In a two- or three-dimensional (field) system, the water can be pushed laterally aside from the foam front (visually observed in experiments in a previous study; see Figure 4.20). In that two-dimensional system, foam containing a phosphate solution was injected in the center of the 140-cm-wide by 40-cm-tall by 5-cm-thick system. Most of the sediment in the system was a medium sand (0.3 mm), with a lens of coarser sand on the left (dark rectangle, Hanford Site sediment), and two lenses of finer sand on the right (two tan rectangles of 0.15-mm sand). Over time, the foam front expanded, with a "halo" of higher water content in front of the foam front. By 24 h, foam was exiting both sides of the flow system, but most of the flow was toward the high-K zone (left side). Foam was exiting the system in the bottom one-third of the system, and the water content halo was now seen laterally (above) the foam front. Samples taken after the experiment confirmed high water content in these areas, and most phosphate was deposited in the high water content area above the high-K zone.

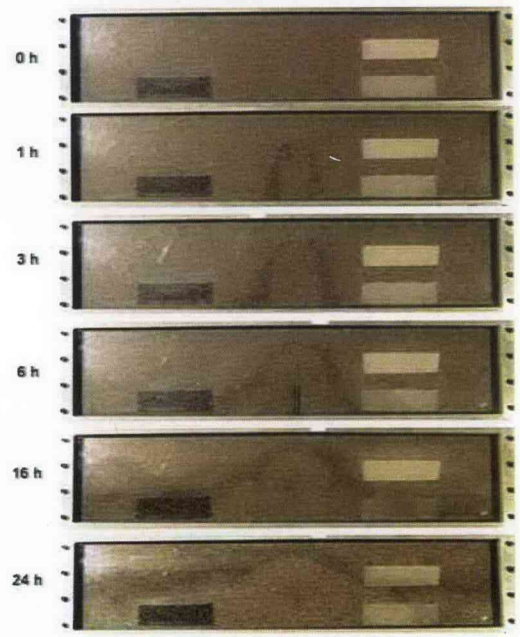

Figure 4.20. Development of the residual water content halo over time for foam injection in a two-dimensional system (Szecsody et al. 2009).

In this project, three one-dimensional column experiments (70 cm to 160 cm in length) were conducted to evaluate transport of phosphate using foam. For a 50-mM phosphate injection, although the foam front reached 40 cm and the pore water was in front of this foam front (Figure 4.21a), the phosphate only reached 10 cm (Figure 4.21b). For a 250-mM phosphate injection at a higher foam flow rate, the foam front reached 105 cm (visual observation, Figure 4.21d), with the pore water being pushed ahead of it (Figure 4.21c), and phosphate reaching 30 cm (Figure 4.21d).

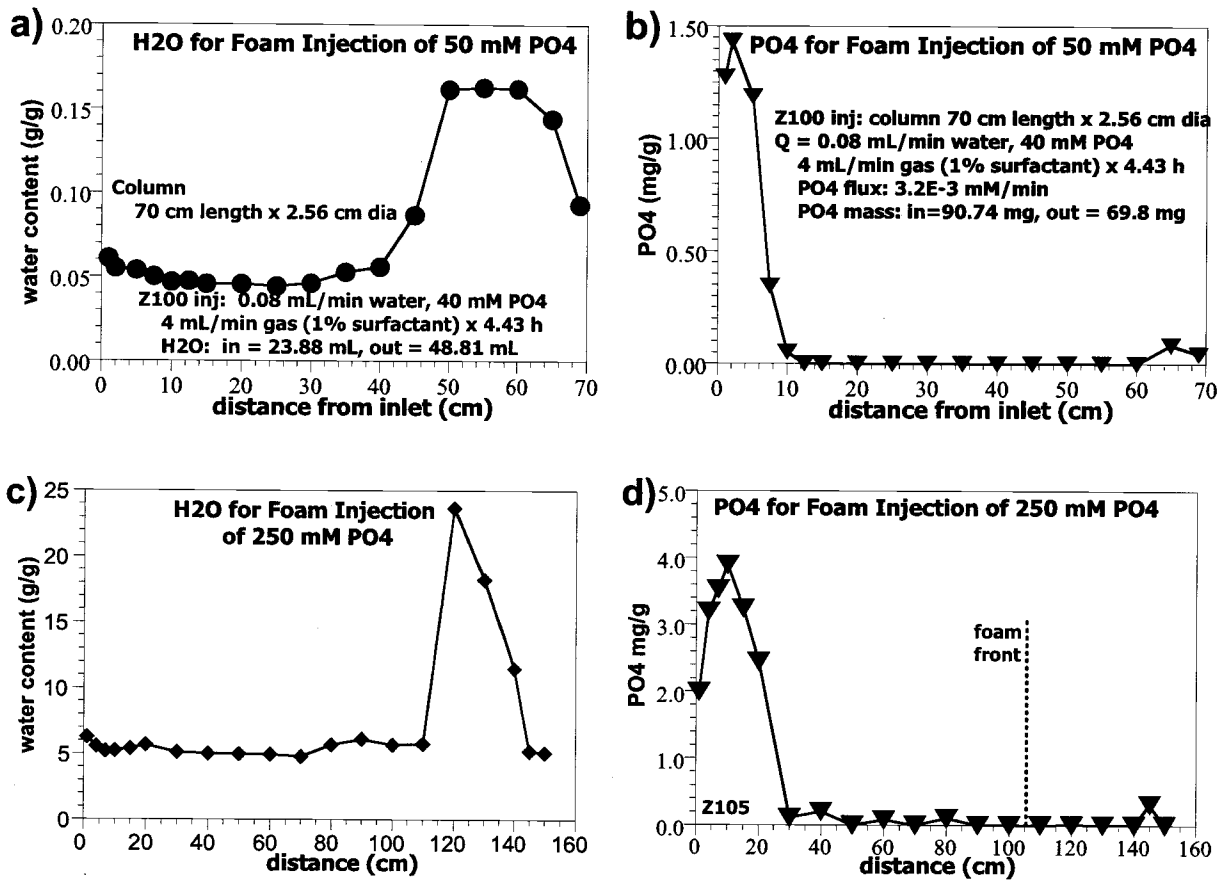

Figure 4.21. Foam injection with PO_4 into unsaturated one-dimensional columns with 50 mM PO_4 (a, water content; b, PO_4) and with 250 mM PO_4 (c, water content; d, PO_4).

One additional foam injection experiment was conducted to further quantify questions related to the foam advection process. Foam injection involves gas movement, the surfactant, pore water (initially in the column), water advected with the foam, and chemicals (phosphate in this case) in the injected water. An understanding of the interaction between processes that control the relative lag of these different phases/chemicals is needed to understand the transport of phosphate in the foam injection. It was hypothesized that the foam is breaking and reforming (thereby lagging relative to the air being injected with the foam). This processes was investigated by initially filling the sediment column with pure nitrogen gas, then injecting foam using air (21% oxygen) and having oxygen electrodes monitor the effluent oxygen breakthrough. It was also hypothesized that the foam front is limited by the surfactant concentration. To quantify this process, sediment samples taken after the experiment were analyzed for the surfactant concentration. Visually, the foam front showed some bubbles reaching 140 cm after 6.5 h

(Figure 4.22a) as the pressure approached 35 psi at the inlet. In contrast, the gas (air) used to make up the bubbles broke through in 1.1 h (Figure 4.22b). Because the foam front reached halfway through the column (75 cm) in 4.6 h, the foam had a retardation of 8.4 relative to the gas in the foam. This indicated significant bubble breakage, but bubbles clearly reformed, or the front would not have advanced.

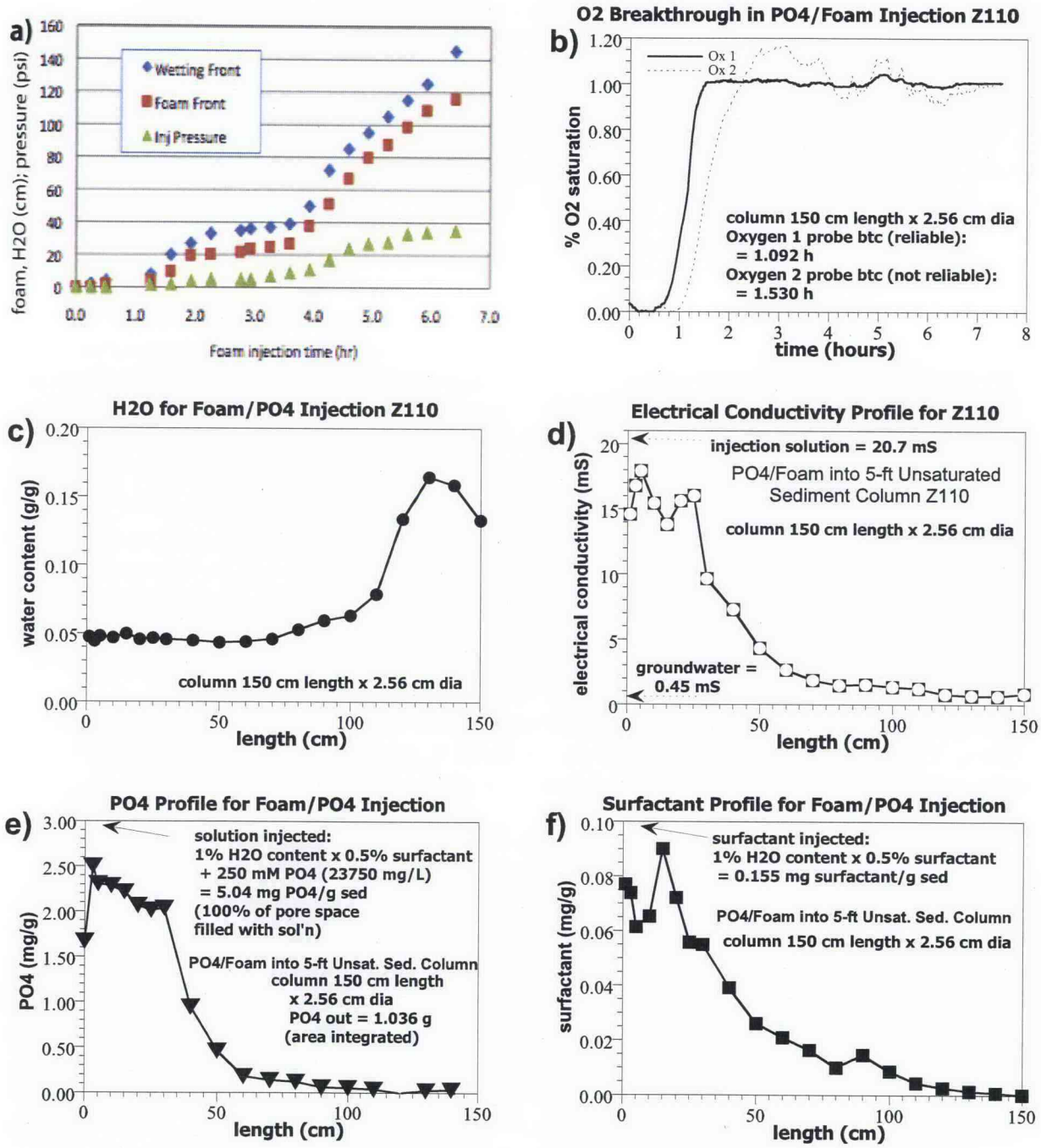

Figure 4.22. Foam with 250 mM PO_4 injection into a 150-cm-long sediment column: a) foam advance and pressure increase over time, b) O_2 breakthrough, c) moisture profile, d) electrical conductivity profile of pore water, e) phosphate profile of pore water, and f) surfactant profile of pore water.

At the end of this foam injection experiment, samples taken along the 150-cm length were analyzed for moisture content, electrical conductivity, phosphate, and surfactant concentration. As shown in previous experiments, a pore-water front advanced ahead of the foam front (Figure 4.22c). To quantify whether any of the chemicals in the foam (and the water) associated with the foam are advancing, the electrical conductivity of the pore water was measured (Figure 4.22d), which clearly showed that the water in ahead of the plume front is original pore water and not water associated with the foam injection. The surfactant (Figure 4.22f) advanced to about 100 cm (at low concentration), so the visual observation correctly identified that front. It is likely this front stops due to bubbles not being able to reform at the low surfactant concentration. The phosphate (Figure 4.22e) lagged somewhat relative to the surfactant front. The pressure increase is caused by resistance transporting the foam (i.e., Figure 4.23), not movement of the water front ahead of the foam (Figure 4.21c).

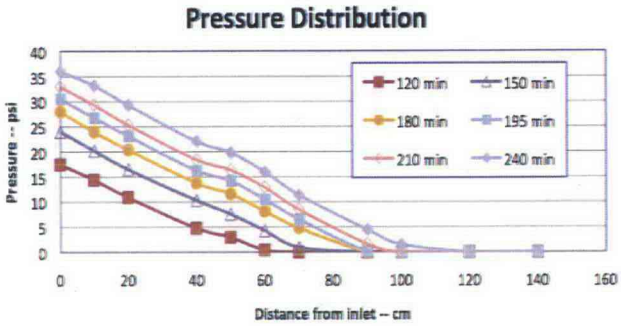

Figure 4.23. Pressure profile in 160-cm column.

At field scale, if foam were injected into a well (radial flow), there would be a smaller pressure increase than noted in these one-dimensional experiments. However, eventually the same processes of pressure limited foam injection would occur if a fully screened injection were to occur. At field scale, this pressure increase limitation could be minimized by changing the foam injection strategy. For example, if limited vertical zones were used to inject foam into (for example, alternating 5-ft injection zones with 5 ft of no injection in between), then the pore-water front could be pushed laterally rather than ahead of the wetting front (as shown in Figure 4.19), thus minimizing the pressure needed to move the water ahead of the wetting front.

The changes in uranium surface phases for sediments 1, 2, and 3 were characterized by sequential extractions (Table 4.18). These experiments were conducted in small (10-cm long) columns in which the phosphate was injected with the surfactant as a foam with 1% water content.

In contrast to the 70- to 160-cm-long columns previously discussed, there was significant (and relatively uniform) foam and phosphate transport in the 10-cm-long columns. Results of the uranium phase changes over 1 to 3 months (Table 4.10); for those PO_4 injections using foam, results were similar to the phase changes described in Table 4.16 for the PO_4 mist injections. The most mobile aqueous and adsorbed uranium phases generally increased, but there was an apparent significant loss in carbonate associated uranium and a significant increase in oxide and PO_4/silicate uranium phases. Compared to the PO_4 injected with a mist, the foam-injected PO_4 experiments resulted in smaller increases in the immobile uranium phases, and there were larger gains in the aqueous and adsorbed uranium fractions (changes in Table 4.19 compared to Table 4.17). This appears to indicate the presence of the surfactant may increase the uranium mobility. Experiments were not conducted investigating the partitioning of uranium between the solution and surface in the presence of the surfactant. Even though somewhat less effective than the PO_4-mist injections, the foam-injected PO_4 still produced significant (41% to 51%) change in the fraction of uranium associated with immobile surface phases (Figure 4.24).

Table 4.10. Results of Sequential Liquid Extractions of Uranium Phases for PO_4 Foam-Treated Sediment

						Sequential Extractions, Fraction of Total U Mass						
Sed.	Treat-ment	Time (months)	T (°C)	H2O (%)	Total U (ug/g)	#1 aq.	#2, ion exch.	#3, pH 5 acetate	#4, pH2.3 acetate	#5 oxalate	#6 8M H+	K_d (cm^3/g)
1	none	0 (3 samples)	22	5	376.6±6.2	0.0152	0.010	0.0277	0.800	0.0818	0.0649	1.45
	PO4 foam	1 month	22	5	246.3	0.0070	0.0019	0.015	0.727	0.102	0.148	0.44
	PO4 foam	2 months	82	5	297.9	0.0619	0.0270	0.047	0.201	0.143	0.520	0.69
	PO4 foam	3 months	82	5	205.8	0.1395	0.0283	0.022	0.162	0.140	0.508	0.31
2	none	0 (5 samples)	22	5	74.3±2.3	0.0129	0.011	0.0385	0.744	0.137	0.0507	0.87
	PO4 foam	1 month	22	5	50.3	0.010	0.0073	0.033	0.290	0.463	0.198	1.08
	PO4 foam	2 months	82	5	62.5	0.028	0.0070	0.062	0.166	0.357	0.380	0.35
	PO4 foam	3 months	82	5	51.9	0.037	0.0133	0.071	0.168	0.338	0.373	0.53
3	none	0 (6 samples)	22	5	28.1±1.8	0.0606	0.107	0.291	0.336	0.061	0.149	1.84
	PO4 foam	1 month	22	5	25.2	0.015	0.018	0.351	0.363	0.103	0.149	3.07
	PO4 foam	2 months	82	5	25.9	0.035	0.026	0.098	0.223	0.280	0.340	1.90
						Fraction Change to End of Experiment						Mobile*
1	PO4 foam	3 months	82	5		0.1243	0.0180	-0.0055	-0.638	0.0578	0.443	0.137
2	PO4 foam	3 months	82	5		0.024	0.0030	0.032	-0.576	0.201	0.323	0.059
3	PO4 foam	3 months	82	5		-0.026	-0.081	-0.193	-0.113	0.219	0.191	-0.300

fraction loss (-) or gain (+) *sum of extractions 1, 2, and 3

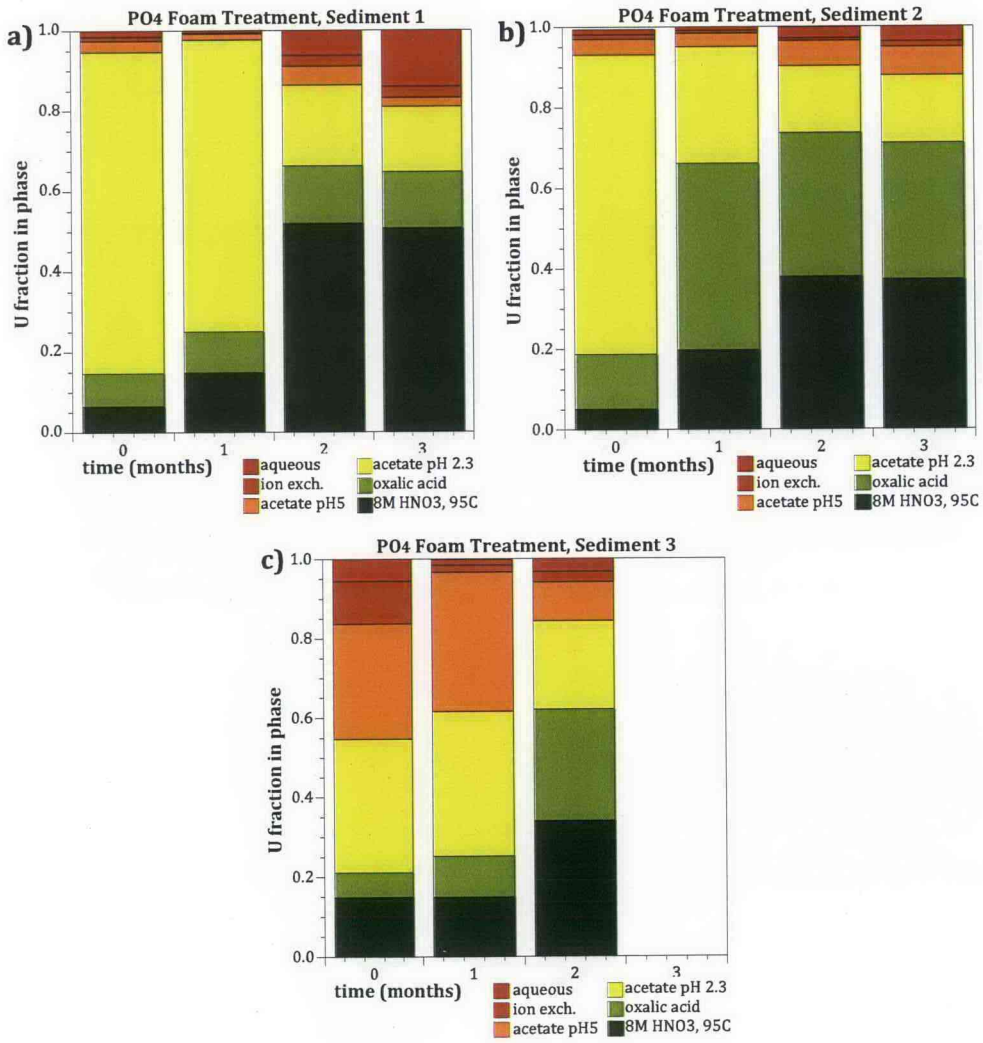

Figure 4.24. Phosphate treatment of sediments by foam/surfactant delivery with changes in uranium surface phases shown for a) sediment 1, b) sediment 2, and c) sediment 3.

5.0 Discussion

Evaluation of these geochemical technologies to alter uranium surface phases involves not only a comparison of the geochemical results, and additional consideration of the following:

- uncertainty in the sequential extraction results to accurately identify the uranium surface phase changes
- variability in the uranium surface phase change between sediments (containing a different mixture of surface phases)
- ability to upscale the advection technology used (i.e., gas, mist, or foam)
- long-term implication of the uranium surface phase changes to alter uranium mass mobility in the vadose zone.

The geochemical performance of the technologies is described in Section 5.1, and the physical performance of the advection method used is described in Section 5.2. Finally, one-dimensional vertical infiltration simulations in the vadose zone to address the long-term implications of the uranium surface phase changes are described in Section 5.3.

5.1 Short-Term Geochemical Performance: Change in Uranium Mobility

A comparison of the uranium surface phase changes observed by sequential extractions (Table 5.1) is reported as fraction change relative to untreated sediment. All nine of the technologies were used with sediment 3 (Figure 5.1), and seven technologies were used with sediment 2 (Figure 5.2). The most mobile uranium surface phases are the aqueous (extraction 1), adsorbed (extraction 2), and rind-CO_3 phases (extraction 3), and progressively less mobile surface phases are uranium associated with all of the carbonate (extraction 4), oxides (extraction 5), and silicates/phosphates (extraction 6). Minerals in natural sediments are not completely accessed by the extraction liquid due to mineral coatings on other minerals. If a harder to extract phase (silicate, for example) is partially coating a more mobile phase (carbonate, for example), the carbonate extraction will not completely dissolve all of the carbonates. As such, liquid extractions provide some useful information as to the uranium surface phases (and are considered operational definitions of extracted phases), but more positive identification (by XRD, electron microprobe, or other techniques) are needed to positively identify uranium phases in the natural and treated sediment. It should also be noted that the additional process of slow diffusion of uranium out of sediment microfractures along with the slow dissolution of different uranium surface phases all contribute to the complex pattern of uranium release over time observed in the field.

The two reductive gas treatments (H_2S and SO_2) in general showed little change. For H_2S gas, there was no observed change over 3 months for sediment 3, and a slight increase in aqueous uranium for sediment 2. For SO_2 gas, there was also a slight increase in aqueous uranium for sediment 2. SO_2 treatment of sediment 3 (Figure 5.1i) showed almost no change from the untreated sediment for 2 months, then less aqueous, adsorbed, and rind-CO_3 at 3 months. Since this is an inconsistent change relative to previous months, the results are likely not valid.

Table 5.1. Sediment Treatment and Change in Uranium Surface Phases by 3 Months

Treat-ment	Sed.	H_2O %	Fraction increase (+) or loss (-) by 3 months #1 aq.	#2, ion exch.	#3,pH 5 acetate	#4,pH2.3 acetate	#5 oxalate	#6 8M H+	Mobile #1+#2+#3	Immobile #5+#6
H_2S gas	2	5	0.007	0.002	0.001	0.015	-0.050	0.030	0.011	-0.020
	3	5	-0.006	-0.011	-0.034	0.034	0.035	-0.022	-0.051	0.012
SO_2 gas	2	5	0.023	0.003	0.023	-0.015	-0.055	0.027	0.050	-0.028
	3	5	-0.019	-0.055	-0.181	0.305	0.005	-0.059	-0.255	-0.055
HCl mist	3	5	-0.047	-0.096	-0.186	0.178	0.069	0.079	-0.329	0.148
CO_2 gas	2	5	0.002	-0.004	-0.005	-0.054	0.022	0.089	-0.008	0.067
	3	5	-0.027	-0.071	-0.124	-0.035	0.059	0.193	-0.222	0.252
	3*	15	-0.047	-0.075	-0.092	-0.040	-0.077	0.330	-0.213	0.253
NaOH mist	3	5	-0.06	-0.103	-0.089	0.052	0.094	0.101	-0.252	0.196
NH3 gas	2	5	0.000	-0.002	-0.018	-0.001	-0.044	0.073	-0.021	0.028
	3	5	-0.026	-0.064	-0.167	-0.035	0.041	0.247	-0.257	0.288
	3*	15	-0.081	-0.109	-0.162	0.086	0.043	0.222	-0.352	0.265
Fe^{III}mist	2	5	-0.010	-5E-04	0.143	-0.231	-0.011	0.116	0.133	0.105
	3	5	-0.058	-0.106	-0.074	0.128	0.058	0.048	-0.238	0.106
PO4 mist	1	5	0.069	0.004	-0.010	-0.738	0.086	0.588	0.063	0.674
	2	5	0.015	0.000	0.015	-0.599	0.212	0.363	0.030	0.575
	3	5	-0.023	-0.089	-0.018	-0.138	0.096	0.167	-0.131	0.263
PO4 foam	1	5	0.124	0.018	-0.005	-0.638	0.058	0.443	0.137	0.501
	2	5	0.024	0.003	0.032	-0.576	0.201	0.323	0.058	0.524
	3	5	-0.026	-0.081	-0.193	-0.113	0.219	0.191	-0.300	0.410
			mobile phases			immobile phases				

Three treatments that acidified the sediment pore water were CO2 gas, HCl mist, and ferric iron mist, although there were additional geochemical differences between the treatments. The HCl mist added only acid, and decreased the most mobile uranium phases (aqueous and adsorbed uranium), and increased oxide and silicate uranium (Figure 5.1f). The HCl mist was only conducted on sediment 3 in a single column analyzed at 3 months. CO_2 gas treatment did result in similar uranium surface phase changes, with decreased aqueous and adsorbed uranium, with increased oxide and silicate uranium (sediment 3) and a minor oxide/silicate uranium for sediment 2 (Figure 5.2b). In addition, there was a significant increase in mobile uranium phases at 1 month during the CO_2 treatment (i.e., CO_2 was flushed out of the columns after 1 month). Although pore-water pH changed with water content for CO_2 gas treatment (Figure 4.7a), uranium surface phase changes did not (Figure 5.1d, e). These results for CO_2 gas treatments show promising—yet somewhat inconsistent—results between sediments. In comparison to the HCl treatment, the addition of the extra carbonate with the CO_2 gas maintained or increased uranium in the most mobile phases. In general, it appears that a two-step treatment of acidifying, then neutralizing the sediment pH did immobilize some uranium, likely in iron, manganese, and aluminum oxides. Mist injection of ferric nitrate at pH 1.5 showed a greater decrease aqueous and adsorbed uranium, an increase in rind-CO_3-associated uranium (somewhat mobile phase), and equal or lesser increase in oxides/silicates compared to CO_2 gas or HCl treatment.

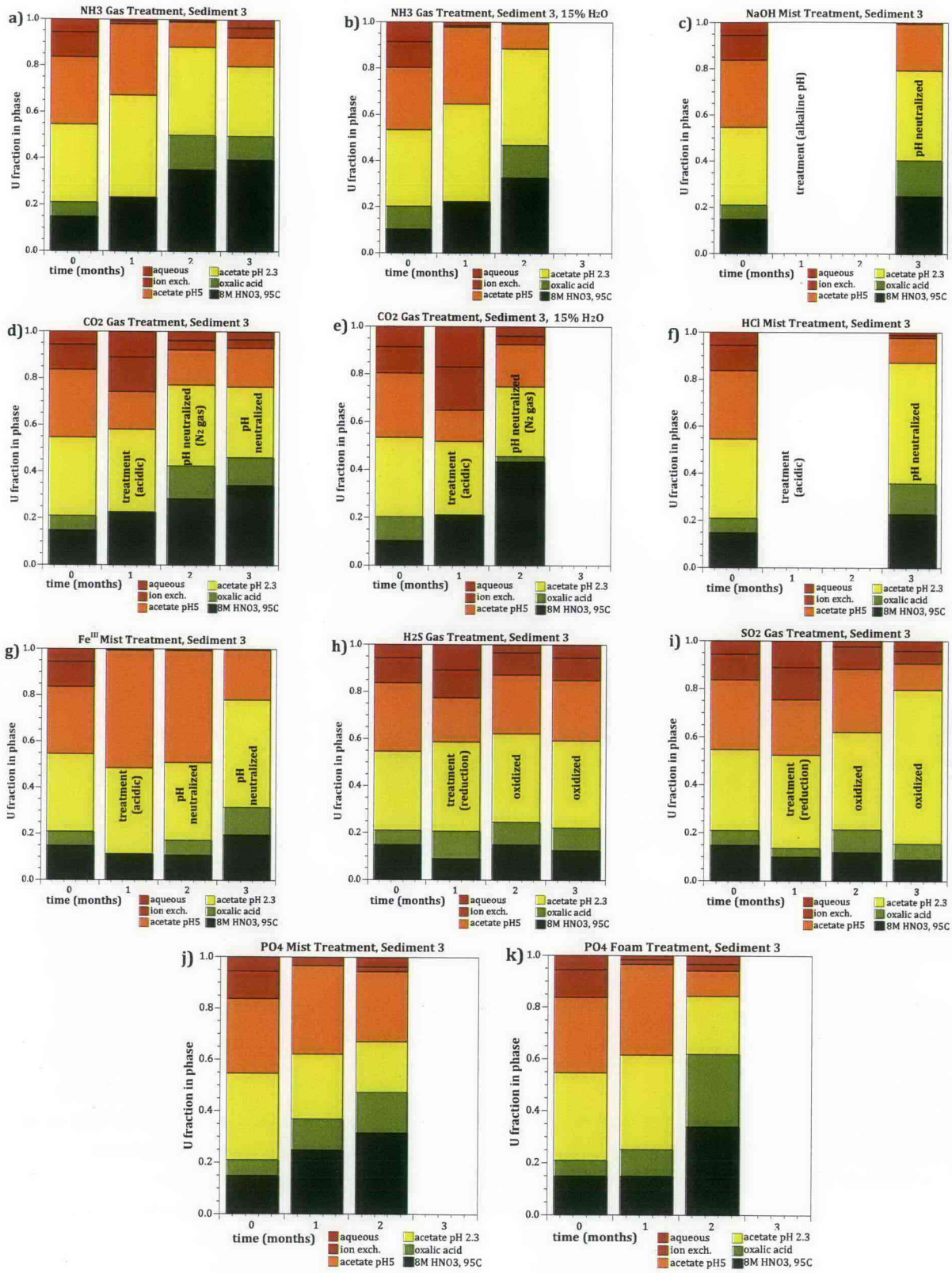

Figure 5.1. Sediment 3 treatment by a) NH_3 gas at 5% water content, b) NH_3 gas at 15% water content, c) NaOH mist, d) CO_2 gas at 5% water content, e) CO_2 gas at 15% water content, f) HCl mist, g) ferric iron mist, h) H_2S gas, i) SO_2 gas, j) PO_4 mist, and k) PO_4 foam.

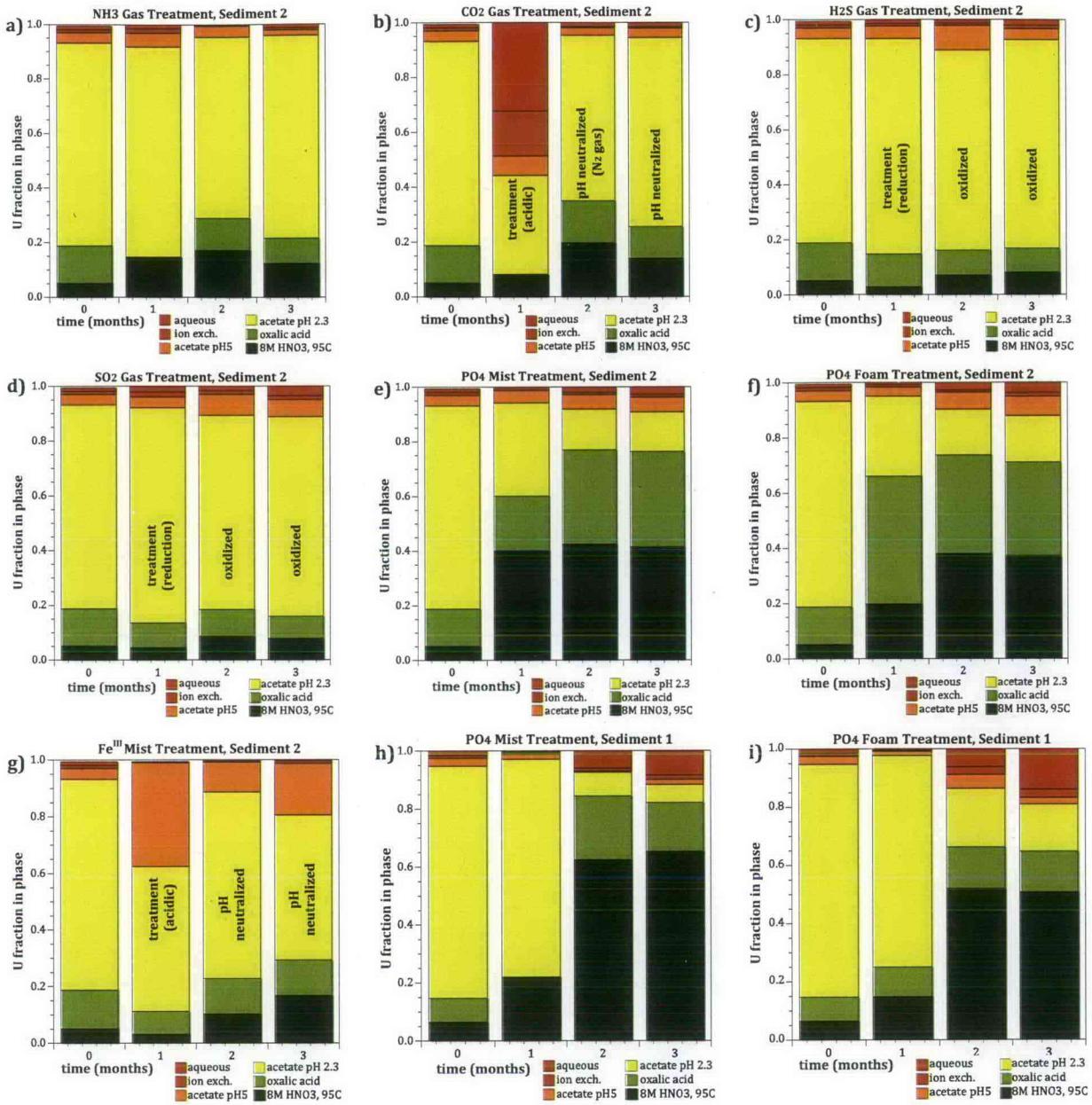

Figure 5.2. Sediment 2 treatment by a) NH_3 gas, b) CO_2 gas, c) H_2S gas, d) PO_4 mist, e) PO_4 foam, f) SO_2 gas, and g) ferric iron mist. Sediment 1 treatment by h) PO_4 mist, and i) PO_4 foam.

Two treatments that increased sediment pore-water pH to temporarily dissolve aluminosilicates were NH_3 gas and NaOH mist. The NaOH mist treatment (Figure 5.1c) greatly decreased aqueous and adsorbed uranium (25%) and significantly increased uranium in oxides/silicates for sediment 3. Unfortunately, the NaOH mist treatment was not tested on sediment 2. The NH_3 gas treatment showed similar results, with decreased aqueous and adsorbed uranium, and increased oxide/silicate-associated uranium that were consistent changes for both sediment 2 (Figure 5.2a) and sediment 3 (Figure 5.1a, b). Increased water content (15% versus 5%), which had little effect on the sediment pH (Figure 4.11a), had little effect on changes in uranium surface phases (Figures 5.1a, b). The NH_3 gas showed less reactivity

for sediment 2 (Figure 5.2a), which may be related to the specific aluminosilicate(s) that are readily dissolved in sediment 3 (Figure 5.1a) are at a lower concentration. Further identification of the major mineral phases involved in dissolution/precipitation is needed.

Finally, phosphate treatment of sediments at near neutral pH (pH = 7.5) was delivered as a mist and used a surfactant (foam). Apparent changes (Table 5.1) show a large (10% to 50%) increase in silicates/ phosphates for sediments 1, 2, and 3, and a corresponding decrease in CO_3-U. Sediment 2 showed a significant apparent change in surface uranium phases, which was not observed with CO_2 or NH_3 treatment, likely because phosphate treatment is not dependent on the dissolution of specific mineral phases (i.e., precipitate components are added).

Because carbonates are not dissolved by the near neutral solution, it is likely phosphate precipitates formed are coating some of the carbonates. This hypothesis would need to be proven by additional experiments (demonstrating the carbonate-associated uranium is not decreased). Thus, there may be in actuality a smaller increase in silicate-PO_4-associated uranium, but once that phosphate precipitate is dissolved (extraction 6, 8M HNO_3), the underlying carbonate is also dissolved. Phosphate treatment of sediment also increased (sediment 2) or decreased (sediment 3) the most mobile uranium (aqueous, adsorbed). Phosphate treatment with foam showed similar results to mist treatment, but the uranium immobilization was not as great, implying the additional presence of the surfactant increased uranium mobility. Additional experiments would be needed to investigate the uranium-surfactant reactions.

Overall, alkaline sediment treatment (NH_3 gas, NaOH mist) decreased uranium mobile phases (aqueous, adsorbed, rind-CO_3) by 25% to 35%, and created lower solubility oxides/silicates. Acidic sediment treatments (CO_2 gas, HCl mist) also decreased uranium mobile phases by 21% to 33%, but treatment with CO_2 did greatly increase uranium mobility during the actual treatment phase (i.e., before pH neutralization). Reductive treatments (H_2S gas, SO_2 gas) were ineffective. Phosphate treatments (delivered by mist or foam) showed an inconsistent 14% increase to 30% decrease in uranium mobile phases, and an apparent large increase in phosphate/silicates. The phosphates formed likely coated some carbonates, so actual uranium associated with phosphates may not be as great as reported.

5.2 Short-Term Performance: Evaluation of Injection Technology

Three different phases were used to advect reactants into the uranium-contaminated sediment: gas (for CO_2, NH_3, H_2S, and SO_2), mist (for NaOH, Fe(III), HCl, and PO_4), and foam (for PO_4). The primary focus of this 2009 study was to evaluate the different reactants for changes in uranium surface phases, and not to optimize the injection strategy. For the uranium surface phase tests, short (10-cm long) one-dimensional columns were used, and in general, the reactant was advected into the column in excess. Some experiments were conducted in longer one-dimensional columns (to 160-cm length) to provide some characterization of the transport and reactivity of the gas-, mist-, or foam-advected reactant.

Reactive gasses (CO_2, NH_3, H_2S, and SO_2) have advantages relative to mist or foam advection for vadose zone remediation due to no increase in the pore water content, which can increase uranium (and other contaminant) mobility. Reactive gasses can also likely achieve the greatest areal extent from the injection well. At the field scale, long-term gas injection would have to be humidified to not dry out sediments, as some pore water is needed for reactions to occur. Of the gasses used, H_2S, SO_2 (Figure 4.3b), and CO_2 (Figure 4.7a) showed more reactivity at lower water content. Ammonia gas

(Figure 4.11a) reactivity only increased a small extent at lower water content (2%). Scale up of the use of reactive gasses to field scale would involve evaluation of concentration obtained during radial injection considering the effects of gas diffusion, and vertical buoyancy (i.e., gas density difference relative to air will move the gas up or down). In addition, the geochemical change effected by the reactive gas injection may need to be neutralized. Both ammonia and carbon dioxide effect a pH change, and experiments were conducted to evaluate whether the carbonate-saturated sediment would buffer the pH over time. Ammonia-gassed sediment showed a pH decrease from 11.8 (at 1 week) to 9.5 by 90 days (Figure 4.11b), whereas CO_2-gassed sediment showed a pH increase from 5.8 (at 1 week) to 7.1 by 90 days (Figure 4.7b), so both were approaching the natural sediment pH (8.0). Although further evaluation is needed, these preliminary results indicate that pH neutralization (i.e., by a second step such as air injection) may not be needed.

Mist injection refers to a high volume of air with a low volume of aqueous reactant present in fine droplets. Advantages of using a mist is any aqueous reactant can be used, a low water content can be generally maintained, and there are no additional chemicals to evaluate (i.e., foam uses a surfactant). Mist injection has been used at field scale for injection of ZVI particles, but in this study was used to advect an aqueous reactant (HCl, NaOH, $Fe^{III}(NO_3)_3$ at pH 1.5, PO_4). Although mist can successfully advect water into a 160-cm-long one-dimensional column and results in a uniform water content deposited (Figure 4.9a), scale up to the field will be significantly different for a radial flow field of a well. Nonuniform water content profiles can also result (Figure 4.9b). Because the volume of pore space increases with the square of the distance from a well, at field scale, as the mist velocity will decrease, water (and reactant) will be deposited closer to the injection source compared to a linear flow system. Therefore, it is hypothesized that mist technology will suffer from limited areal extent relative to gas injection. Laboratory experiments could be conducted in radial flow systems (i.e., wedge shaped) to develop the mist technology. ARS Consultants use a four-nozzle system for spraying water with ZVI through a well screen, moving the system up and down in the well. Several of these mist technologies (HCl, NaOH, ferric iron at pH 1.5) also suffer from a complication that a second step of pH neutralization is needed. If the first mist injection results in a nonuniform water content with distance (i.e., Figure 4.9b), the second mist injection to neutralize pH is more difficult to emplace uniformly, and in a few limited cases, is deposited closer to the injection source (i.e., Figure 4.10b for second injection; Figure 4.10a is the first injection).

Foam was also used as a carrier of an aqueous reactant (PO_4) in this study. Foam at 1% water content using 0.5% sodium laurel sulfate (a surfactant) was generated with a 10-micron frit, which resulted in 0.1- to 0.6-mm sized bubbles. No attempt was made to improve the longevity of the foam (i.e., smaller bubbles and/or a solution with stabilizers have a greater stability half-life). Advantages of using foam are that a low water content aqueous reactant can be injected relatively uniformly into sediment. This technology is in the development stage, and experiments in this technology and other studies have had limited results advecting foam more than 100 cm (even in a 600-cm-long one-dimensional column). The foam used in this study has a relatively short half-life, as shown by significant bubble breakage (Figure 4.21b, breakthrough of the gas in the bubbles). The limited areal extent of the foam (Figure 4.21a) is controlled by the decreasing surfactant concentration (Figure 4.21f) and pressure buildup (Figure 4.22). Modification of the foam technology for greater bubble longevity should result in greater transport of aqueous reactants. Foam transport at field scale will involve optimizing multiple processes, including the gas in the foam, the moisture content front that is advected ahead of foam front, degradation of the foam, and transport of the reactant in the foam. Even with these complications, foam is a promising remediation

technology, and has significant advantages compared with water injection of the same chemical. Comparison of foam- versus water-injection of a reductant (sodium polysulfide) in a separate study (Zhong et al. 2009a, b) showed that both chromate and pertechnetate mobilization was significant for the water injection, but much more limited in extent for the foam injection. Another disadvantage of foam is that another chemical (the surfactant in this case) is introduced into the system. A comparison of PO_4 injection using mist to foam showing somewhat minor increases in uranium mobile phases for the foam may be indirect evidence for the influence of the surfactant. It was hypothesized that the presence of the surfactant may increase uranium mobilization, although experiments were not conducted to assess the influence of the surfactant on uranium mobilization.

5.3 Long-Term Predicted Performance – Simulation of Uranium Transport

Laboratory experiments with the different sediment treatments quantified some aspects of the change in sediment geochemical and physical environment and changes in uranium surface phases. Although it was desired to decrease the most mobile surface phases (aqueous, adsorbed, rind-CO_3) and increase less mobile surface phases (uranium associated with total carbonates, oxides, silicates, and phosphates), simulations were used to provide an estimate of the long-term impact of these phase changes. A total of five uranium phases were used in this modeling (aqueous uranium, adsorbed uranium, rind-CO_3, carbonate-CO_3, and oxide/silicate/PO_4 associated uranium), as described in detail in Section 3.0. Because actual uranium speciation is not being used, these simulations are only an approximation of the time delay and concentration decrease of uranium surface phase changes, and are not intended to be used to predict actual uranium concentrations leaching out of the vadose zone. In addition, the slow physical release (i.e., diffusion) of uranium from sediment microfractures that is observed in Hanford Site sediments was not included in these simulations.

The hypothetical plume is based on a profile from the BX-BY Tank Farm, with uniform uranium (in multiple phases) at an elevation of 99 to 170 ft (land surface at 270 ft, water table at 17 ft). For the base case (no treatment), the uranium laden zone has a total of 160 μg U/g of sediment (327.5 μg U/cm^3) partitioned between 5.4% aqueous; 14% adsorbed; 33% rind-CO_3; 40% balance of the CO_3; and 7.6% oxide, silicate, and phosphate (Figure 5.3). This distribution is the uranium phase distribution for sediment 3. There is downward migration of the different phases due to infiltration of precipitation (6 cm/year) and the slow dissolution/reprecipitation of carbonate and oxide phases. Simulation results in this section are shown as a vertical profile, and reported as breakthrough curves at a 98-ft elevation (i.e., directly beneath the current uranium plume location to assess migration) and at a 27-ft depth (10 ft above the water table, outside the influence of the capillary zone).

The relatively rapid movement of aqueous and adsorbed uranium (Figure 5.3) is due to a low K_d (0.1 cm^3/g, retardation factor = 2.0), and the center of the adsorbed uranium plume reaches a 27-ft elevation in 180 years (second series of profiles are at 130 years). A tracer reaches the water table in 90 years (shown). The rind carbonate associated uranium reaches the 27-ft elevation by 400 years, with the center of this plume at 800 years. The balance of carbonate with incorporated uranium migrates more slowly, so the center of this plume reaches the 27-ft elevation in 4000 years. The oxide, silicate, and phosphate plume is the slowest to migrate, with the lowest solubility (slower dissolution and reprecipitation rate). This small amount of mass (7.6%) is dispersed over time, but the center of the plume reaches 27 ft by 8000 years.

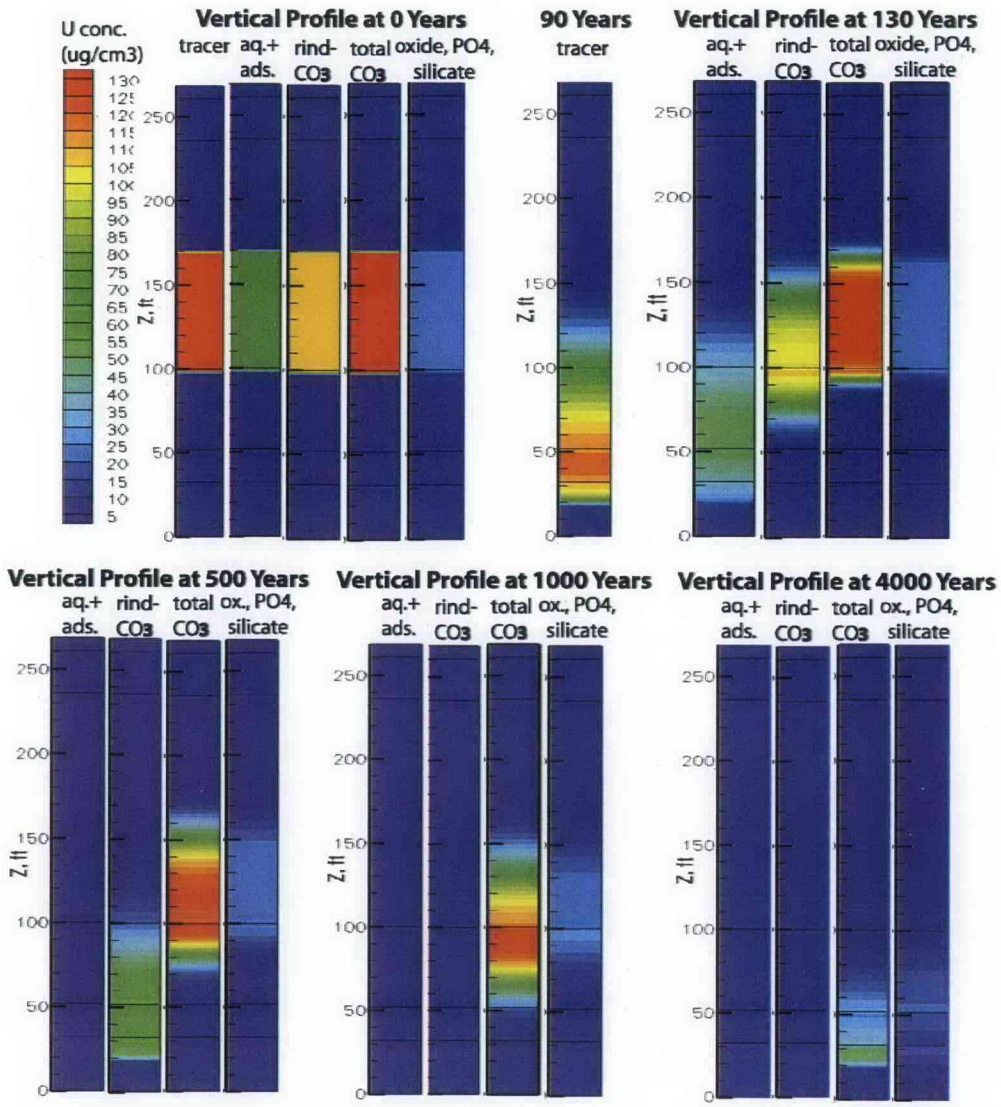

Figure 5.3. Simulation of downward uranium migration in the vadose zone for the untreated sediment. Vertical profiles at different times shown.

Mass migration is more clearly illustrated in breakthrough curves at a 98-ft elevation (directly under the initial uranium plume) and at 27 ft (Figure 5.4). Over the first 1000 years (Figure 5.4a), a tracer plume quickly migrates (plume center at 56 years), with the adsorbed/aqueous plume lagged slightly (plume center of mass at 90 years). The rind carbonate (solid phase) center of mass moves more slowly (plume center 230 years). The balance of the carbonate-associated uranium center of mass moves past the 98-ft elevation in 1100 years (Figure 5.4b, scale to 10,000 years), and the oxide, silicate, and phosphate associated uranium center of mass migrates past the 98-ft elevation in 1900 years. The total sum of the different uranium masses (red line, Figure 5.4b) shows the multiple curves associated with the different uranium surface phases. Note that these plots do not represent concentration breakthrough curves, which would be only for mobile (aqueous) uranium mass. Movement of the solid uranium phases and associated solubility in the vadose zone (and in the saturated zone) result in a lower concentration of uranium in the aqueous phase from these solid phases.

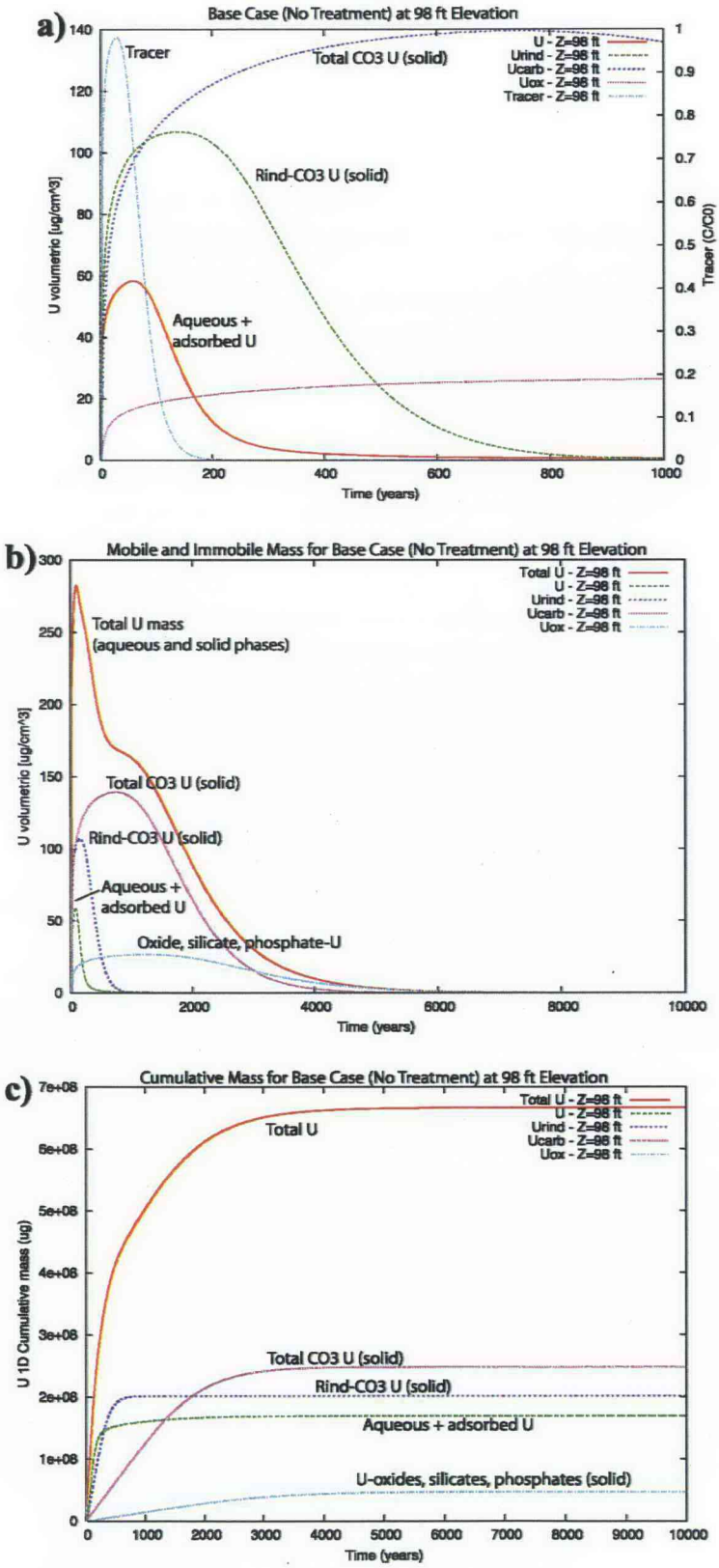

Figure 5.4. Simulation of uranium downward migration for the untreated sediment case directly beneath initial uranium inventory (97-ft elevation).

The relative mass migration of different uranium surface phases at the 27-ft elevation (10 ft above the water table) is similar to that at 98 ft, but masses are more separated because of the longer migration distance from the source at 99- to 170-ft elevation. The tracer (plume center of mass) reaches the 27-ft elevation by 93 years (Figure 5.5a), followed by the adsorbed and aqueous uranium mass at 220 years (exhibiting significant tailing), then the larger rind carbonate-associated uranium at 580 years. The balance of the carbonate-associated uranium mass has migrated to the 27-ft elevation by 3100 years (Figure 5.5b) and the oxide-, silicate-, and phosphate-associated uranium migrates in 5000 years.

The cumulative uranium mass (both aqueous and solid phases) show that half the mass has migrated to this near water-table location by 700 years (Figure 5.5c), and 90% of the mass by 4300 years. This cannot be directly translated to corresponding aqueous uranium concentration, as the different uranium surface phases have different solubility.

Although this one-dimensional simulation task was originally intended to be just migration in the vadose zone, in order to predict approximate uranium aqueous concentration in the groundwater, a moving water table was incorporated in the code. Different surface phase dissolution parameters are needed for these surface phases after they migrate into the water-saturated zone (i.e., higher rates of dissolution) due to the higher water content, as shown conceptually in Figure 5.6. Although the simulations are incomplete at this time, there is high certainty on the aqueous uranium concentration during the first 200 years, as the mass is only from the adsorbed uranium surface phase (green line, Figure 5.6). The subsequent peaks of uranium solid phases (i.e., rind-CO_3 at 580 years; balance of the CO_3 at 3100 years; and oxide, silicate, phosphate at 5000 years) would also leach some uranium into aqueous solution. The leach rate will be different in the saturated zone compared with the vadose zone (and also be dependent on the groundwater flow rate). Although the solid phase masses of rind-carbonate, carbonate, and oxide-uranium are larger than the adsorbed uranium, the resulting aqueous concentrations are smaller due to a considerably slower release rate from the solid phase (i.e., green line).

The sediment treatments described in the results section move uranium mass between the different surface phases. Obviously if adsorbed/aqueous mass is transformed into oxide, silicate, and phosphate mass, two changes occur: a) the timing of when the uranium mass eludes at the water table increases from 100s to 1000s of years; and b) the uranium concentration decreases. A comparison of the transport of just the adsorbed fraction of uranium to the 27-ft elevation (Figure 5.7) was based on simulations of the uranium surface phase changes that occurred for seven different treatments. Simulations for H_2S- and SO_2-treated sediments are not shown, although there were essentially no uranium surface phase changes. The base case (solid red line, Figure 5.7), phosphate by mist and foam, and CO_2 gas treatments all had similar uranium peak concentration, as according to the sequential extractions there were minimal changes in the fraction of uranium in aqueous and adsorbed phases. Note the phosphate and CO_2 treatments did effect major changes in other surface phases, which do highly influence the leaching of uranium at later time periods (not shown). Ammonia gas and NaOH mist decreased the uranium aqueous concentration 50%, and HCl mist and ferric iron mist decreased the uranium aqueous concentration by 75%.

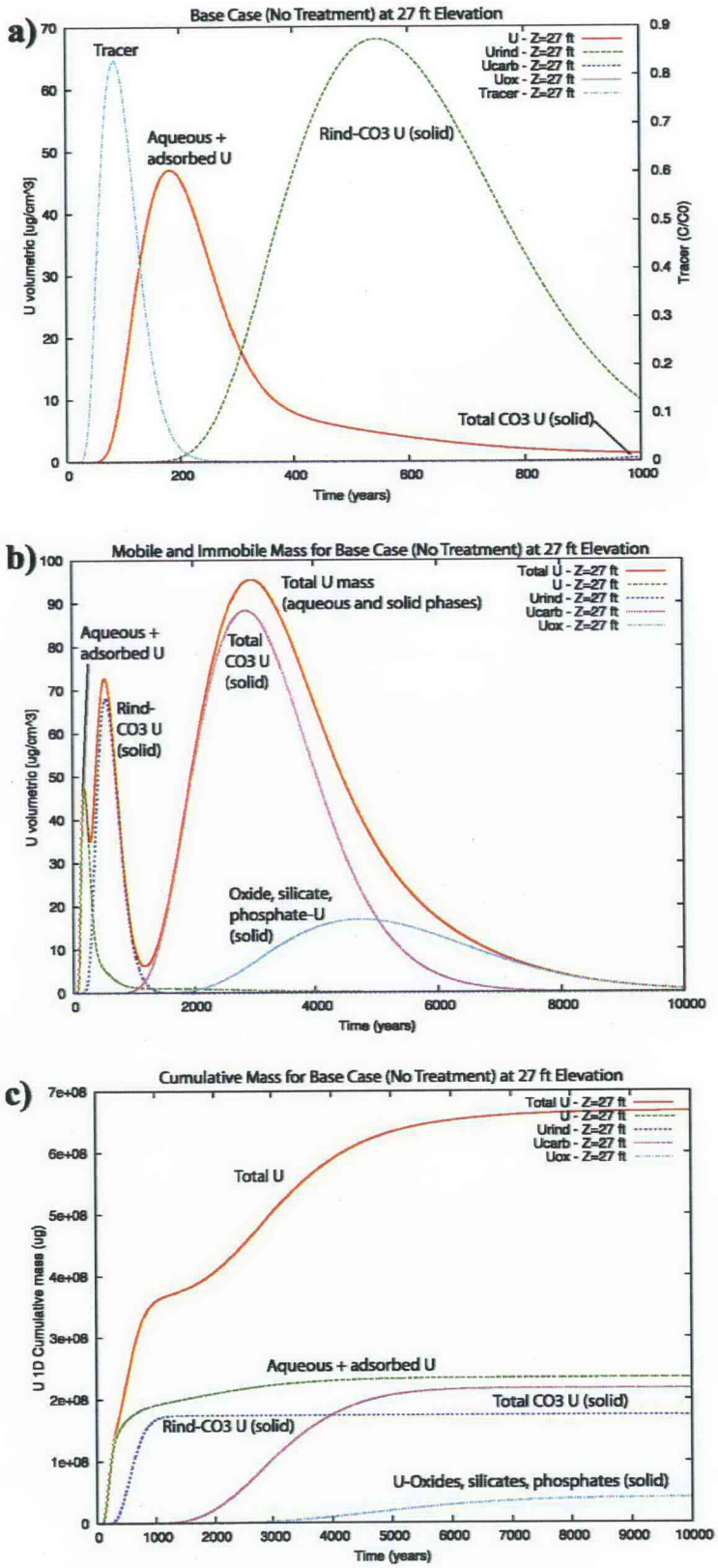

Figure 5.5. Simulation of uranium downward migration for the untreated sediment case at 10 ft above the water table (27-ft elevation).

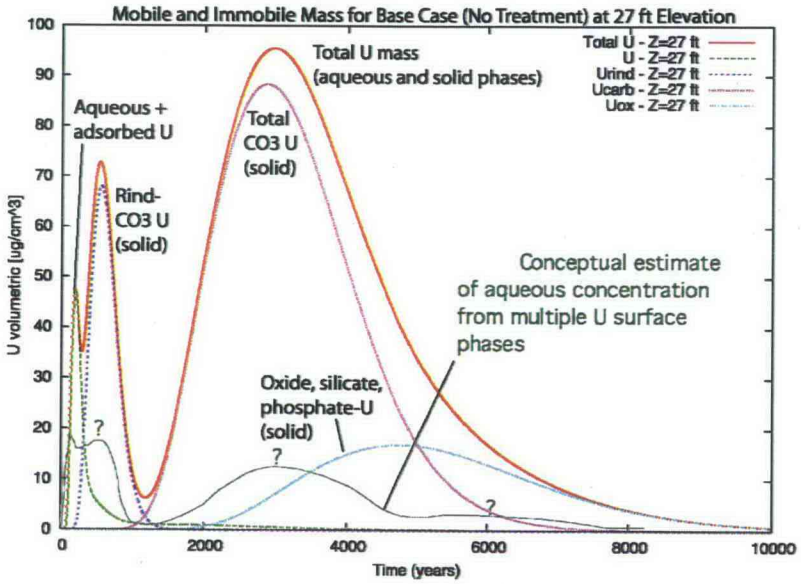

Figure 5.6. Conceptual diagram of uranium aqueous concentration at the water table.

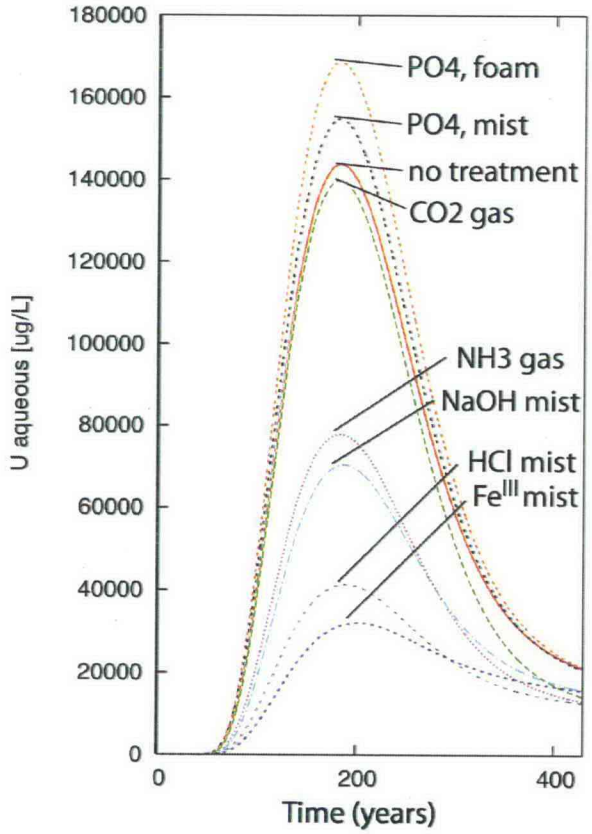

Figure 5.7. Simulation of uranium downward migration for all treatments at 10 ft above the water table (27-ft elevation) from only the fraction of uranium that was adsorbed.

The total cumulative mass of aqueous and all solid phases that have migrated to the 27-ft depth for all treatment cases illustrates (Figure 5.8) that the performance of a treatment varies with time. The Fe(III) mist and HCl mist, which showed the greatest decrease in aqueous peak concentration (<400 years) have only moved this uranium mass to rind-CO_3, and are, therefore, the worst performers at >3000 years. Ammonia gas shows the greatest lag in mass of any of the treatments over most of the time period (2000 to 10,000 years). Phosphate treatments (delivered in a mist or by foam advection) do not decrease aqueous uranium mass (<400 years, Figure 5.7), but are among the best performers to delay mass break-through over most of the time period. In general, most treatments delayed 50% of the mass breakthrough from 700 years (untreated sediment) to 2300 to 2800 years (excluding phosphate treatments). This 4x delay does not illustrate the risk decrease, which is the uranium aqueous concentration that results from the delayed movement of these uranium solid phases to the water table (i.e., green conceptual line in Figure 5.6). Those results will be available in an update to this report.

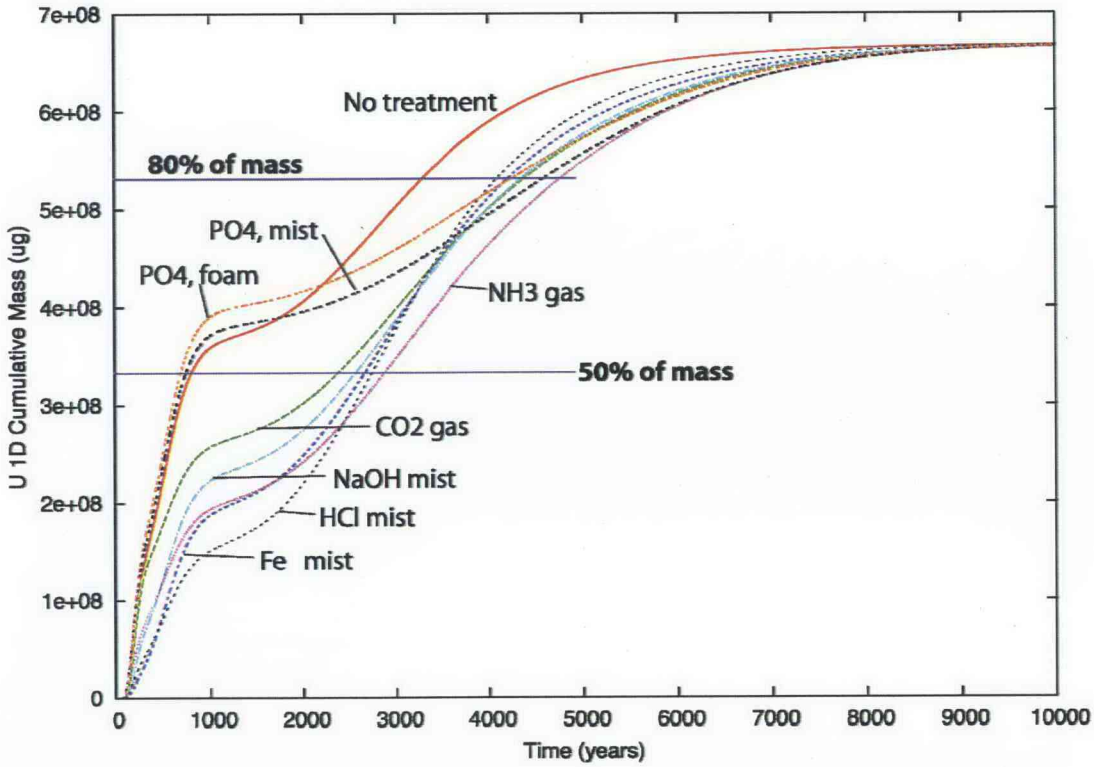

Figure 5.8. Simulation of uranium downward migration for all treatments at 10 ft above the water table (27-ft elevation). Shown is the total aqueous and solid phase accumulated mass.

6.0 Summary and Conclusions

This project was initiated to evaluate the potential for candidate gas-transported reactant technologies to decrease the mobility of uranium in Central Plateau vadose zone sediments at the Hanford Site. The investigation is focused on assessing the geochemical reaction processes for uranium immobilization through geochemical evaluation and proof-of-principle experiments. Although the project is focused on changes in uranium mobility, some of the geochemical changes that result from injection of the reactive gasses and liquid do not directly affect uranium, yet still have a significant influence on uranium mobility. For example, aluminosilicate precipitates produced from ammonia gas (and subsequent pH neutralization) likely coat uranium surface phases such as carbonates. Sequential extractions showed general changes in uranium surface phases, but do not correctly identify surface coatings of less soluble minerals on more soluble minerals. Positive identification of uranium surface phases by the described technologies is currently in progress using electron microprobe techniques.

6.1 Technology Influence on Sediment and Uranium Geochemistry

A brief description of the geochemical changes that result from each technology is as follows:

Hydrogen sulfide gas injection into sediment (H_2S): H_2S gas injection creates mild reducing conditions (Eh -40 to -50 mV) and acidic conditions in the sediment (pH 5.3 to 7.2). An increase in water content from 2% to 15% (g/g, half saturation) did not change the Eh, but did increase the pH. The H_2S may dissolve and reduce some amorphous and crystalline iron oxides. The resulting reductive capacity is small (1.2 μmol e-donor/g of sediment). It is not known if H_2S can directly reduce U(VI) aqueous or solid phases. Changes in uranium surface phases over 1 or 2 months of reduction and over 2 to 3 months of subsequent oxidation by sequential liquid extractions are small and within experimental error.

Sulfur dioxide gas injection into sediment (SO_2): SO_2 gas injection has similar effects to H_2S gas, although slightly milder reducing conditions are created (Eh -25 to -50 mV) and less acidic pH (5.7 to 7.5). The reductive capacity (1.3 μmol e^-/g) was small and about the same as H_2S gas. In comparison, similar Hanford Site sediments when treated with 0.1M sodium dithionite had an average reductive capacity of 11.3 μmol/g (although this is water saturated). Uranium surface phase changes, as characterized by sequential liquid extractions showed essentially no significant or reproducible phase changes. What appears to be a substantial increase in carbonate associated uranium for the third month (sediment 3, Table 4.4) is not backed up by month one and month two data.

Therefore, both H_2S and SO_2 gas treatment were concluded to have no to very little influence on uranium mobility in unsaturated sediments. In addition, because the reducing conditions are short term (years to even 10 years at best), over the transport timescale of uranium in 200 Area sediments (1000s of years to reach the water table), even substantial surface phase changes over this short a timescale (<100 years) would not be of any significant benefit. Although gasses are relatively easy to inject at field scale, both of these gasses are toxic, so this treatment would require additional safety constraints.

Carbon dioxide gas injection into sediment (CO_2): CO_2 gas injection into sediment results in mildly acidic pH (5.4 to 7.1), which was dependent on the water content (pH 5.4 at 2% water content, Figure 4.7). For these experiments, 100% CO_2 was used, so the amount of carbonate in the sediment pore water greatly increases over natural conditions. Both the increased carbonate and acidic pH should

increase uranium mobilization by forming more Ca-U-CO_3 aqueous complexes and less adsorption at this pH. Subsequent pH neutralization should then precipitate uranium-carbonate complexes. Other minerals, such as iron oxides, are also likely partially dissolved at the lower pH. Experiments conducted in this study gassed the sediment with 100% CO_2 for 1 month, then gassed the sediment with air for the subsequent 2 months. There were substantial uranium surface phase changes, as characterized by the sequential extractions. Apparent changes were decreased adsorbed and carbonate associated uranium, and increased silicate/oxide uranium (8% to 33%). During the 1-month treatment with CO_2 gas (before pH neutralization), there was a substantial increase in uranium mobilization (which may or may not be a concern for field-scale application). It should be noted that liquid extractions are problematic in the complex sediment environment when a more resistive precipitate coats a higher solubility mineral. Therefore, the observed phase changes may not be as substantial as observed, and electron microbe may eventually positively identify the actual phase changes that take place. Although the sediment columns were treated with CO_2 and in a second step pH neutralized with air, in separate experiments the sediment pH with just CO_2 treatment (i.e., no pH neutralization) showed a slow trend to natural conditions (i.e., pH was 7.3 by 3 months, Figure 4.7b). At field scale, it is possible that a single treatment of just CO_2 gas without a subsequent pH neutralization step could be used.

Hydrochloric acid mist injection into sediment (HCl mist): The injection of 0.5M HCl as a 0.1% liquid mist with air into sediment was tested to help evaluate CO_2 gas, as similar sediment acidification results, but without the increase in carbonate. The mist technology has been used at field scale for decades for injecting ZVI particles into the subsurface, but the mass at different distances from the injection source has not been quantified. In this study, mist can result in an even deposition of water with distance from the injection source (Figure 4.9a) or decreasing water content (Figure 4.9b), which is likely the result of experimental artifacts (need to refine the venturi used to consistently create the mist). The resulting sediment pH was as low as 5.0 (with 8% water content), which increased to natural sediment pH as the water content decreased. Only one sediment column was treated with the HCl mist for 1 month, then pH neutralized with 0.5M NaOH mist for 2 months. The resulting apparent uranium surface phase changes were substantial (33%), which was better than the CO_2 gas for the same sediment (3). The surface phase changes were more consistent for the HCl mist, with decreases in aqueous, ion exchangeable and CO_3 rind-associated uranium, and increases in CO_3-, oxide-, and silicate-associated uranium. Therefore, although the CO_2 gas has the advantage of being a reactive gas injection into the vadose zone with (likely) greater radial extent possible, the increase in carbonate is not beneficial. The process of sediment acidification followed by pH neutralization appears to be more successful (without the carbonate).

Ferric nitrate liquid mist treatment of sediment: The injection of ferric iron (at pH 1.5) as a 0.1% liquid mist will form ferric hydroxides after the pH is neutralized. The pH < 2 was necessary to keep the ferric iron in solution during injection. Although this process is originally intended to only produce ferric hydroxide (with uranium substitution in the hydroxide), because acidic conditions are used, similar sediment geochemical changes will occur as was previously described with the HCl mist injection. A substantial mass of ferric iron was injected into the system (Figure 4.15), which resulted in measureable ferric iron surface phases clearly greater than that already present in the natural Hanford Site sediment. Consistent changes measured in uranium surface phases were a decrease in aqueous and ion exchangeable uranium, and an apparent increase in silicate-associated uranium (Table 4.15). There were inconsistent changes in carbonate-associated uranium, which likely reflects the iron oxide coating being uneven. The phase changes were substantial (23% to 25% for two sediments). In general, ferric nitrate addition

resulted in somewhat short-term geochemical changes, with the most mobile aqueous and adsorbed uranium replaced by iron oxides of moderate solubility. Ferric nitrate addition also required a two-step process, with pH neutralization. Because the mist was somewhat inconsistent in delivery, it is also possible the ferric oxides produced could have clogged some pore space near the injection location.

Ammonia gas treatment of sediment (NH_3): NH_3 gas treatment of sediment (10% NH_3) for 1 week results in a substantial pH increase (pH 11.8 to 12.8, Figure 4.11a), which did not vary with water content (2% to 15%). These alkaline conditions cause significant aluminosilicate dissolution (Qafoku et al. 2004), and also decrease uranium sorption (Zachara et al. 2007). The subsequent pH neutralization will result in aluminosilicate precipitation, which may coat some of the surface uranium phases. In this study, uranium-contaminated sediment was treated with NH_3 gas for 1 month, then pH neutralized (by air injection) for the subsequent 2 months. The apparent changes in uranium surface phases (by sequential liquid extractions) were substantial, from 7% to 35% (different sediments). All sediments and different water content showed a consistent decrease in aqueous, adsorbed, carbonate uranium concentrations, and an increase in oxide- and silicate-associated uranium surface phases (Table 4.11). Ammonia gas treatment at field scale may be possible without the subsequent pH neutralization step. Treatment over 3 months (without pH neutralization) showed that the pH was decreasing from 11.8 to 9.5 (at 3 months). Because ammonia gas is primarily causing aluminosilicate dissolution and reprecipitation, the process likely does not directly involve uranium phases, so is generally independent of uranium surface concentrations.

Sodium hydroxide mist injection into sediment (NaOH mist): The mist injection of 0.5M NaOH as a 0.1% liquid mist was tested to help evaluate NH_3 gas, as similar sediment alkalinity results. One sediment at one time period (3 months) was tested with NaOH mist, where the NaOH was misted into the sediment and allowed to react for 1 month, followed by pH neutralization by injection of HCl mist and subsequent reaction for 2 months. There were very similar uranium surface phase changes for the NaOH mist as the NH_3 gas, with decreases in aqueous, adsorbed and carbonate-associated uranium, and increases in oxide and silicate uranium. The total apparent change in uranium surface phases (25%) was almost identical to NH_3 treatment (29%) for the same sediment (3 at 5% water content). As stated earlier, it was hypothesized there are aluminosilicate coatings on some of the uranium surface phases, and not as much change in the actual uranium surface phases.

Phosphate treatment by mist injection (PO_4 mist): The treatment of sediment with phosphate delivered by a 0.1% aqueous mist or foam (following section) was investigated as a low solubility uranium-phosphate can form [autunite, $Ca(UO_2)_2(PO_4)_2 \cdot XH_2O$] and other phosphate minerals will coat mineral phase surfaces. In contrast to most of the other gas and mist technologies, this phosphate treatment is nearly neutral pH (pH 7.5), which is optimum for the formation of autunite and apatite. Mist injection of a 50-mM phosphate solution resulted in a decreasing water content (Figure 4.17), and decreasing phosphate concentration with distance from the injection source (Figure 4.17b). Experiments in which uranium surface phase changes were quantified were short (10-cm long) columns, so uniform high phosphate concentration was obtained. There were substantial (23% to 75%) apparent changes in uranium surface phases, as quantified by sequential liquid extractions. There were apparent decreases in carbonate-associated uranium, which would not occur with a pH 7.5 phosphate solution. Although unproven, it is likely that the apparent changes from the extraction data represent phosphate coatings on carbonates, and the acetic acid used for the two carbonate extractions was not dissolving the phosphate precipitates. This does not mean that there were no changes in uranium surface phases, but the conceptual model is different between a decrease in carbonate-uranium (and corresponding increase in

phosphate-uranium) versus the same carbonate- with surface precipitate of phosphate-uranium and other phosphate precipitates. Phosphate coatings on uranium-carbonate phases have a lower uranium leach rate than uncoated uranium-carbonate phases. Interestingly, the most mobile uranium (aqueous and adsorbed) did not uniformly decrease, and in fact, increased in two of three sediments tested. Therefore, it appears that PO_4 treatment of sediment most likely does result in a substantial decrease in uranium mobility (precipitates formed need to be confirmed by electron microprobe), but the short-term migration of uranium by the most mobile aqueous and adsorbed phases may not show much treatment. The addition of phosphate to sediment may increase microbial activity, as phosphate is typically a limiting nutrient in the subsurface. Because phosphate is added at pH 7.5 (both by mist and foam), the microbial population is not influenced by a major pH change such as with the ammonia addition (which is also a limiting nutrient, but the pH is 12). Experiments were not conducted to quantify the influence on microbial growth (and PO_4 utilization by microbes).

Phosphate treatment by foam injection (PO_4 foam): The treatment of sediment with phosphate delivered by a 1.0% aqueous liquid containing 0.5% surfactant (sodium laureth sulfate) was advected into the sediment after the gas/aqueous solution was pumped through a foam generator (10-μm porous steel plate) to generate a stream of 0.5- to 1.0-mm foam. Foam transport of aqueous reactants may have some advantages than mist injection in that is appears to be easier to control the advection. Foam transport is complex with substantial foam breakage and reformation (foam is retarded 8.4 times relative to the gas in the foam; see Figure 4.21), and movement of sediment pore water ahead of the foam front. A significant pressure is required to advect foam into the sediment (Figure 4.22) due to higher viscosity of the foam relative to either air or water. Results in changing uranium surface phases for foam-advected phosphate were slightly less than the mist-advected phosphate. This might indicate that the surfactant may increase uranium mobility (i.e., forming complexes). Experiments are needed to investigate partitioning of uranium between pore water and mineral phases in the presence of the surfactant.

Other treatments: Other technologies in use for groundwater remediation were initially considered (Table 2.1) but not investigated further included reduction by addition of solids (ZVI or sulfur modified iron or sodium dithionite), adsorption (specialized nanoparticles), and organophosphate addition (triethyl phosphate). The advantages and disadvantages of these technologies are described in Section 2.0.

6.2 Comparison of Technologies and Potential for Field-Scale Use

Reactive gasses, mist-advected reactants, and foam-advected reactants were compared in terms of the following: a) the measured changes in short-term uranium mobilization (as measured mainly by sequential liquid extractions); b) estimated long-term changes in uranium mobilization, as predicted from vadose zone simulation given the changes in uranium surface phases; c) advection aspects of the technology; and d) potential issues associated with field-scale implementation, as shown in Table 6.1. Short-term changes are uranium surface phases that are transported somewhat retarded relative to a tracer, and include the aqueous, adsorbed, and rind carbonate uranium phases. In the vadose zone simulations of downward migration of uranium phases due to infiltration of precipitation (Section 5.3), the tracer reaches the water table in 90 years, adsorbed/aqueous uranium reaches the water table in 180 years (i.e., Rf = 2), and rind-CO_3-associated uranium reaches the water table in 800 years (i.e., Rf = 10). The sequential extraction data (Section 4.0) was used to quantify the changes in "short-term" uranium mobility, which includes the aqueous, adsorbed, and rind carbonate uranium phases.

Table 6.1. Comparison of Technologies for Decreasing Uranium Mobility

Technology	Geochemistry: Short-Term*	Geochemistry: Long-Term*	Physical Transport*	Field Scale*	Rating**
Reactive Gas					
H_2S	1. almost no influence on U surface phases 2. oxidation remobilizes U	1. some reduced U will remain immobilized (aging), although this process is poorly characterized	gas reactant easy to advect in lab and at field scale	safety issues H2S gas, low reductant mass injected, field tested	N
SO_2	1. almost no influence on U surface phases 2. oxidation remobilizes U	1. some reduced U will remain immobilized (aging), although this process is poorly characterized	gas reactant easy to advect in lab and at field scale	not previously evaluated at field scale	N
CO_2	1. significant phase changes (20-25% less mobile U) 2. some geochemical changes need further characterization 3. increased short-term mobilization	1. does not reduce aq. and adsorbed U fraction 2. two step process (CO2 gas injection, pH neutralization) may be required	gas reactant easy to advect in lab and at field scale	fewer safety issues than other reactive gasses	17
NH_3	1. significant phase changes (29-35% less mobile U) 2. some geochemical changes need further characterization 3. consistent between sediments	1. most mobile phases (aq., ads, rind-CO3) reduced, but not eliminated 2. increase in least mobile phases (silicates)	gas reactant easy to advect in lab and at field scale	1. some safety issues with field scale NH3 gas 2. potential for increase in microbial activity	19
Gas Advection of Aqueous Reactant (+0.1% to 0.3% H2O)					
HCl mist	1. significant (33%) less mobile U 2. two-step process 3. similar geochem. to CO2, but greater % changes	1. significant decrease in aq. peak, but since CO3 minerals created, moderate U leaching at later times (not as good as a silicate/phosphate)	1. technology needs refinement; mist stream inconsistent 2. . no additional chemicals used	1. mist injection has been used for decades at field scale, 2. limited (but uncharacterized) lateral extent in field system	13
$Fe^{III}NO_3$ mist	1. significant decrease in mobile U (aq., ads.); increase in oxide U 2. two-step process 3. inconsistent between sediments	1. oxides produced are not as low a solubility as silicates/phosphates	1. technology needs refinement; mist stream inconsistent 2. precipitate may cause clogging	1. mist injection has been used for decades at field scale, 2. limited (but uncharacterized) lateral extent in field system	11
Na_2HPO_4 mist	1. phosphate precipitates formed are low solubility 2. slight increase in aq and ads. U 3. single step (pH neutral)	1. since aq. and ads. U are not decreased, initial pulse does not decrease 2. PO4 ppt and coatings substantially decreases bulk of U mobility	1. technology needs refinement; mist stream inconsistent 2. no additional chemicals used	1. mist injection has been used for decades at field scale, 2. limited (but uncharacterized) lateral extent in field 3. may increase microbial activity	14
NaOH mist	1. significant phase changes (25% less mobile) 2. similar coatings to NH3	1. most mobile phases (aq., ads, rind-CO3) reduced, but not eliminated 2. increase in least mobile phases (silicates)	1. technology needs refinement; mist stream inconsistent 2. no additional chemicals used 3. two step process	1. mist injection has been used for decades at field scale, 2. limited (but uncharacterized) lateral extent in field system	16
Foam Advection of Aqueous Reactant (+1% H2O)					
Na_2HPO_4	1. phosphate precipitates formed are low solubility 2. slight increase in aq and ads. U 3. unknown U-surfactant reactions	1. since aq. and ads. U are not decreased, initial pulse does not decrease 2. PO4 ppt and coatings substantially decreases bulk of U mobility	1. foam transport is complex, needs refinement 2. long term chemical and physical influence of surfactant unknown	1. pressure needed; foam high resistance to flow in sediment 2. targets high-K zones 3. limited (uncharacterized) lateral extent in field 4. may increase microbial activity	13

* scale of 0• (low) to 5• (high) rating **sum of category ratings (maximum = 20) N = not recommended, as technology failed to decrease U mobility

Long-term changes in uranium mobilization refer to the balance of the uranium surface phases, in which there is still some dissolution and reprecipitation vertically. These phases include the balance of the uranium-carbonate, uranium-oxides, uranium-silicates, and uranium-phosphates. For comparison, simulations in Section 5.3 show uranium-carbonates on average reach the water table in 4000 years, and oxides/silicates/phosphates in 8000 years. Physical transport of each technology was characterized by additional laboratory experiments that were conducted with each technology to determine how easily reactants could be moved into a long sediment column (described in Section 4.0 for each technology).

In terms of the short-term decrease in uranium mobility (in decreasing order), NH_3, NaOH mist, CO_2, HCl mist, and Fe(III) mist resulted in moderate to high decreases. Phosphates (mist or foam advected) showed inconsistent change in aqueous and adsorbed uranium. For long-term estimated change in uranium reduction, mineral phases created that had low solubility (phosphates, silicates) were desired, so phosphates (mist and foam delivered), NH_3, and NaOH mist showed the greatest formation of these minerals. The evaluation of the physical transport of the reactants into the sediment packed in columns was based on the ease of treatment in laboratory experiments as well as any associated issues. The four gasses (NH_3, CO_2, H_2S, SO_2) were obviously the easiest to advect. Mist delivered reactants were more difficult to implement, due to inconsistent mist formation. Foam advection was relatively easy to implement, but foam advection is a complex process, and the additional presence of the surfactant has somewhat unknown influence on uranium mobility. Evaluation of the ability to treat sediment at field scale with the current technologies was the highest for CO_2 and NH_3 gas. Mist delivery, although being implemented at field scale for other purposes, is likely to be more limited in areal extent. Foam delivery may be feasible but requires more development and potentially a different foam than the one used in these studies.

Overall, the ammonia and carbon dioxide gas had the greatest overall geochemical performance and ability to implement at field scale. Corresponding mist-delivered technologies (NaOH mist for ammonia and HCl mist for carbon dioxide) performed as well or better geochemically, but are not as easily upscaled. Phosphate delivery by mist was rated slightly higher than by foam delivery simply because of the need for more information about foam injection, and the unknown effect of uranium mobility in the presence of the surfactant.

7.0 References

Ahn M. 2003. *Remediation of Chromium(VI) in the Vadose Zone: Stoichiometry and Kinetics of Chromium(VI) Reduction by Sulfur Dioxide.* MS Thesis, Texas A&M University, Texas.

Behrends T and P van Cappellen. 2005. "Competition Between Enzymatic and Abiotic Reduction of Uranium(VI) Under Iron Reducing Conditions." *Chemical Geology* 220:315–327.

Cantrell KJ, DI Kaplan, and TW Wietsma. 1995. "Zero-Valent Iron for the In Situ Remediation of Selected Metals in Groundwater." *Journal of Hazardous Materials* 42:201–212.

Cantrell KJ, SB Yabusaki, MH Engelhard, AV Mitroshkov, and EC Thornton. 2003. "Oxidation of H_2S by Iron Oxides in Unsaturated Conditions." *Environmental Science & Technology* 37:2192–2199.

Charlet L, E Liger, and P Gerasimo. 1998. "Decontamination of TCE- and U-Rich Water by Granular Iron: Role of Sorbed Fe(II)." *Journal of Environmental Engineering* 124:25–30.

Chou L and R Wollast. 1984. "Study of the Weathering of Albite at Room Temperature and Pressure with a Fluidized Bed Reactor." *Geochimica et Cosmochimica Acta* 48:2205–2217.

Chowdiah P, BR Misra, JJ Kilbane II, VJ Srivastava, and TD Hayes. 1998. "Foam Propagation Through Soils for Enhanced In Situ Remediation." *Journal of Hazardous Materials* 62:265–280.

Davydov A, KT Chuang, and AR Sanger. 1998. "Mechanism of H_2S Oxidation by Ferric Oxide and Hydroxide Surfaces." *Journal of Physical Chemistry B* 102:4745–4752.

Denham M and B Looney. 2007. "Gas: A Neglected Phase in Remediation of Metals and Radionuclides." *Environmental Science & Technology* 41(12):4193–4198.

DOE/RL. 2008. *Deep Vadose Zone Treatability Test Plan for Hanford Central Plateau.* DOE/RL-2007-56, Rev. 0, U.S. Department of Energy, Richland Operations Office, Richland, Washington.

Dong W, WP Ball, C Liu, Z Wang, AT Stone, J Bai, and JM Zachara. 2005. "Influence of Calcite and Dissolved Calcium on Uranium (VI) Sorption to a Hanford Subsurface Sediment." *Environmental Science and Technology* 39:7949–7955.

Enzien MV, DL Michelsen, RW Peters, JX Bouillard, and JR Frank. 1995. "Enhanced In Situ Bioremediation Using Foams and Oil Aphrons. Chapter in *In-Situ Aeration: Air Sparging, Bioventing, and Related Remediation Processes*, eds RE Hinchee, RN Miller, and PC Johnson, Battelle Press, Columbus, Ohio.

Finch R and T Murakami. 1999. "Systematics and Paragenesis of Uranium Minerals." *Reviews in Mineralogy and Geochemistry* 38(1):91–179.

Freedman VL, MD Williams, CR Cole, MD White, and MP Bergeron. 2002. *Initial Assessments for B-BX-BY Field Investigation Report (FIR): Numerical Simulations.* PNNL-13949, Pacific Northwest National Laboratory, Richland, Washington.

Hua B, H Xu, J Terry, and B Deng. 2006. "Kinetics of Uranium(VI) Reduction by Hydrogen Sulfide in Anoxic Aqueous Systems." *Environmental Science & Technology* 40:4666–4671.

Huang CW and CH Chang. 2000. "A Laboratory Study on Foam-Enhanced Surfactant Solution Flooding in Removing N-Pentadecane Form Contaminated Columns." *Colloids and Surfaces A.* 173:171–179.

Jeong SW, MY Corapcioglu, and SE Roosevelt. 2000. "Micromodel Study of Surfactant Foam Remediation of Residual Trichloroethylene." *Environmental Science & Technology* 34:3456–3461.

Kovscek AR and HJ Bertin. 2003. "Foam Mobility in Heterogeneous Porous Media II: Experimental Observations." *Transport in Porous Media* 52:37–49.

Lancy LE. 1954. "Integrated Treatment for Metal Finishing Wastes." *Sewage and Industrial Wastes* 26(9):1117–1125.

Liger E, L Charlet, and P van Cappellen. 1999. "Surface Catalysis of Uranium(VI) Reduction by Iron(II)." *Geochmica et Cosmochimica Acta* 63:2939–2955.

Liu C, J Zachara, O Qafoku, J McKinley, S Heald, and Z Wang. 2004. "Dissolution of Uranyl Microprecipitates in Subsurface Sediments at Hanford Site, USA." *Geochimica et Cosmochimica Acta* 68(22):4519–4537.

Livens FR, MJ Jones, AJ Hynes, JM Charnock, JFW Mosselmans, C Hennig, J Steele, D Collison, DJ Vaughan, RAD Pattrick, WA Reed, and LN Moyes. 2004. "X-Ray Absorption Spectroscopy Studies of Reactions of Technetium, Uranium and Neptunium with Mackinawite." *Journal of Environmental Radioactivity* 74:211–219.

McKinley J, J Zachara, J Smith, and C Liu. 2007. "Cation Exchange Reactions Controlling Desorption of Sr from Coarse-Grained Contaminated Sediments at the Hanford Site, Washington." *Geochimica et Cosmochimica Acta* 71(2):305–325.

Mulligan CN and F Eftekhari. 2003. "Remediation with Surfactant Foam of PCP-Contaminated Soil." *Engineering Geology* 70(3):269–279.

Mulligan CN and S Wang. 2006. "Remediation of a Heavy Metal-Contaminated Soil by a Rhamnolipid Foam." *Engineering Geology* 85:75–81.

Naftz DL, CC Fuller, JA Davis, SJ Morrison, EM Feltcorn, RC Rowland, GW Freethey, RC Rowland, C Wilkowske, and M Piana. 2002. "Field Demonstration of Three Permeable Reactive Barriers to Control Uranium Contamination in Groundwater, Fry Canyon, Utah, USA." In *Groundwater Remediation Using Permeable Reactive Barriers*, Academic Press, New York, p 401–434.

Payne T, J Davis, and T Waite. 1994. "Uranium Retention by Weathered Schists – the Role of Iron Minerals." *Radiochimica Acta* 66/67:297–303.

Peters RW, MV Enzien, JX Bouillard, JR Frank, VJ Srivastava, J Kilbane, and T Hayes. 1994. "Nonaqueous Phase Liquids Contaminated Soil/Groundwater Remediation Using Foams." Chapter in *In-Situ Remediation: Scientific Basis for Current and Future Technologies*, eds GW Gee and NR Wing, Battelle Press, Columbus, Ohio.

Qafoku NP, CC Ainsworth, JE Szecsody, and OS Qafoku. 2004. "Transport-Controlled Kinetics of Dissolution and Precipitation in the Sediments Under Alkaline and Saline Conditions." *Geochimica et Cosmochimica Acta* 68(14):2981–2995.

Rai D, AR Felmy, and JL Ryan. 1990. Uranium(IV) Hydrolysis Constants and Solubility Product of UO_2*H_2O (am)." *Inorganic Chemistry* 29:260–264.

Rockhold M, T Johnson, J Szecsody, J McKinley, T Blake, T Wietsma, M Covert, and M Oostrom. 2008. *Experimental Evaluation of Gas-Phase Transport and Reactivity of Two Organophosphate Compounds (TEP and DMMP) in Unsaturated Porous Media.* Abstract #H13A-0906, American Geophysical Union, Annual Fall Meeting, San Francisco, California. Available at http://adsabs.harvard.edu/abs/2008AGUFM.H13A0906R.

Rothmel RK, RW Peters, EST Martin, and MF Deflaun. 1998. "Surfactant Foam/Bioaugmentation Technology for In Situ Treatment of TCE-DNAPLs." *Environmental Science & Technology* 32:1667–1675.

Sani RK, BM Peyton, JE Amonette, and GG Geesey. 2004. "Reduction of Uranium(VI) Under Sulfate-Reducing Conditions in the Presence of Fe(III)-(Hydr)oxides." *Geochimica et Cosmochimica Acta* 68:2639–2648.

Serne RJ, GV Last, GW Gee, HT Schaef, DC Lanigan, CW Lindenmeier, MJ Lindberg, RE Clayton, VL LeGore, RD Orr, IV Kutnyakov, SR Baum, CF Brown, MM Valenta, and TS Vickerman. 2002. *Characterization of Vadose Zone Sediment: Borehole 299-E33-45 Near BX-102 in the B-BX-BY Waste Management Area.* PNNL-14083, Pacific Northwest National Laboratory, Richland, Washington.

Serne RJ, MJ Lindberg, SR Baum, GV Last, RE Clayton, KN Geiszler, GW Gee, VL LeGore, CF Brown, HT Schaef, RD Orr, MM Valenta, DC Lanigan, IV Kuthyakov, TS Vickerman, CW Lindenmeier. 2008a. *Characterization of Vadose Zone Sediment: Borehole 299-E33-45 Near BX 102 in the B-BX-BY Waste Management Area.* PNNL-14083, Rev. 1, Pacific Northwest National Laboratory, Richland, Washington.

Serne RJ, MJ Lindberg, MM Valenta, BN Bjornstad, RE Clayton, IV Kutnyakov, DG Horton, VL LeGore, TS Vickerman, DC Lanigan, KN Geiszler, RD Orr, HT Schaef, SR Baum, CF Brown, and CW Lindenmeier. 2008b. *Characterization of Vadose Zone Sediments Below the T Tank Farm: Boreholes C4104, C4105, 299-W10-196, and RCRA Borehole 299-W11-39.* PNNL-14849, Rev. 1, Pacific Northwest National Laboratory, Richland, Washington.

Simpson BC, RA Corbin, MJ Anderson, CT Kincaid, and JM Zachara. 2006. *Identification and Classification of the Major Uranium Discharges and Unplanned Releases at the Hanford Site Using the Soil Inventory Model (SIM) Rev. 1 Results*. NUV-06-21106-ES-001-DOC Rev. 1, Novotec, USA Inc., Cincinnati, Ohio.

Smith S and J Szecsody. 2009. "Influence of Contact Time on the Extraction of 233 Uranyl Spike and Contaminant Uranium from Hanford Sediment." *Radiochimica Cosmochemica Acta* (In Press).

Szecsody J, K Cantrell, K Krupka, C Resch, M Williams, and J Fruchter. 1998. *Uranium Mobility During In Situ Redox Manipulation of the 100 Areas of the Hanford Site*. PNNL-12048/UC-2000, Pacific Northwest National Laboratory, Richland, Washington.

Szecsody J, N Hess, and JP McKinley. 2001. "Pertechnetate Reduction During Transport at High Ph in Natural Sediments." Presented at *U.S. DOE Environmental Management Science Program Vadose Zone Principal Investigator Workshop*, Environmental Molecular Sciences Laboratory, November 5–6, 2001, Pacific Northwest National Laboratory, Richland, Washington.

Szecsody J, M Williams, J Fruchter, V Vermeul, D Sklarew. 2004. "In Situ Reduction of Aquifer Sediments: Enhancement of Reactive Iron Phases and TCE Dechlorination." *Environmental Science and Technology* 38:4656–4663.

Szecsody J, M Rockhold, M Oostrom, R Moore, C Burns, M Williams, L Zhong, J Fruchter, J McKinley, V Vermeul, M Covert, T Wietsma, A Breshears, and B Garcia. 2009. *Sequestration of Sr-90 Subsurface Contamination in the Hanford 100-N Area by Surface Infiltration of a Ca-Citrate-Phosphate Solution*. PNNL-18303, Pacific Northwest National Laboratory, Richland, Washington.

Thomas R and L Macaskie. 1996. "Biodegradation of Tributyl Phosphate by Naturally Occurring Microbial Isolates and Coupling to the Removal of Uranium from Aqueous Solution." *Environmental Science and Technology* 30:2371–2375.

Thornton EC. 2000. "In Situ Gaseous Reduction." Chapter in *Vadose Zone Science and Technology Solutions*, p. 1302–1307, eds BB Looney and RW Falta, Battelle Press, Columbus, Ohio.

Thornton EC and JE Amonette. 1999. "Hydrogen Sulfide Gas Treatment of Cr(VI)-Contaminated Sediment Samples from a Plating-Waste Disposal Site: Implications for In-Situ Remediation." *Environmental Science and Technology* 33:4096–4101.

Thornton EC, L Zhong, M Oostrom, and B Deng. 2007. "Experimental and Theoretical Assessment of the Lifetime of a Gaseous-Reduced Vadose Zone Permeable Reactive Barrier." *Vadose Zone Journal* 6:1050–1056.

Tokunaga TK, Y Kim, and J Wan. 2009. *Searching for Sustainable Approaches for Remediating Uranium-Contaminated Groundwaters and Sediments*. Poster at U.S. Department of Energy, Environmental Remediation Science Program Annual Meeting, May 2009, Washington DC. Available at http://esd.lbl.gov/files/research/projects/sustainable_systems/Exploratory_Toxic_Tetsu.pdf.

Um W, Z Wang, J Serne, B Williams, C Brown, C Dodge, and A Francis. 2009. "Uranium Phase in Contaminated Sediments Below Hanford's U Tank Farm." *Environmental Science and Technology* 43(12):4280–4286.

Vermeul VR, BN Bjornstad, CJ Murray, DR Newcomer, ML Rockhold, JE Szecsody, MD Williams, and YL Xie. 2004. *In Situ Redox Manipulation Permeable Reactive Barrier Emplacement: Final Report Frontier Hard Chrome Superfund Site, Vancouver, WA.* PNWD-3361, Pacific Northwest National Laboratory, Richland, Washington.

Waite, TD, JA Davis, TE Payne, GA Waychunas, and N Xu. 1994. "Uranium(VI) Adsorption to Ferrihydrite: Application of a Surface Complexation Model." *Geochimica et Cosmochimica Acta* 58(24):5465-5478.

Wang S and CN Mulligan. 2004a. "Rhamnolipid Foam Enhanced Remediation of Cadmium and Nickel Contaminated Soil." *Water, Air, and Soil Pollution* 157:315–330.

Wang S and CN Mulligan. 2004b. "An Evaluation of Surfactant Foam Technology in Remediation of Contaminated Soil." *Chemosphere* 57:1079–1089.

Wellman DM, JP Icenhower, AP Gamerdinger, and SW Forrester. 2006a. "Effects of Ph, Temperature, and Aqueous Organic Material on the Dissolution Kinetics of Meta-Autunite Minerals (Na, $Ca)_{2-1}[(UO_2)(PO_4)]_2\ 3H_2O$." *American Mineralogist* 91:143–158.

Wellman DM, JP Icenhower, and AT Owen. 2006b. "Comparative Analysis of Soluble Phosphate Amendments for the Remediation of Heavy Metal Contaminants: Effect on Sediment Hydraulic Conductivity." *Environmental Chemistry* 3:219–224.

Wellman DM, EM Pierce, EL Richards, BC Butler, KE Parker, JN Glovack, SD Burton, SR Baum, ET Clayton, and EA Rodriguez. 2007. *Interim Report: Uranium Stabilization Through Polyphosphate Injection - 300 Area Uranium Plume Treatability Demonstration Project.* PNNL-16683, Pacific Northwest National Laboratory, Richland, Washington.

Wellman DM, EM Pierce, DH Bacon, M Oostrom, KM Gunderson, SM Webb, CC Bovaird, EA Cordova, ET Clayton, KE Parker, RM Ermi, SR Baum, VR Vermeul, and JS Fruchter. 2008a. *300 Area Treatability Test: Laboratory Development of Polyphosphate Remediation Technology for In Situ Treatment of Uranium Contamination in the Vadose Zone and Capillary Fringe.* PNNL-17818, Pacific Northwest National Laboratory, Richland, Washington.

Wellman DM, JM Zachara, C Liu, NP Qafoku, SC Smith, and SW Forrester. 2008b. "Advective Desorption of Uranium(VI) from Contaminated Hanford Vadose Zone Sediments Under Saturated and Unsaturated Conditions." *Vadose Zone Journal* 7(4):1144–1159.

White MD, M Oostrom, and MD Williams. 2002. *Initial Assessments for S-SX Field Investigation Report: Simulations of Contaminant Migration with Surface Barriers.* PNWD-3111, Pacific Northwest National Laboratory, Richland, Washington.

Zachara J, C Liu, C Brown, S Kelly, J Christensen, J McKinley, J Davis, J Serne, E Dresel, and W Um. 2007. *A Site-Wide Perspective on Uranium Geochemistry at the Hanford Site*. PNNL-17031, Pacific Northwest National Laboratory, Richland, Washington.

Zhong L, EC Thornton, and B Deng. 2007. "Uranium Immobilization by Hydrogen Sulfide Gaseous Treatment Under Vadose Zone Conditions." *Vadose Zone Journal* 6:149–157.

Zhong L, NP Qafoku, JE Szecsody, PE Dresel, and ZF Zhang. 2009a. "Foam Delivery of Calcium Polysulfide to the Vadose Zone for Chromium (VI) Immobilization: A Laboratory Evaluation." *Vadose Zone Journal* 8(4) (In Press).

Zhong L and J Szecsody. 2009b. "Foam Delivery of Calcium Polysulfide in Hanford Deep Vadose Zone for Cr(VI)/Tc-99 Remediation." Pacific Northwest National Laboratory, Laboratory Directed Research and Development (LDRD) project final report.

Appendix

Uranium Sequential Extraction Data

Table A.1. Sequential Extraction Results for Untreated Sediment

Sed.	Treat-ment	Time (months)	T (°C)	H_2O (%)	sequential liquid extractions (ng U/g sed) #1 aq.	#2 ion exch.	#3 acetate pH5	#4 acetate pH2.3	#5 oxalate	#6 8M H+	total U (ug/g)	sequential extractions, fraction of total U mass #1 aq.	#2, ion exch.	#3, pH 5 acetate	#4, pH2.3 acetate	#5 oxalate	#6 8M H+	Kd (cm^3/g)	fraction aq.in vad. zone
1	none	0 (3 samples)	22	5	5731±672	3897±480	10440±920	301400±4200	30820±72	24640±5780	376.6±6.2	0.015	0.0103	0.028	0.800	0.0818	0.065	1.45	0.0016
2	none	0 (5 samples)	22	5	962±53	792±44	2864±172	54600±1980	10170±1220	3770±215	74.3±2.3	0.013	0.0107	0.039	0.744	0.137	0.051	0.87	0.0024
3	none	0 (6 samples)	22	5	1706±148	3003±297	8181±1081	9738±997	1718±336	4210±678	28.1±1.8	0.061	0.107	0.291	0.336	0.061	0.149	1.84	0.0086
3	none	0 (3 samples)	22	15	2397±308	3051±391	7448±375	9194±958	2741±392	2872±1030	27.7±1.8	0.086	0.110	0.270	0.331	0.099	0.104	1.90	0.0098
												±12%	±12%	±8.8%	±3.6%	±11%	±16%		

Table A.2. Sequential Extraction Results for H_2S Gas Treated Sediment

Sed.	Treat-ment	Time (months)	T (°C)	H_2O (%)	sequential liquid extractions (ng U/g sed) #1 aq.	#2 ion exch.	#3 acetate pH5	#4 acetate pH2.3	#5 oxalic acid	#6 8M H+	total U (ug/g)	sequential extractions, fraction of total U mass #1 aq.	#2, ion exch.	#3, pH 5 acetate	#4, pH2.3 acetate	#5 oxalate	#6 8M H+	Kd (cm^3/g)	fraction aq.in vad. zone
2	none	0 (5 samples)	22	5	962±53	792±44	2864±172	54600±1980	10170±1220	3770±215	74.3±2.3	0.013	0.0107	0.0385	0.744	0.137	0.0507	0.87	0.0024
	H_2S	1 mo.	22	5	924.1	630.5	3100	53284	8174	1919	68.0	0.014	0.0093	0.0456	0.783	0.120	0.0282	1.07	0.0020
	H_2S	1mo, 1mo oxic	22	5	995	626	6674	54511	6719	5356	74.9	0.013	0.0084	0.0891	0.728	0.090	0.0715	1.13	0.0018
	H_2S	2 mo.	82	5	491	959	6587	50073	6860	7661	72.6	0.007	0.0132	0.0907	0.689	0.094	0.1055	3.25	0.0006
	H_2S	2mo, 1mo oxic	82	5	1615	1012	3158	60382	6910	6453	79.5	0.02	0.0127	0.0397	0.759	0.087	0.0811	0.99	0.0030
3	none	0 (6 samples)	22	5	1706±148	3003±297	8181±1081	9738±997	1718±336	4210±678	28.1±1.8	0.061	0.107	0.291	0.336	0.061	0.149	1.84	0.0086
	H_2S	1 mo.	22	5	3683	4019	6416	12965	3952	3090	34.1	0.108	0.118	0.188	0.380	0.116	0.0905	3.30	0.0066
	H_2S	1mo, 1mo oxic	22	5	1050	3017	7905	11875	3020	4747	31.6	0.033	0.095	0.250	0.376	0.0955	0.150	8.43	0.0015
	H_2S	2 mo.	82	5	1422	2493	6640	9574	2484	3274	25.9	0.055	0.096	0.257	0.370	0.0959	0.126	5.23	0.0028

Table A.3. Sequential Extraction Results for SO_2 Gas Treated Sediment

Sed.	Treat-ment	Time (months)	T (°C)	H_2O (%)	sequential liquid extractions (ng U/g sed) #1 aq.	#2 ion exch.	#3 acetate pH5	#4 acetate pH2.3	#5 oxalic acid	#6 8M H+	total U (ug/g)	sequential extractions, fraction of total U mass #1 aq.	#2, ion exch.	#3, pH 5 acetate	#4, pH2.3 acetate	#5 oxalate	#6 8M H+	Kd (cm^3/g)	fraction aq.in vad. zone
2	none	0 (5 samples)	22	5	962±53	792±44	2864±172	54600±1980	10170±1220	3770±215	74.3±2.3	0.013	0.0107	0.0385	0.744	0.137	0.0507	0.87	0.0024
	SO_2	1 mo.	22	5	1591.3	1409.0	3033	60098		10378	76.5	0.021	0.0184	0.0396	0.7855		0.1356	1.38	0.0026
	SO_2	1mo, 1mo oxic	22	5	1263	1018	5732	53250	7247	6581	75.1	0.017	0.0136	0.0763	0.7091	0.0965	0.0876	1.26	0.0022
	SO_2	2 mo.	82	5	942	881	6801	54708	6988	7273	77.6	0.012	0.0113	0.0876	0.7051	0.0901	0.0937	1.55	0.0014
	SO_2	2mo, 1mo oxic	82	5	2734	1067	4702	55483	6252	5909	76.1	0.036	0.014	0.0618	0.7286	0.0821	0.0776	0.66	0.0066
3	none	0 (6 samples)	22	5	1706±148	3003±297	8181±1081	9738±997	1718±336	4210±678	28.1±1.8	0.061	0.107	0.291	0.336	0.061	0.149	1.84	0.0086
	SO_2	1 mo.	22	5	3252	4051	6883	11639	0	4076	29.9	0.109	0.135	0.230	0.389		0.136	3.58	0.0066
	SO_2	1mo, 1mo oxic	22	5	702	2817	7887	12178	2841	3583	30.0	0.023	0.094	0.263	0.406	0.0947	0.119	12.3	0.0009
	SO_2	2 mo.	82	5	1334	2328	6646	11261	2592	3483	27.6	0.048	0.084	0.240	0.407	0.0938	0.126	5.12	0.0025
	SO_2	2mo, 1mo oxic	82	5	1392	1756	3696	21544	2204	3017	33.6	0.041	0.0522	0.110	0.641	0.0656	0.090	4.84	0.0019

Table A.4. Sequential Extraction Results for HCl Mist-Treated Sediment

					sequential liquid extractions (ng U/g sed)							sequential extractions, fraction of total U mass							fraction
Sed.	Treat-ment	Time (months)	T (°C)	H_2O (%)	#1 aq.	#2 ion exch.	#3 acetate pH5	#4 acetate pH2.3	#5 oxalic acid	#6 8M H+	total U (ug/g)	#1 aq.	#2, ion exch.	#3, pH 5 acetate	#4, pH2.3 acetate	#5 oxalate	#6 8M H+	Kd (cm^3/g)	aq.in vad. zone
3	none	0 (6 samples)	22	5	2253±196	3965±393	10800±1430	12860±1320	2270±444	5560±895	28.1±1.8	0.061	0.107	0.291	0.336	0.061	0.149	1.84	0.0086
	HCl	3 months	82	5	309	252	2352	11515	2907	5107	22.4	0.014	0.0112	0.105	0.514	0.130	0.228	2.13	0.0011

Table A.5. Sequential Extraction Results for CO_2 Gas Treated Sediment

					sequential liquid extractions (ng U/g sed)							sequential extractions, fraction of total U mass							fraction
Sed.	Treat-ment	Time (months)	T (°C)	H_2O (%)	#1 aq.	#2 ion exch.	#3 acetate pH5	#4 acetate pH2.3	#5 oxalate	#6 8M H+	total U (ug/g)	#1 aq.	#2, ion exch.	#3, pH 5 acetate	#4, pH2.3 acetate	#5 oxalate	#6 8M H+	Kd (cm^3/g)	aq.in vad. zone
2	none	0 (5 samples)	22	5	962±53	792±44	2864±172	54600±1980	10170±1220	3770±215	74.3±2.3	0.013	0.0107	0.0385	0.744	0.137	0.0507	0.87	0.0024
	CO_2	1 month	22	5	26719.2	13592.3	5925	29967		6775	83.0	0.322	0.164	0.071	0.361		0.082	0.77	0.0558
	CO_2	2 mo., N_2 flush	82	5	1262	372	2615	55441	14086	18093	91.9	0.014	0.004	0.028	0.603	0.153	0.197	0.41	0.0035
	CO_2	3 mo., N_2 flush	82	5	1030	456	2400	49258	8220	9979	71.3	0.014	0.006	0.034	0.690	0.115	0.140	0.64	0.0028
3	none	0 (6 samples)	22	5	1706±148	3003±297	8181±1081	9738±997	1718±336	4210±678	28.1±1.8	0.061	0.107	0.291	0.336	0.061	0.149	1.84	0.0086
	CO_2	1 month	22	5	3171	4257	4673	10156		6521	28.8	0.110	0.148	0.162	0.353		0.227	1.38	0.0174
	CO_2	2 mo., N_2 flush	82	5	862	882	3314	7677	3096	6267	22.1	0.039	0.040	0.150	0.347	0.1401	0.284	1.07	0.0067
	CO_2	3 mo., N_2 flush	82	5	856	899	4234	7621	3027	8641	25.3	0.034	0.0356	0.167	0.3015	0.1197	0.342	1.08	0.0059
3	none	0 (3 samples)	22	15	2397±308	3051±391	7448±375	9194±958	2741±392	2872±1030	27.7±1.8	0.086	0.110	0.270	0.331	0.099	0.104	1.90	0.0098
	CO_2	1 month	22	15	5032	5360	3911	9078		6280	29.7	0.170	0.181	0.132	0.306		0.212	1.21	0.0267
	CO_2	2 mo., N_2 flush	82	15	959	851	4299	7019	537	10468	24.1	0.04	0.035	0.178	0.291	0.0223	0.434	1.01	0.0068

Table A.6. Sequential Extraction Results for NaOH Mist-Treated Sediment

					sequential liquid extractions (ng U/g sed)							sequential extractions, fraction of total U mass							fraction
Sed.	Treat-ment	Time (months)	T (°C)	H_2O (%)	#1 aq.	#2 ion exch.	#3 acetate pH5	#4 acetate pH2.3	#5 oxalate	#6 8M H+	total U (ug/g)	#1 aq.	#2, ion exch.	#3, pH 5 acetate	#4, pH2.3 acetate	#5 oxalate	#6 8M H+	Kd (cm^3/g)	aq.in vad. zone
3	none	0 (6 samples)	22	5	1706±148	3003±297	8181±1081	9738±997	1718±336	4210±678	28.1±1.8	0.061	0.107	0.291	0.336	0.061	0.149	1.84	0.0086
	NaOH	3 months	82	5	16	82	3939	7568	3027	4883	19.5	8E-04	0.0042	0.202	0.388	0.155	0.250	13.3	3.79E-05

Table A.7. Sequential Extraction Results for NH_3 Gas-Treated Sediment

					sequential liquid extractions (ng U/g sed)							sequential extractions, fraction of total U mass							fraction
Sed.	Treat-ment	Time (months)	T (°C)	H_2O (%)	#1 aq.	#2 ion exch.	#3 acetate pH5	#4 acetate pH2.3	#5 oxalate	#6 8M H+	total U (ug/g)	#1 aq.	#2, ion exch.	#3, pH 5 acetate	#4, pH2.3 acetate	#5 oxalate	#6 8M H+	Kd (cm^3/g)	aq.in vad. zone
2	none	0 (5 samples)	22	5	962±53	792±44	2864±172	54600±1980	10170±1220	3770±215	74.3±2.3	0.013	0.0107	0.0385	0.744	0.137	0.0507	0.87	0.0024
	NH_3	1 month	22	5	1018.7	1160.9	3570	54267		10346	70.4	0.014	0.016	0.051	0.771		0.147	1.66	0.0018
	NH_3	2 months	82	5	169	32	1850	29821	5243	7710	44.8	0.004	0.0007	0.041	0.665	0.117	0.172	0.27	0.0012
	NH_3	3 months	82	5	994	652	1568	58118	7240	9661	78.2	0.013	0.008	0.020	0.743	0.093	0.123	0.95	0.0020
3	none	0 (6 samples)	22	5	1706±148	3003±297	8181±1081	9738±997	1718±336	4210±678	28.1±1.8	0.061	0.107	0.291	0.336	0.061	0.149	1.84	0.0086
	NH_3	1 month	22	5	216	307	8038	11502	0	6097	26.2	0.008	0.012	0.307	0.440	0.000	0.233	1.46	0.0013
	NH_3	2 months	82	5	168	86	2437	8596	3371	7955	22.6	0.007	0.004	0.108	0.380	0.1491	0.352	0.52	0.0018
	NH_3	3 months	82	5	847	1058	3039	7396	2501	9728	24.6	0.034	0.0431	0.124	0.301	0.1018	0.396	1.27	0.0057
3	none	0 (3 samples)	22	15	2397±308	3051±391	7448±375	9194±958	2741±392	2872±1030	27.7±1.8	0.086	0.110	0.270	0.331	0.099	0.104	1.90	0.0098
	NH_3	1 month	22	15	392	181	8755	11145		5864	29.7	0.015	0.007	0.332	0.423		0.223	0.49	0.0037
	NH_3	2 months	82	15	168	29	3109	12002	4093	9398	24.1	0.006	0.001	0.108	0.417	0.1421	0.326	0.18	0.0024

Table A.8. Sequential Extraction Results for Ferric Iron Mist-Treated Sediment

					sequential liquid extractions (ng U/g sed)							sequential extractions, fraction of total U mass							fraction
Sed.	Treat-ment	Time (months)	T (°C)	H_2O (%)	#1 aq.	#2 ion exch.	#3 acetate pH5	#4 acetate pH2.3	#5 oxalate	#6 8M H+	total U (ug/g)	#1 aq.	#2, ion exch.	#3, pH 5 acetate	#4, pH2.3 acetate	#5 oxalate	#6 8M H+	Kd (cm^3/g)	aq.in vad. zone
2	none	0 (5 samples)	22	5	962±53	792±44	2864±172	54600±1980	10170±1220	3770±215	74.3±2.3	0.013	0.0107	0.0385	0.744	0.137	0.0507	0.87	0.0024
	Fe^{III}mist	1 month	22	5	197.8	22.3	23306	32622		7445	63.6	0.003	0.0004	0.366	0.513		0.117	0.16	0.0013
	Fe^{III}mist	2 months	82	5	373	82	6634	41533	7780	6487	62.9	0.006	0.0013	0.105	0.660	0.124	0.103	0.33	0.0017
	Fe^{III}mist	3 months	82	5	134	418	7437	20979	5143	6824	40.9	0.003	0.010	0.182	0.512	0.126	0.167	4.49	0.0003
3	none	0 (6 samples)	22	5	1706±148	3003±297	8181±1081	9738±997	1718±336	4210±678	28.1±1.8	0.061	0.107	0.291	0.336	0.061	0.149	1.84	0.0086
	Fe^{III}mist	1 month	22	5	53	57	10769	7891	0	2422	21.2	0.003	0.0027	0.508	0.372		0.114	3.04	0.0002
	Fe^{III}mist	2 months	82	5	80	24	9530	6648	1287	2128	19.7	0.004	0.0012	0.484	0.337	0.065	0.108	0.80	0.0006
	Fe^{III}mist	3 months	82	5	41	18	3581	7653	1961	3249	16.5	0.002	0.0011	0.217	0.464	0.119	0.197	1.15	0.0003

Table A.9. Sequential Extraction Results for PO_4 Mist-Treated Sediment

Sed.	Treat-ment	Time (months)	T (°C)	H_2O (%)	sequential liquid extractions (ng U/g sed) #1 aq.	#2 ion exch.	#3 acetate pH5	#4 acetate pH2.3	#5 oxalate	#6 8M H+	total U (ug/g)	sequential extractions, fraction of total U mass #1 aq.	#2, ion exch.	#3, pH 5 acetate	#4, pH2.3 acetate	#5 oxalate	#6 8M H+	Kd (cm^3/g)	fraction aq.in vad. zone
1	none	0 (3 samples)	22	5	5731±672	3897±480	10440±920	301400±4200	30820±72	24640±5780	376.6±6.2	0.015	0.0103	0.0277	0.800	0.0818	0.0649	1.45	0.0016
	PO4 mist	1 month	22	5	1187.3	2108.6	5029	220027		64572	292.9	0.004	0.0072	0.017	0.751		0.220	2.79	0.0004
	PO4 mist	2 months	82	5	18284	2803	1285	24780	66309	188822	302.3	0.06	0.0093	0.004	0.082	0.219	0.625	0.24	0.0205
	PO4 mist	3 months	82	5	20479	3550	4439	15230	41028	159751	244.5	0.084	0.0145	0.018	0.062	0.168	0.653	0.28	0.0259
2	none	0 (5 samples)	22	5	962±53	792±44	2864±172	54600±1980	10170±1220	3770±215	74.3±2.3	0.013	0.0107	0.0385	0.744	0.137	0.0507	0.87	0.0024
	PO4 mist	1 month	22	5	55.0	828.5	3143	24038		42333	70.4	8E-04	0.0118	0.045	0.341		0.601	21.2	0.0001
	PO4 mist	2 months	82	5	1377	609	3861	10846	25076	30840	72.6	0.019	0.0084	0.053	0.149	0.345	0.425	0.70	0.0034
	PO4 mist	3 months	82	5	1479	569	2843	7690	18520	21971	53.1	0.028	0.0107	0.054	0.145	0.349	0.414	0.54	0.0060
3	none	0 (6 samples)	22	5	1706±148	3003±297	8181±1081	9738±997	1718±336	4210±678	28.1±1.8	0.061	0.107	0.291	0.336	0.061	0.149	1.84	0.0086
	PO4 mist	1 month	22	5	244	896	9284	6817		9649	26.9	0.009	0.0333	0.345	0.253		0.359	9.43	0.0004
	PO4 mist	2 months	82	5	865	422	6324	4595	3642	7333	23.2	0.037	0.0182	0.273	0.198	0.157	0.316	1.30	0.0040

Table A.10. Sequential Extraction Results for PO_4 Foam-Treated Sediment

Sed.	Treat-ment	Time (months)	T (°C)	H_2O (%)	sequential liquid extractions (ng U/g sed) #1 aq.	#2 ion exch.	#3 acetate pH5	#4 acetate pH2.3	#5 oxalate	#6 8M H+	total U (ug/g)	sequential extractions, fraction of total U mass #1 aq.	#2, ion exch.	#3, pH 5 acetate	#4, pH2.3 acetate	#5 oxalate	#6 8M H+	Kd (cm^3/g)	fraction aq.in vad. zone
1	none	0 (3 samples)	22	5	5731±672	3897±480	10440±920	301400±4200	30820±72	24640±5780	376.6±6.2	0.015	0.010	0.0277	0.800	0.0818	0.0649	1.45	0.0016
	PO4 foan	1 month	22	5	1733.5	467.0	3603	179098	25030	36409	246.3	0.0070	0.0019	0.015	0.727	0.102	0.148	0.44	0.0017
	PO4 foan	2 months	82	5	18425	8056	13912	59904	42527	155036	297.9	0.062	0.0270	0.047	0.201	0.143	0.520	0.69	0.0113
	PO4 foan	3 months	82	5	28712	5822	4573	33440	28738	104564	205.8	0.14	0.0283	0.022	0.162	0.140	0.508	0.31	0.0409
2	none	0 (5 samples)	22	5	962±53	792±44	2864±172	54600±1980	10170±1220	3770±215	74.3±2.3	0.013	0.0107	0.0385	0.744	0.137	0.0507	0.87	0.0024
	PO4 foan	1 month	22	5	485.5	365.9	1677	14583	23286	9938	50.3	0.010	0.0073	0.033	0.290	0.463	0.198	1.08	0.0014
	PO4 foan	2 months	82	5	1758	441	3859	10364	22315	23727	62.5	0.028	0.0070	0.062	0.166	0.357	0.380	0.35	0.0078
	PO4 foan	3 months	82	5	1905	688	3659	8703	17546	19378	51.9	0.037	0.0133	0.071	0.168	0.338	0.373	0.53	0.0079
3	none	0 (6 samples)	22	5	1706±148	3003±297	8181±1081	9738±997	1718±336	4210±678	28.1±1.8	0.061	0.107	0.291	0.336	0.061	0.149	1.84	0.0086
	PO4 foan	1 month	22	5	388	461	8844	9143	2589	3755	25.2	0.015	0.018	0.351	0.363	0.103	0.149	3.07	0.0011
	PO4 foan	2 months	82	5	897	672	2540	5775	7248	8802	25.9	0.035	0.026	0.098	0.223	0.280	0.340	1.90	0.0030

Distribution

No. of Copies		
21	**DOE Richland Operations Office**	
	RD Hildebrand (20 printed, CD)	A6-38
	JG Morse (printed, CD)	A5-11
7	**CH2M HILL Plateau Remediation Company**	
	MW Benecke	R3-60
	GB Chronister (6)	R3-60

No. of Copies		
8	**Pacific Northwest National Laboratory**	
	JE Szecsody (4)	K3-61
	MJ Truex (2)	K6-96
	MD Williams	K6-96
	L Zhong	K6-96

Pacific Northwest
NATIONAL LABORATORY

Proudly Operated by **Battelle** *Since 1965*

U.S. DEPARTMENT OF
ENERGY

902 Battelle Boulevard
P.O. Box 999
Richland, WA 99352
1-888-375-PNNL (7665)
www.pnl.gov